

Proposal of Optimized Intravenous Coronary  
Angiography System Using Two-Dimensional  
Monochromatic Synchrotron Radiation

Yasunari OKU

Doctor of Philosophy

Department of Synchrotron Radiation Science,  
School of Mathematical and Physical Science,  
The Graduate University for Advanced Studies

1997

# CONTENTS

1. Introduction.....	1
1-1 Availability of coronary angiography with the intravenous injection of a contrast agent using 2D-SR	
1-2 Merits and demerits of 2D-SR coronary angiography .....	2
1-3 Studies for improving the image contrast and suppressing the radiation dose.....	4
1-4 Necessity of a screening coronary angiography system using synchrotron-radiation .....	7
2. Simulation of image contrast .....	12
2-1 Simulation program	
2-2 Experiments for verification of the simulation program.....	18
2-2-1 Scattered x-rays and their injection into the detector	
2-2-2 Image contrast .....	20
2-3 Result.....	25
2-3-1 Characteristic of x-rays scattered in phantom	
2-3-2 Characterization and improvement of image contrast .....	32
3. Development of the rotating shutter.....	40
3-1 Principle and design	
3-2 Safety analysis against thermal load.....	46
3-3 Experiment for verification of synchronization.....	49
3-4 Application for clinical examination.....	49
4. Proposal of an optimized system for intravenous angiography using synchrotron-radiation source.....	56
4-1 Fixing the basic specifications	
4-2 Design of the storage ring.....	61
4-3 Optical element.....	65

4-4 Contrast agent.....	69
4-5 Penumbra.....	73
4-6 Detector.....	75
5. Conclusions.....	82
5-1 Summary	
5-2 Outcome.....	83
Acknowledgments.....	84
References.....	85
Appendix.....	89

## 1. Introduction

### 1-1 Availability of coronary angiography with the intravenous injection of a contrast agent using 2D-SR

Heart disease is the largest cause of death in the U.S., while it is the third in Japan, the percentages of which are 60% and 15%, respectively. That number is increasing in Japan due to a westernization of the diet. Furthermore, ischemic heart disease provides poor subjective symptoms in the early stage, even though there exists an important stenosis in the coronary arteries, and 50% of all patients can not be helped after reaching the stage of certain symptoms. Therefore, the early discovery of heart disease is of vital importance for any successful treatment to save the patient's lives. Periodic medical examinations of the heart are desired. Such examinations will give significant benefit to society.

For the diagnosis of ischemic heart disease, coronary angiography is effective. It can directly provide effective information for diagnosis. However, the arterial catheterization procedure, which is commonly used in hospitals as a coronary angiography method, requires skilled technique and the hospitalization of patients. Furthermore, it has some risks due to the injection of a catheter into the coronary artery through a thigh artery. Also heart specialists and technicians who handle emergency equipment must wait for treatment due to occurrence of an accident. Thus, periodic examinations such as for screening seems impossible using this procedure.

If the coronary angiography is carried out by intravenous injection, the examination could be carried out more safely and simply. Thus, it could be applied to a screening examination for heart diseases. However, since the contrast agent is diluted until reaching the coronary arteries, distinct images for a successful diagnosis would not be obtained.

The K-edge subtraction method is useful for resolving this problem. In this method, a subtraction image is generated between two images taken by monochromatic x-rays just above and below of K-edge of the contrast agent (iodine), and gives high-contrast images of the blood vessels without images of soft tissues or bones. The mass-attenuation coefficient of iodine, bone and soft tissue

as a function of the x-ray photon energy is shown in Fig. 1. Although this method is expected to be effective for intravenous coronary angiography, it has not been put in practical use because of insufficient intensity and energy resolution of the usual x-ray sources. Monochromatized synchrotron radiation with such intense x-rays is expected to be applied to clinical use of the intravenous coronary angiography method.

The K-edge subtraction method using synchrotron radiation was proposed first by E. Rubenstein of Stanford University et al. in 1981 (Rubenstein E. et al. 1981). The development of the systems and studies are being carried out not only in the U.S., but throughout the world. A sheet-type beam (one-dimensional imaging) coupled to a linear-position detector has been used in the U.S. (Hughes E. B. et al. 1983, Suortti P. et al. 1988, Thomlinson W. et al. 1988, Thompson A. C. et al. 1989, Rubenstein E. et al. 1990), Germany (Dix W. -R. et al. 1986, Dix W.-R. et al. 1989) and Russia, (Dementyev E. N. et al. 1986, Dementyev E. N. et al. 1989) while in Japan, a two-dimensional dynamic imaging system has been adopted (Akisada A. et al. 1986, Fukagawa H. et al. 1989, Nishimura K. et al. 1989, Hyodo, K. et al. 1991, Hyodo K. et al. 1992) at the High Energy Accelerator Research Organization (KEK).

Recently, only monochromatic x-rays whose energy is just above the energy of the K-edge of iodine are being used without K-edge subtraction in a basic study of SR coronary angiography in Japan, and, finally, in clinical applications in May 1996 (Hyodo K. et al. to be published, Ohtsuka S. et al. to be published). This is because the difference in the mass-attenuation coefficient between iodine and soft tissue or bone is relatively big at this energy, and distinct images were obtained without subtraction in an animal experiment using a goat without K-edge subtraction. (Ohtsuka S. et al. 1997)

## 1-2 Merits and demerits of 2D-SR coronary angiography

Dynamic imaging using a two-dimensional imaging system is very useful to see the blood flow through coronary arteries on the heart. Furthermore, not only structural diagnosis by using time-sequential images, but also diagnosis of the heart functions are possible. However, it has been pointed out that the exposure

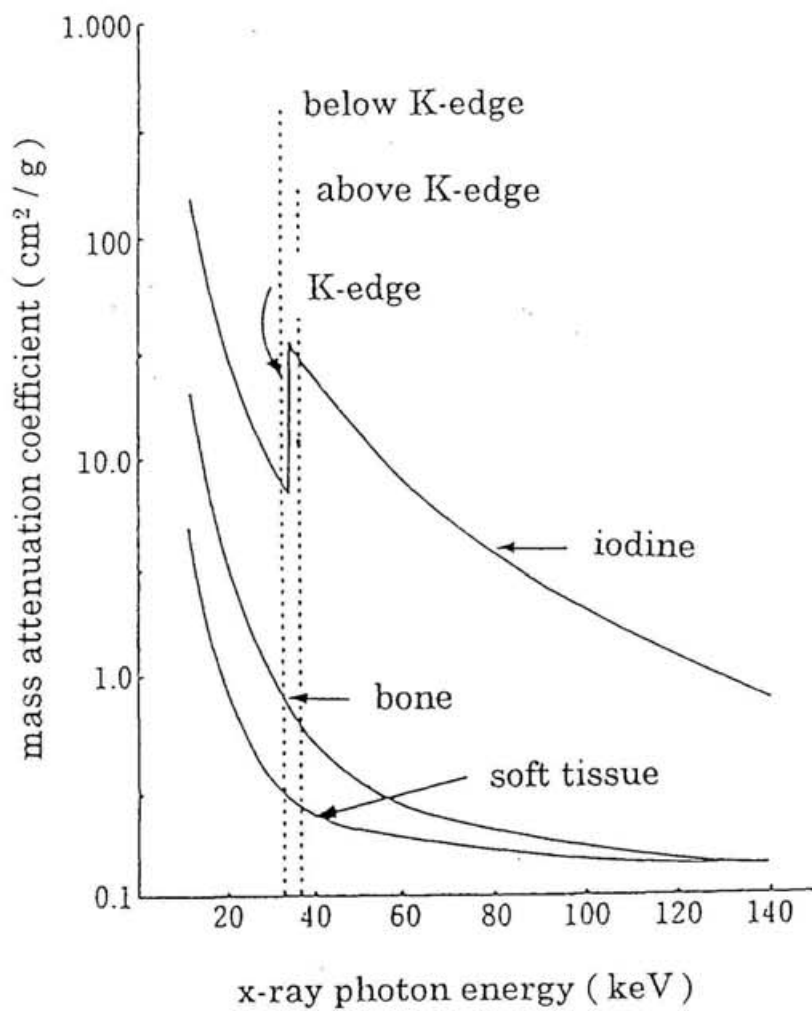


Fig. 1 Mass-attenuation coefficient of x-rays as a function of the photon energy

area covering the whole heart sight is so wide that a scattering of x-rays from a patient's body may cause a deterioration of the image contrast and visibility, as in Fig. 2. X-ray grids are effective for suppressing scattered x-rays. They are commonly used in hospitals when x-ray examinations are performed. The x-ray grid is a plate piled up with thin wood and lead alternately, which stops the scattered x-rays by the lead but allows the primary x-rays to pass through the wood, as in Fig. 3. Thus, it is expected to improve images by suppressing scattered x-rays also in the case of clinical coronary angiography using a monochromatic SR beam.

The image contrast is also deteriorated by the inevitable third higher harmonic diffracted by a monochromator crystal (Konishi K. et al. 1985) as well as scattered x-rays. Since the third higher harmonic and scattered x-rays can not be distinguished on image data, a simulation is very effective for identifying its influence on the deterioration of the image contrast.

In order to see the deterioration of image quality due to scattering and the third higher harmonic, a simulation program for them has been developed (Oku Y. et al. 1995), and their characteristics were investigated.

On the other hand, since a series of images is taken in dynamic imaging, the radiation dose per examination must be relatively larger than that of one-dimensional imaging. Thus, the dose should be suppressed to be as physically small as possible. An Image Intensifier-TV (II-TV) was adopted as an x-ray detector in two-dimensional SR coronary angiography. The TV system reads one image during a period of 1/30 sec; on the other hand, the irradiation period of x-rays per image must be in the range of 2 to 6 msec, because any motional blur of the images due to heart beating must be avoided. Also, continuous and unnecessary irradiation of the x-rays must be avoided. Therefore, SR x-rays should be a pulsed beam with 2~6 msec of beam spill, leading to suppressing any image blurring at a frequency of 30 Hz.

### 1-3 Studies for improving the image contrast and suppressing of the radiation dose

The merits and demerits of intravenous injection and intra-arterial injection

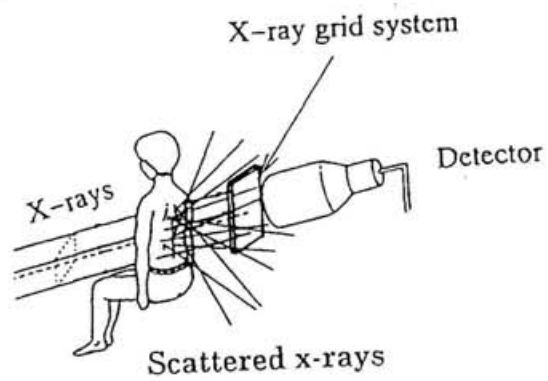


Fig. 2 Scattered x-rays generated when passing through a patient's body. An x-ray grid can suppress them.

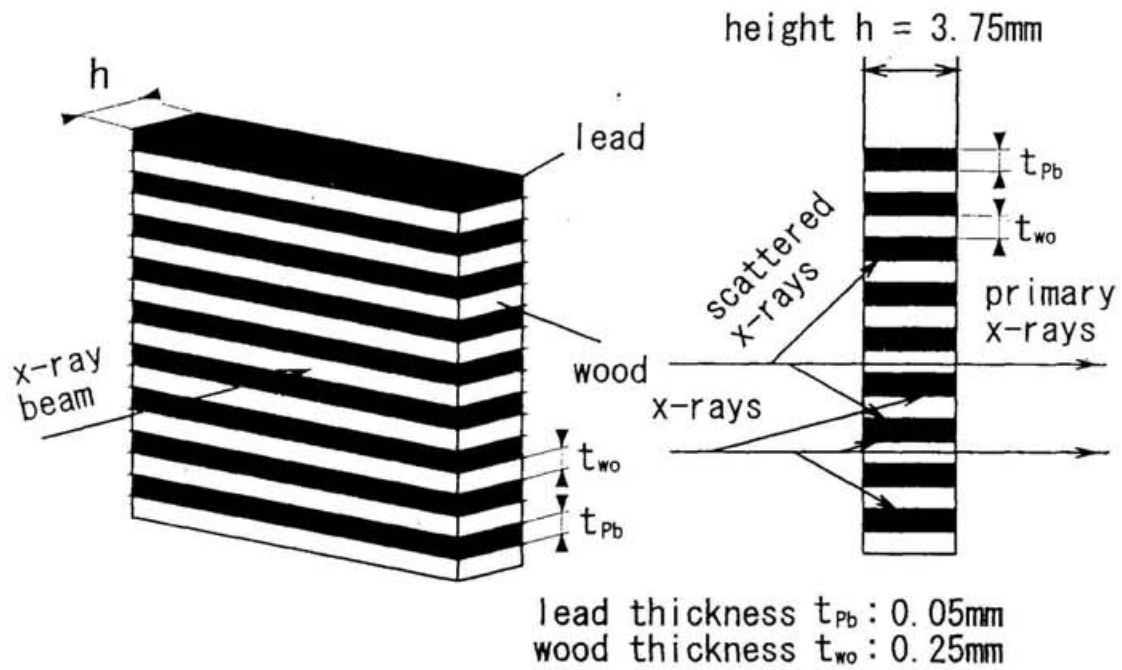


Fig. 3 Structure of the x-ray grid and effect of suppressing scattered x-rays  
 The x-ray grid is a plate piled up with thin wood and lead alternately, which stops the scattering x-rays, but lets primary x-rays pass through.  
 The grid ratio  $h/t_{wo} = 3.75 / 0.25 = 15$ .

of a contrast agent in coronary angiography are given in Table 1, while the merits and demerits of two-dimensional SR coronary angiography and one-dimensional scan method are given in Table 2. In order to make full use of the merits of possible screening examinations as a merit of intravenous injection, constructions of many SR source systems are expected. The arrangement of the SR coronary angiography system is shown in Fig. 4.

From Table 2, it is found that the influence of scattered x-rays must be investigated and an equipment which gives a pulsed SR beam is needed.

#### 1-4 Necessity of a screening coronary angiography system using synchrotron radiation

A realistic intravenous coronary angiography system using SR, which is based on investigations of deterioration of image contrast due to scattered x-rays and the third higher harmonic, its improvement by x-ray grids, in order to avoid of the demerits of two-dimensional coronary imaging, will be needed, if this method is adopted as a screening process. A rotating x-ray shutter for generating a pulsed x-ray beam is also needed in order to suppress image blur and to reduce the skin dose of radiation. A compact radiation source (Wiedemann H. 1985, Wiedemann H. 1988, Oku Y. et al. 1993, Oku Y. et al 1994) will make this method popular. Therefore, the specifications for a practical electron storage ring dedicated to coronary angiography have been fixed on a basis of image-visibility study using the simulation program.

The total photon flux from the source per image is limited by the x-ray shutter. The flux is distributed to the ideal exposure area covering the whole heart sight for coronary angiography. The photon flux per pixel is obtained from the pixel size and photon density in front of the detector. The quantum noise ratio is obtained from the flux per pixel per image, which must be sufficiently small compared to the artery contrast. Thus, the necessary photon flux density at the K-edge of iodine was estimated by quantum noises.

On the other hand, the third higher harmonic at 99.51 keV should be as small as possible in order to avoid any deterioration of the image contrast because of its high transmittance of the contrast agent, and a greater generation of

Table 1 Merits and demerits of intravenous injection and intra-arterial injection of a contrast agent in coronary angiography

	Intravenous injection	Intra-arterial injection
merits	<ul style="list-style-type: none"> <li>• out patients' examination ( screening ) possible due to simple method</li> <li>• small physical load of doctor and patients</li> </ul>	<ul style="list-style-type: none"> <li>• only coronary imaging possible</li> <li>• clear image</li> </ul>
demerits	<ul style="list-style-type: none"> <li>• dilution of contrast agent</li> <li>• imaging other blood vessel together</li> </ul>	<ul style="list-style-type: none"> <li>• hospitalization</li> <li>• high technique</li> <li>• preparation for emergency</li> </ul>

Table 2 Merits and demerits of SR coronary angiography of 2D and 1D imaging

	2D imaging	1D imaging
merits	<ul style="list-style-type: none"> <li>• dynamic imaging</li> <li>→ easy distinction of coronary</li> <li>→ heart function diagnosis possible</li> <li>→ certain timing of contrast agent flowing in coronary</li> </ul>	<ul style="list-style-type: none"> <li>• small scattering x-rays onto detector</li> <li>• smaller dose for one examination</li> <li>• large dynamic range of detector</li> </ul>
demerits	<ul style="list-style-type: none"> <li>• many scattered x-rays onto detector</li> <li>• more dose for one examination</li> </ul>	<ul style="list-style-type: none"> <li>• fixed imaging by patient's scan</li> <li>→ patient's motion necessary</li> <li>→ difficulty of timing of contrast agent flowing in coronary</li> </ul>

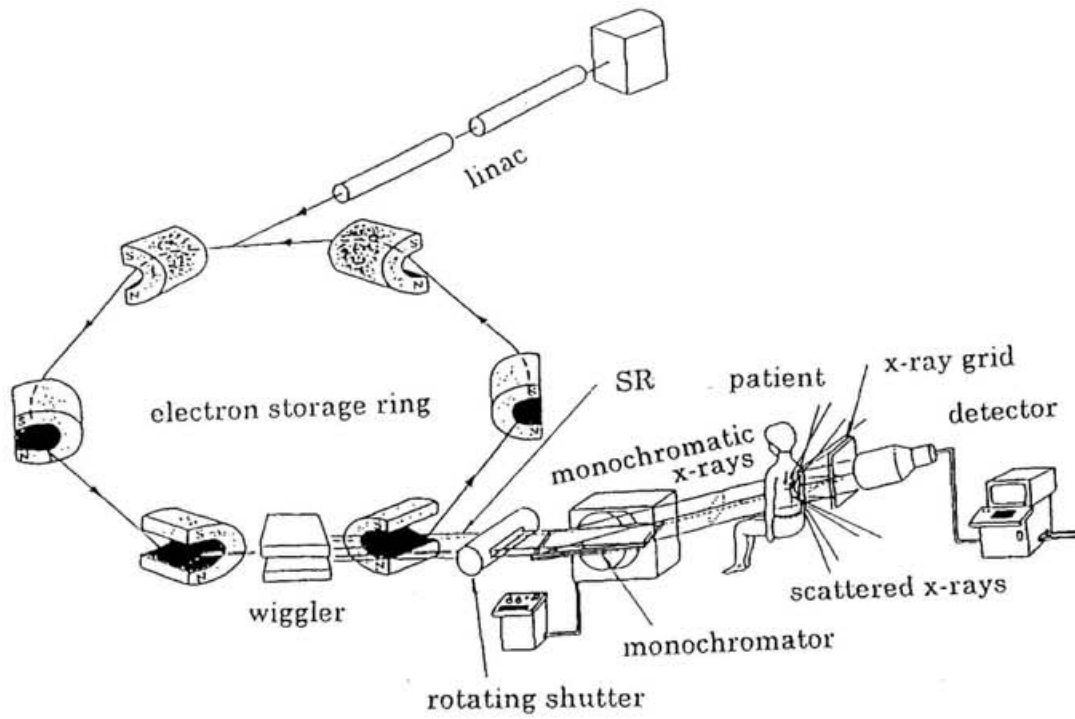


Fig. 4 Constitution of the coronary angiography system using synchrotron radiation

scattered x-rays than that by the x-rays at the iodine K-edge energy of 33.17 keV. Thus, by this study of the simulation program, the limitation of the ratio of the third higher harmonic, 99.17 keV over 33.17 keV, was obtained.

An appropriate beam energy of a storage ring and parameters of an insertion device as a radiation source was determined.

The necessary beam current and the number of poles of the insertion device have been fixed from the necessary photon-flux density of x-rays at the K-edge of iodine. The conceptual design of the dedicated ring was carried out by the program SAD (Oide K. et al. since 1986) . Finally, a consideration of the other system factors, such as optical elements, detectors, contrast agent and the location of a detector was also taken for a complete coronary angiography system. The whole system factors are described in chapter 4.

## 2. Simulation of image contrast

### 2-1 Simulation program

A simulation program using the Monte Carlo method has been developed, in order to study influence of the scattered x-rays and the third higher harmonic on images for medical diagnosis and effect of suppressing scattered x-rays by x-ray grid insertion. The simulation concept is shown in Fig. 5. An acrylic block was used as a simple model of a patient's body. In the program, x-ray photons are injected repeatedly into the acrylic phantom. Basic flow chart of the program is shown in Fig. 6. Two-dimensional image simulation model is shown in Fig. 7. The phantom comprises an acrylic block with a hollow tube analogous to a coronary artery filled with iodine diluted by water. The monochromatic incident x-rays are primarily 33.17 keV and 99.51 keV as the third higher harmonic, and uniformly distributed as a two-dimensional beam. The x-ray grid is inserted between the phantom and the detector, if it is used. Coherent scattering, incoherent scattering, photoelectric effect, and fluorescence x-ray generation by photoelectric effect were considered. The photon energy ranges from 10 to 100 keV. Photon free path was calculated as in the next equation: (Nakamori N. et al. 1980)

$$r = -\frac{1}{\mu_0(E_0)} \ln R, \quad (1)$$

where  $R$  is (0,1) uniform random number,  $\mu_0$  is total x-ray attenuation coefficient of coherent scattering and incoherent scattering, as a function of the photon energy  $E_0$ . The attenuation functions due to each interaction of x-rays were calculated by polynomial expression made from data of XCOM (Berger M. J. et al. 1987). Differential cross sections are given by the following equations (Nakamori N. et al. 1981, Namito Y. et al. 1993) which were modified from formula of Thomson scattering and Klein-Nishina formula, where  $\theta$  is the polar angles (see Fig. 8) of coherent scattering and incoherent scattering :

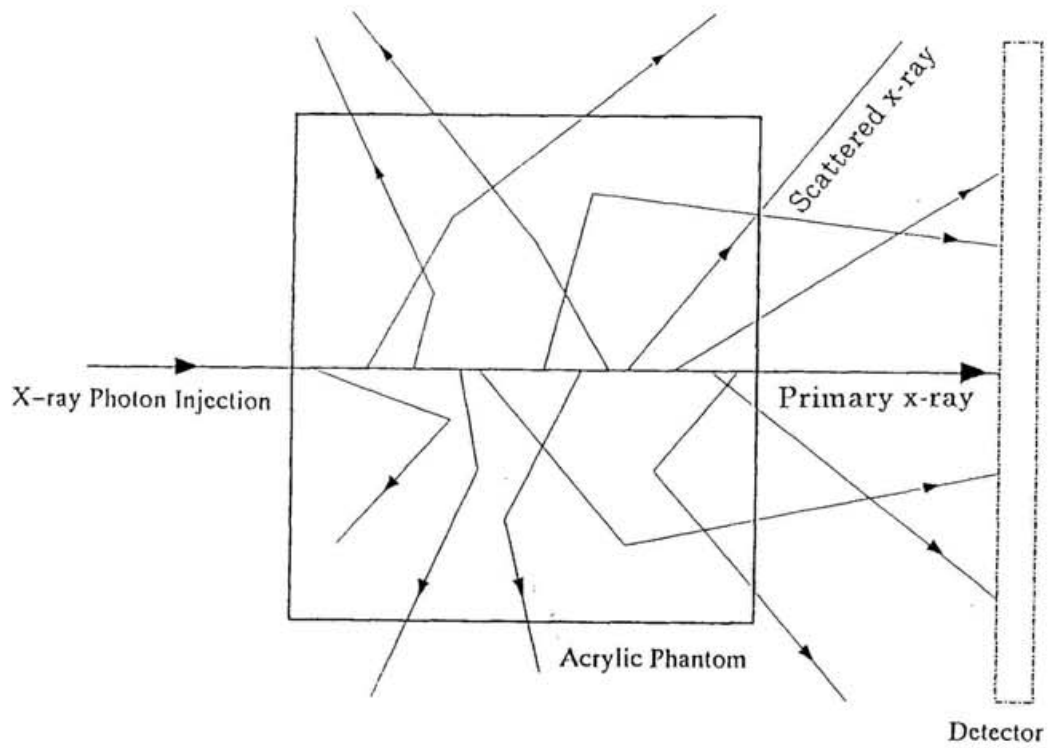


Fig. 5 Monte-Carlo simulation model of scattering x-rays

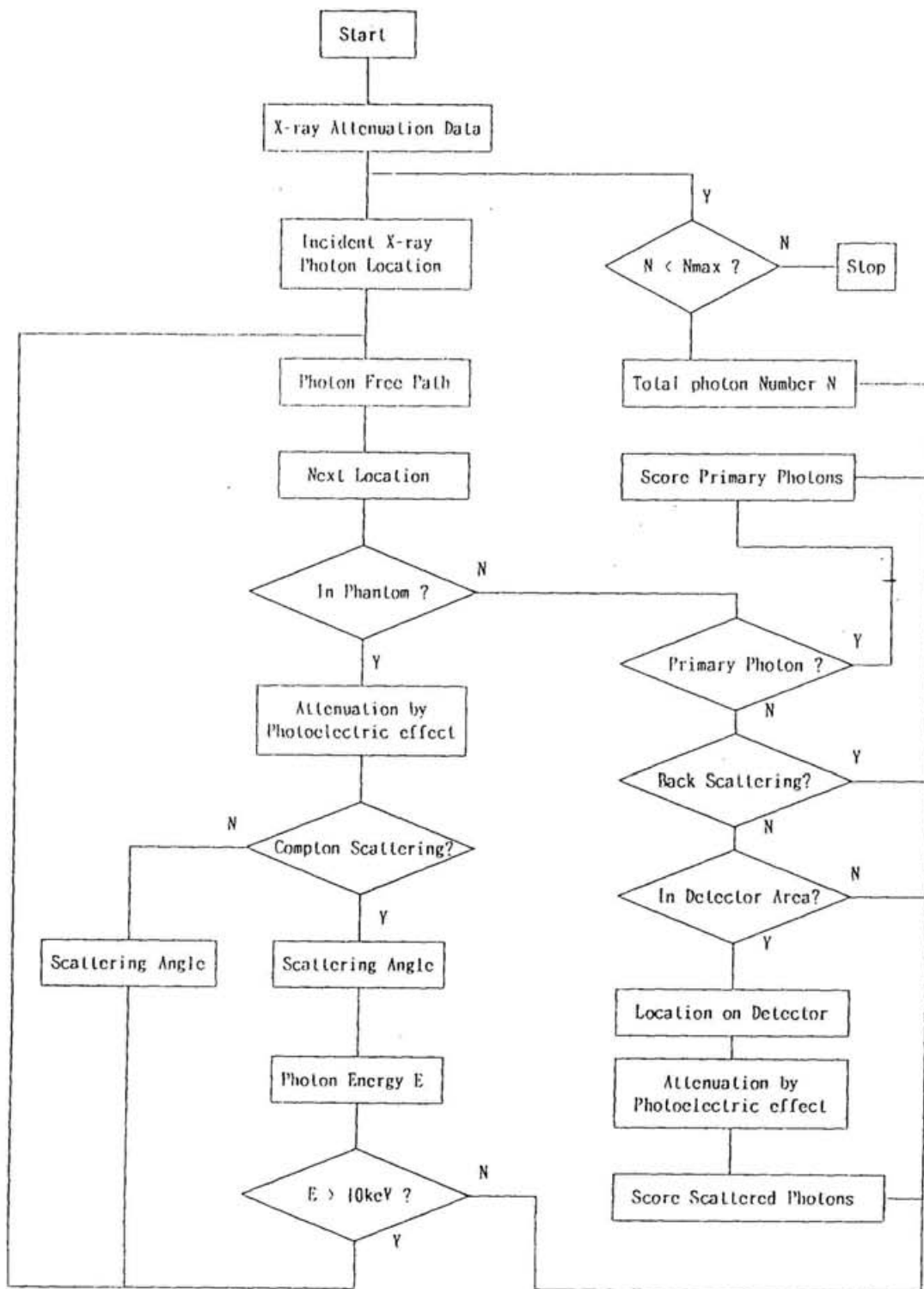


Fig. 6 Flow chart of the scattering x-ray simulation program

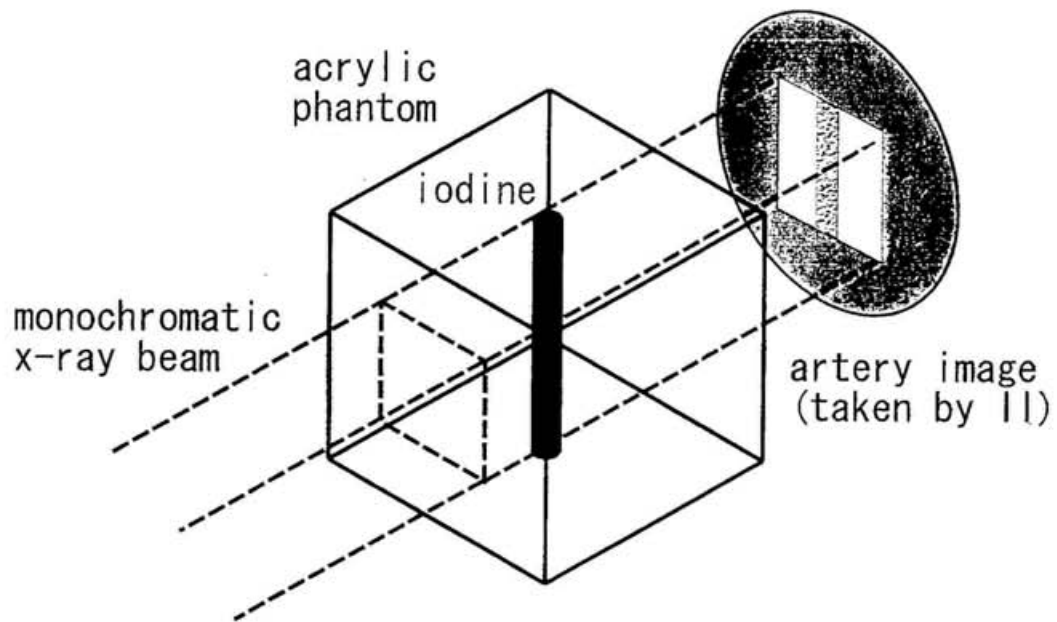


Fig. 7 Model of the two-dimensional image simulation program

The phantom is an acrylic block with a vessel which imitates a coronary artery and contains iodine diluted by water as a simple model of a patient's body and coronaries. In the program, x-ray photons are injected repeatedly into an acrylic phantom as a uniformly distributed two-dimensional beam and photons arriving on the detector plane are integrated as matrix data.

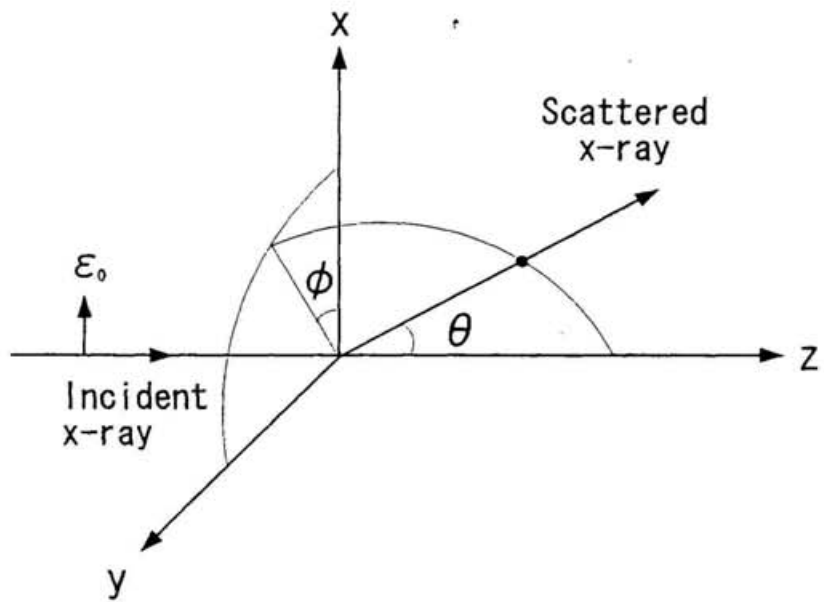


Fig. 8 Scattering polar angle  $\theta$  and scattering azimuth angle  $\phi$  from the plane of polarization vector  $\epsilon_0$

$$\left(\frac{d\sigma}{d\theta}\right)_{coh} = \frac{r_e^2}{2} (1 + \cos^2 \theta) \cdot 2\pi \sin \theta \cdot [F(x,z)]^2, \quad (2)$$

$$\left(\frac{d\sigma}{d\theta}\right)_{incoh} = \frac{r_e^2}{2} \left(\frac{E}{E_0}\right)^2 \left(\frac{E}{E_0} + \frac{E_0}{E} - 2 \sin^2 \theta\right) \cdot 2\pi \sin \theta \cdot S(x,z) \quad (3)$$

where  $r_e$  is the classical electron radius and  $E$  is the photon energy after incoherent scattering expressed by the next equation;

$$E = \frac{E_0}{1 + \gamma (1 - \cos \theta)}, \quad (4)$$

where

$$\gamma = \frac{E_0}{m_0 c^2}$$

$m_0 c^2$  is the rest mass energy of electrons,  $F(x,Z)$  and  $S(x,Z)$  are called the atomic form factor and the incoherent scattering function, respectively; they function as a value of  $x$  expressed by scattering polar angle  $\theta$ , photon wavelength  $\lambda$  (Å) and atomic number  $Z$  of the subject, as following equation;

$$x = \frac{\sin(\theta / 2)}{\lambda}$$

They are given in the table (Hubbell J. H. et al. 1975). In the simulation program, when these scattering occur after a photon passes the distance given by Eq. (1), the scattering angles are decided by random numbers whose birth probability distribution is in proportion to the above differential cross sections as an angle of photon scattering using Eq.(2)(3).

Scattering azimuth angle from the plane of polarization vector  $\phi$  (see Fig. 8) is determined in the same way by Eq.(5) and (6), they give differential cross sections against solid angle ( $\Omega$ ) of the coherent scattering and the incoherent

scattering with substitution of scattering polar angle  $\theta$  obtained from Eq.(2) and (3) (Namito Y. et al. 1993),

$$\left(\frac{d\sigma}{d\Omega}\right)_{coh} = r_e^2 (1 - \sin^2 \theta \cdot \cos^2 \phi) \quad (5)$$

$$\left(\frac{d\sigma}{d\Omega}\right)_{incoh} = \frac{r_e^2}{2} \left(\frac{E}{E_0}\right)^2 \left(\frac{E}{E_0} + \frac{E_0}{E} - 2 \sin^2 \theta \cdot \cos^2 \phi\right) \quad (6)$$

The attenuation by passing through the subject is calculated from the total path length and the value is memorized as each photon reaching the detector. This program gives photon location on the detector, photon energy and attenuation by photoelectric effect. The number of these photons are added to memorize for each pixel located on the detector, and two-dimensional simulation images are generated as digital matrix data.

## 2-2 Experiments for verification of the simulation program

### 2-2-1 Scattered x-rays and their injection into the detector

Two experiments have been carried out in order to verify the simulation program. One experiment was held using 33.17 keV monochromatic x-ray from a silicon (111) double crystal monochromator using SR at NE5A beamline of accumulation ring (AR) in KEK. An acrylic block whose thickness was 200 mm as an x-ray scattering matter. An imaging plate (IP) with size of 200 mm wide and 250 mm high was used as an x-ray detector. The arrangement of the acrylic phantom and the IP is shown in Fig. 9. The x-ray beam whose size was 14 mm wide and 2 mm high was injected to the acrylic.

The specifications of the x-ray grid were as follows: The path length of the grid in the direction of passing x-rays is 3.75 mm, the thickness of wood sheet was 0.25 mm and the thickness of lead sheet was 0.05 mm as in Fig. 3. The simulation of x-ray scattering has been carried out under the same conditions as in the experiment. The number of incident photons in the simulation was  $10^6$  photons, because the ratio of scattered x-rays per 33.17 keV primary photons close

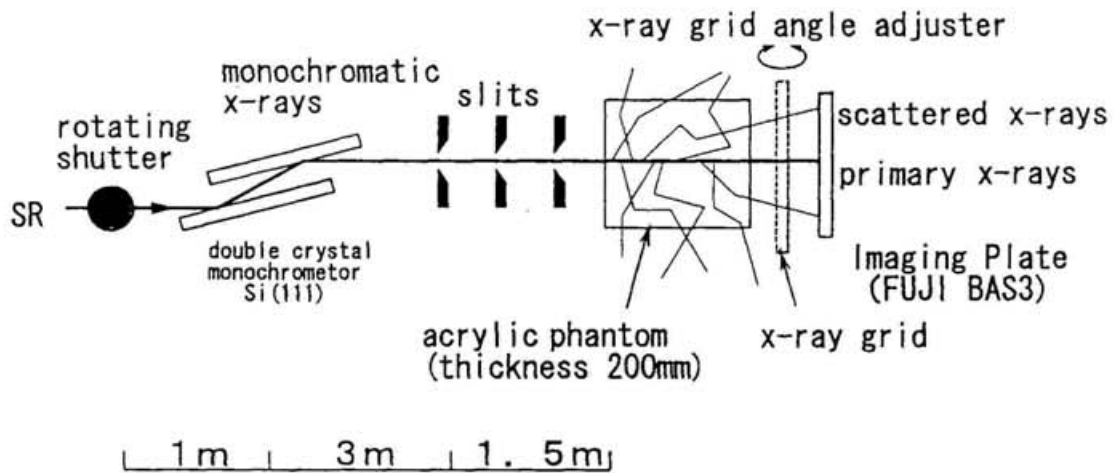


Fig. 9 Arrangement of the experiment to verify the ratio of the scattered x-ray photon flux against the direct x-rays calculated by the simulation program. A silicon (111) double crystal monochromator, an acrylic block whose size was 200 mm long, 250 mm wide, and 250 mm high as x-ray scattering matter and an imaging plate whose size was 200 mm wide and 250 mm high as an x-ray detector were used. The injection x-ray beam to the acrylic was cut by x-ray slits to be a sheet-type beam whose size was 14 mm in width and 2 mm in height.

to the fixed value in the error range due to initial random number, as in Fig. 10. In the experiment, 99.51 keV photons, a third higher harmonic, were also diffracted by silicon monochromator (Konishi K. et al. 1985). Thus, simulation results with 99.51 keV incident photons were added to them of 33.17 keV. Furthermore, the simulation results were corrected using the IP response related to the photon energy of the detected x-rays in order to compare with the experimental result exactly. The IP response was calculated by polynomial expression made from the data of M. Ito et al. ( Ito M. et al. 1991 ).

Figure 11 shows a comparison of a ratio of the number of scattered x-ray photons against the number of primary x-ray photons in the center area of 14 mm  $\times$  2 mm between the simulation and the experiment. The simulation results are in good agreement with the experiment data. The distributions of scattered x-rays and the profiles of the horizontal center lines on IP are shown in Figs. 12 and 13, each of which corresponds to the simulation by the developed program and simulation by program code EGS4 ( Nelson W. R. et al 1985 ), respectively. The image data made by the EGS4 were calculated by Professor H. Hirayama of KEK. The scattered x-ray distributions and profiles of the developed simulation program as well as the result of EGS4 are almost similar to the experimental ones. These results show that the developed simulation program presents the scattered x-rays' behavior well. Furthermore, it was found that the x-ray grid inserted between acrylic and detector was effective for suppressing the scattered x-rays in the case of 127 mm of the distance between acrylic phantom and detector, equivalent to the case of setting the detector from the phantom with distance of 500 mm without the x-ray grid.

### 2-2-2 Image contrast

The other experiment was held at X-17 B1 beamline of NSLS in Brookhaven National Lab. (BNL) in order to verify property of the image contrast made by the simulation program. An asymmetric lapped silicon (311) crystal was used as a monochromator. An acrylic block with a hole, which imitates a coronary artery whose diameter was from 1 to 5 mm, containing iodine diluted by water and an image intensifier (II) as an x-ray detector were used. The II was the same type as

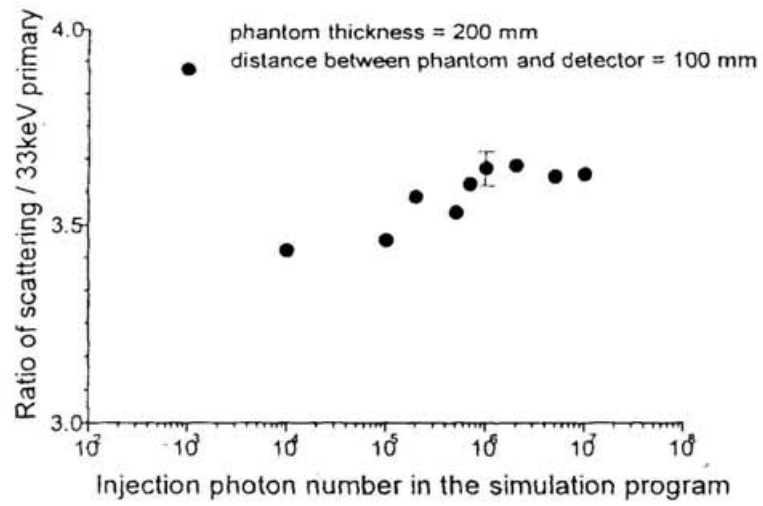


Fig. 10 Ratio of scattered x-rays per 33.17 keV primary photons as a function of injection photon number in the simulation program

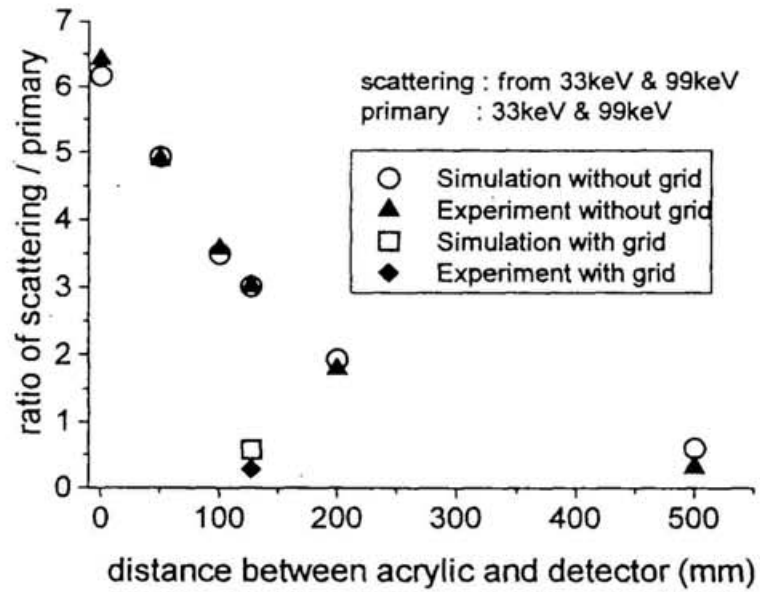
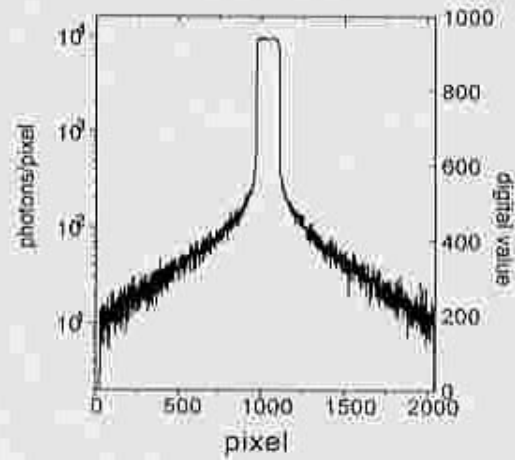
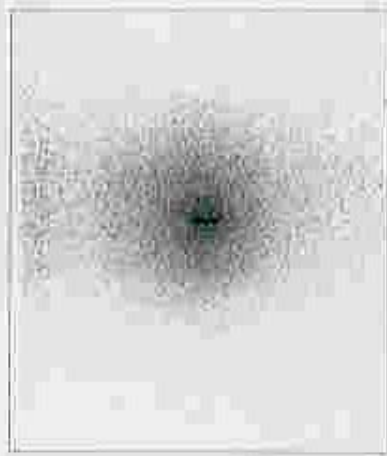
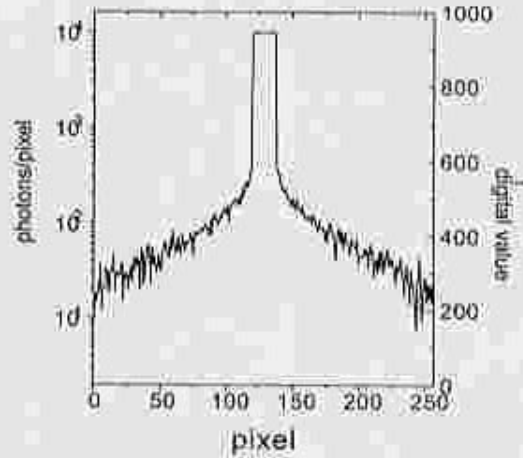
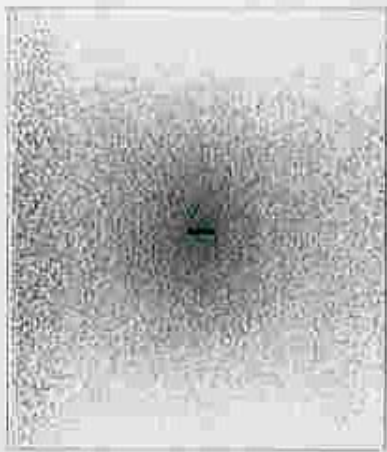


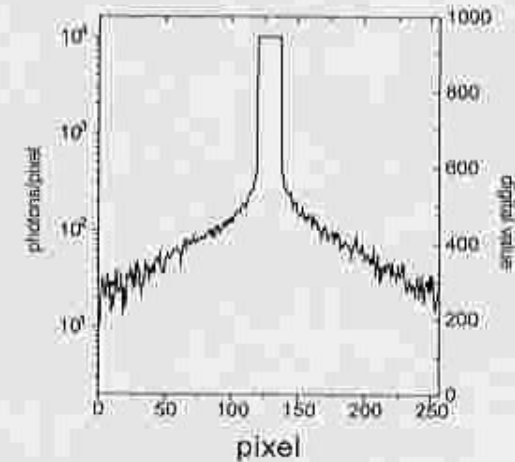
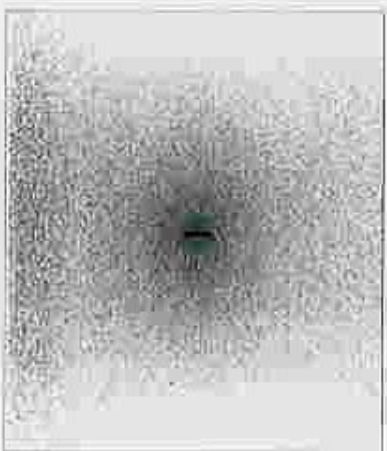
Fig. 11 Comparing result between simulation and experiment of the ratio of the number of scattered x-ray photons per the number of primary x-ray photons as a function of the distance between acrylic phantom and detector (acrylic phantom thickness = 200 mm)



experiment

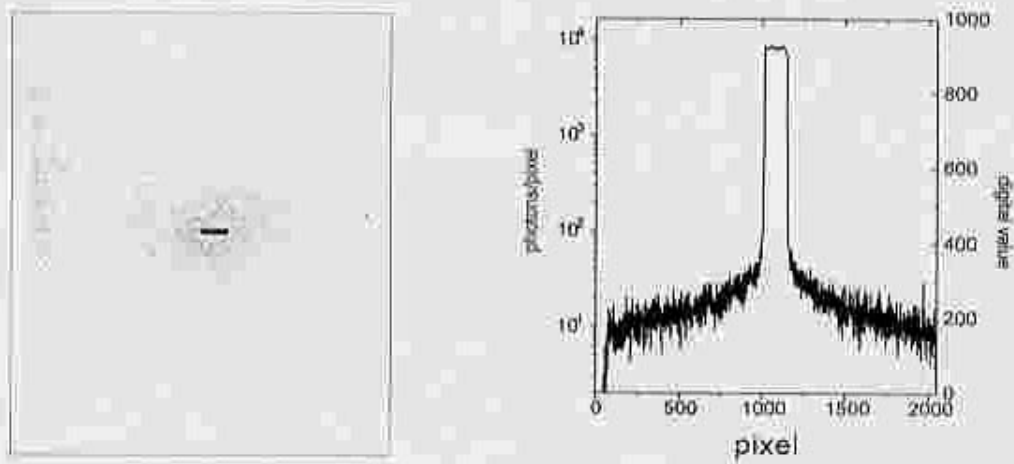


simulation by developed program

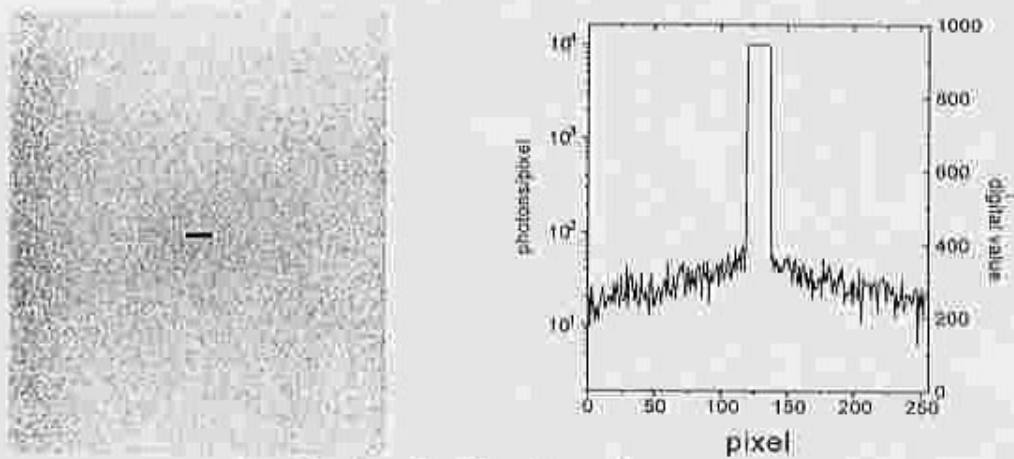


simulation by EGS4

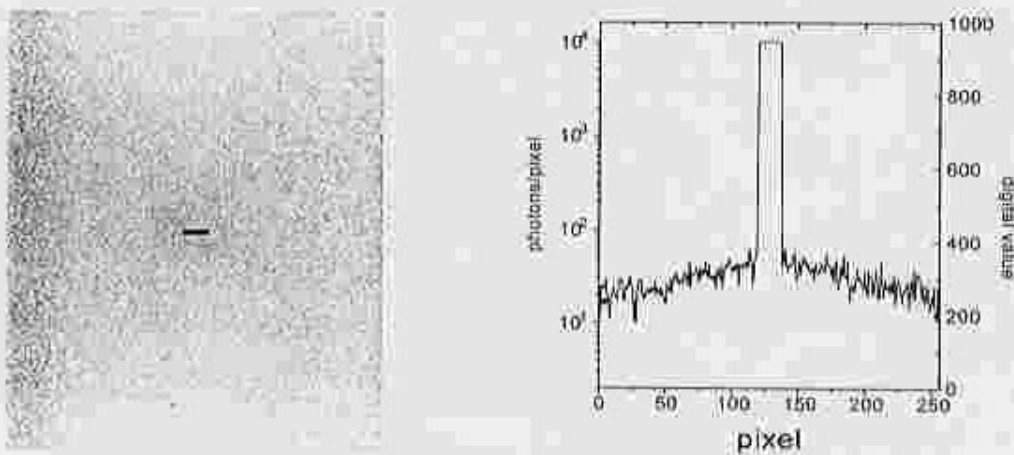
Fig.12 Images of scattered x-ray distributions and their profiles by small beams in the experiment and simulations by the developed program and EGS4. The distance between the phantom and the detector was 0.1 mm.



experiment



simulation by developed program



simulation by EGS4

Fig.13 Images of scattered x-ray distributions and their profiles by small beams in the experiment and simulations by the developed program and EGS4. The distance between the phantom and the detector was 127 mm.

the one used in the clinical application of two-dimensional SR coronary angiography, RTP9211G-G10 made by TOSHIBA (Hyodo K. et al. to be published, Ohtsuka S. et al. to be published). The arrangement of this experiment is shown in Fig. 14. The thickness of the acrylic block was 100 mm, the distance between the acrylic and the detector was 10 mm and the concentration in weight of diluted iodine was 5 %. The experimental images were recorded by a 8 mm video recorder. The analog data of video tapes were transferred to digital data, and analyzed on a personal computer. Fig. 15 shows an example of profile of the image, and contrast against the background is expressed as  $(a-b)/(a-c)$ . The simulations with the same conditions were carried out considering the II response related to the photon energy, and the contrast were compared between the simulation and the experiment as well as the preceding experiment. Comparing result is shown in Fig. 16 as two-dimensional images, Fig. 17 as image profiles and Fig. 18 as the above contrast value; it was found that the image simulation made images with reasonable contrast .

## 2-3 Result

### 2-3-1 Characteristic of x-rays scattered in phantom

As the developed simulation program was verified by comparison with the above two experiments and EGS4 simulation result, it is used for investigations of scattered x-ray characteristics and image contrast with various conditions in this section. The scattered x-rays injected into the exposure area per 33.17 keV and 99.51 keV primary photons of square beam as a function of one side length of beam is shown in Fig. 19. The values were obtained by the developed simulation program. The distance between acrylic and the detector was 100 mm. It was found that scattered x-rays generated from 20% of incident 99.51 keV x-rays against the incident 33.17 keV ones were equivalent to scattered x-rays generated from 33.17 keV x-rays in case where acrylic thickness was 80 mm. In the case of 120 mm, 160 mm and 200 mm of the acrylic thickness, 12%, 7% and 4% of incident 99.51 keV x-rays were equivalent to scattering of 33.17 keV, respectively. The body thickness equivalent to water is 80~120 mm and 160~200 mm, and the length of one side of the exposure area should be 80 mm and 150 mm, in the case

### NSLS X17 beamline

beam energy : 2.5 GeV  
wiggler field : 4.7 T  
beam current : 200 mA  
99keV/33keV : 5 %

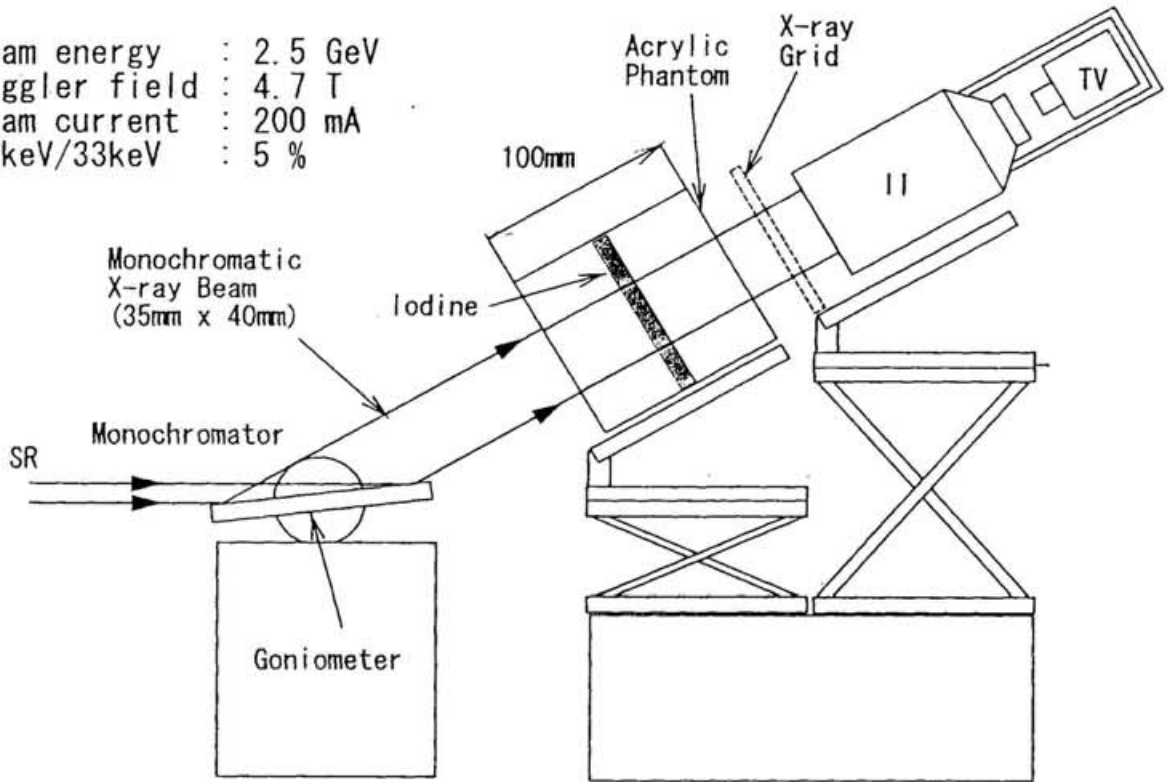


Fig. 14 Arrangement of the experiment to verify the image simulation contrast. An asymmetric lapped silicon (311) crystal as a monochromator, an acrylic block with a hole which imitates a coronary artery whose diameter was from 1 to 5 mm and contained iodine diluted by water and an image intensifier as a x-ray detector were used. The thickness of acrylic block was 100 mm, the distance between the acrylic and the detector was 10 mm and the concentration in weight of diluted iodine was 5 %.

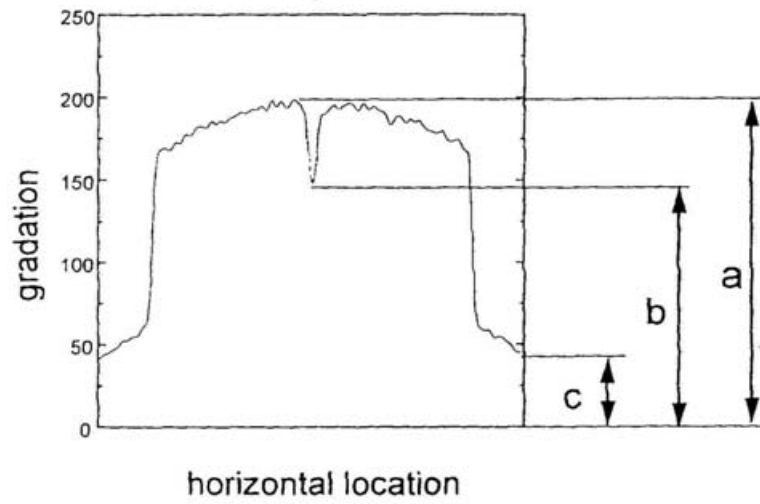
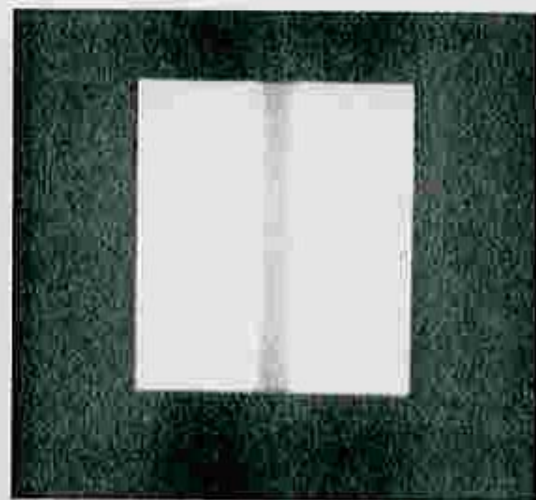
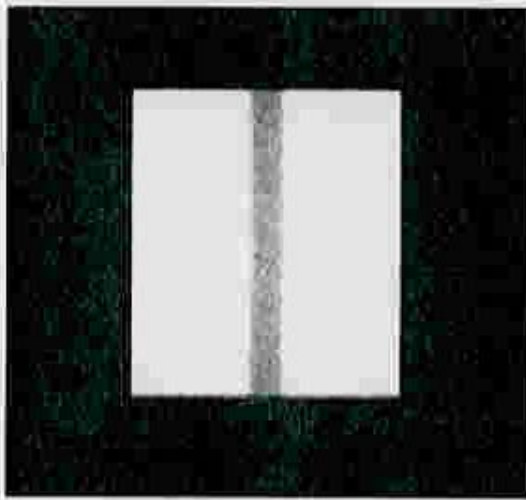


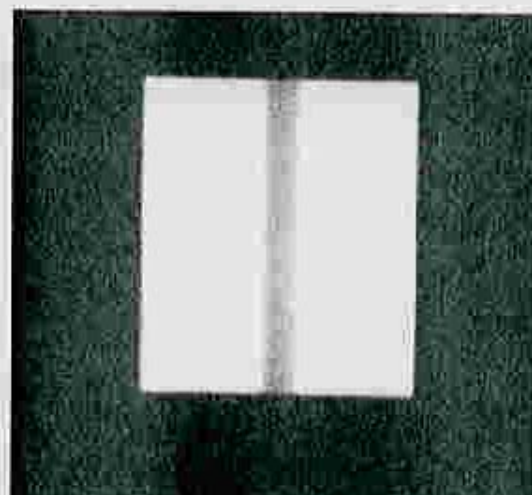
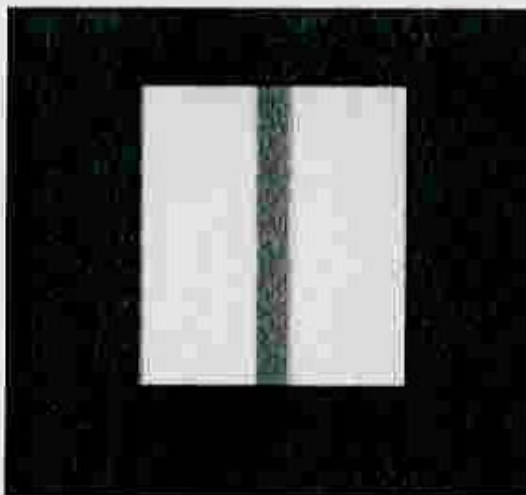
Fig. 15 An example of profile of the image  
The contrast of artery against the background is expressed as  $(a-b)/(a-c)$ .

simulation

experiment



without grid



with grid

Fig. 16 Two-dimensional coronary images of simulation and experiment in case of no grid and with grid

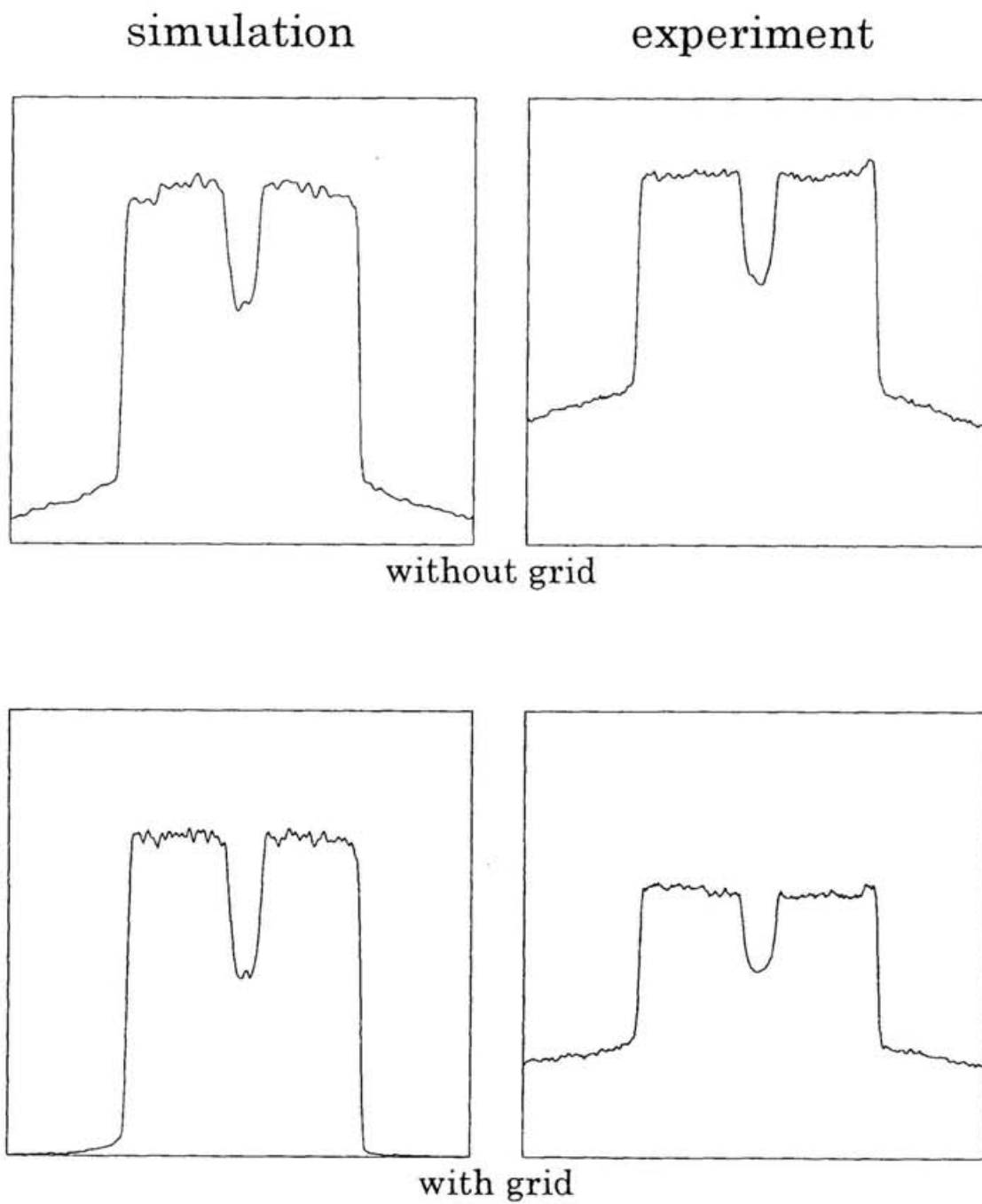


Fig. 17 Profiles of coronary images of simulation and experiment in case of no grid and with grid

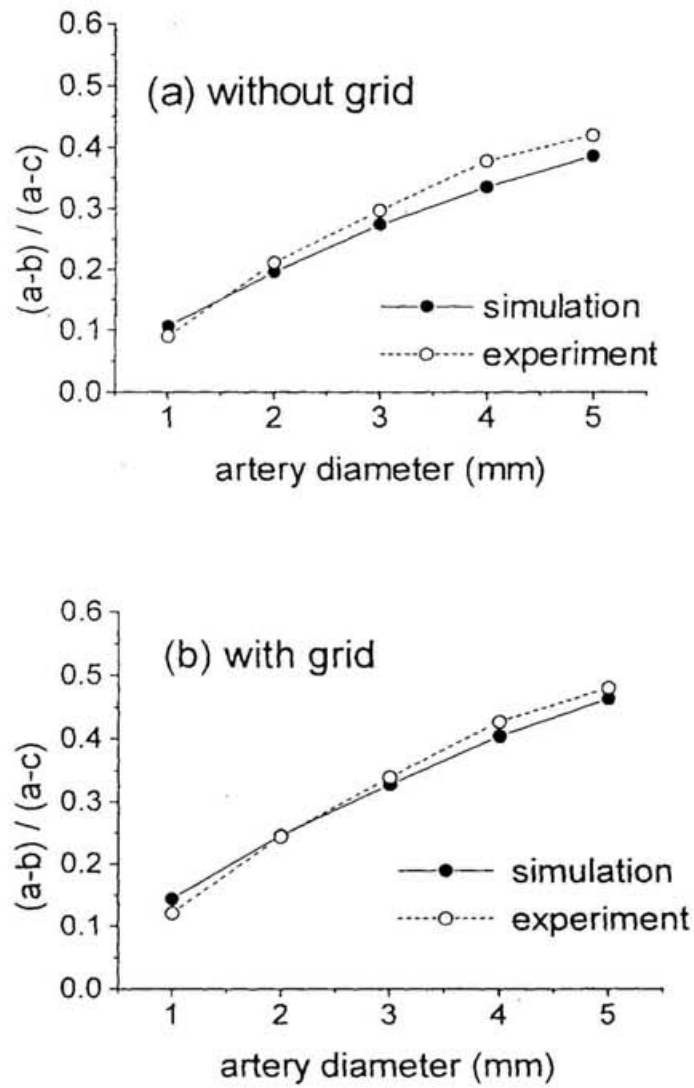


Fig. 18 Comparing result between simulation and experiment of the contrast of artery against the background expressed as  $(a-b)/(a-c)$  as a function of the artery diameter. (a) without grid (b) with grid

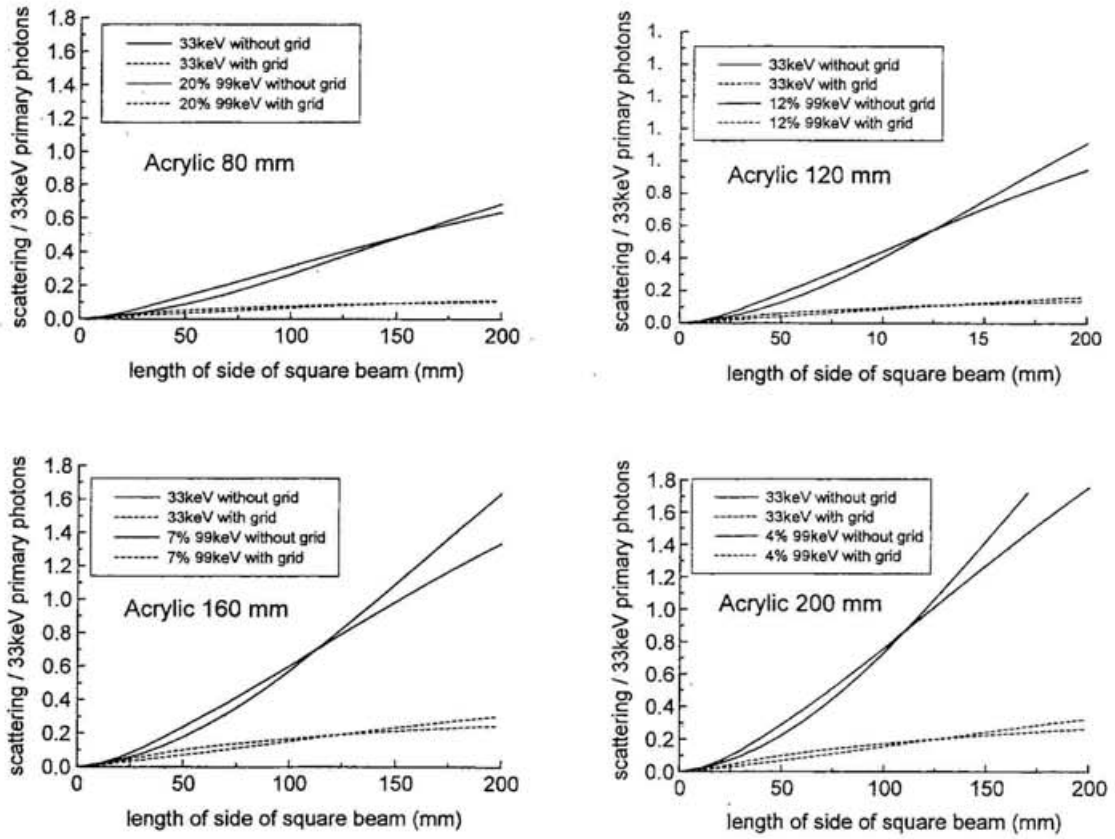


Fig. 19 Scattering x-rays per 33.17 keV direct photons of square beam as a function of one side length of beam

where the experiment use dogs and the clinical applications, respectively. Thus, it was found that the scattered x-rays influence image quality seriously in clinical applications rather than animal experiments, because of the body thickness and the required exposure area size, and especially, the ratio of 99.51 keV contamination is harmful in the case of the higher thickness of body. Energy spectrums of scattered x-rays in the condition of first clinical application at NE1 beamline of KEK are shown in Fig. 20. Real scattered x-ray quantity and one considered energy response of image intensifier are shown. In this case, there were not so many the scattered x-rays due to the distance between the patient's body and the detector of 500 mm. Generally, the distance should be as short as possible in order to make small the penumbra of images. However, the distance was reasonable in the condition of AR NE1, because the penumbra of the artery image was negligible as described in section 4-5.

### 2-3-2 Characterization and improvement of image contrast

The ratio of 33.17 keV primary x-rays per 99.51 keV primary and scattered x-rays as a function of wood thickness of x-ray grids is shown in Fig. 21. The ratio is almost constant in the region where the wood thickness is thicker than 0.15 mm. The bigger the grid ratio (grid height / wood thickness), the bigger the above ratio, it means more suppression of scattered x-rays by the x-ray grid. However, the grid ratio of 15 is the best available value due to the manufacturing skill. An effective transmittance ( $I/I_0$ ) is defined here as

$$\frac{I}{I_0} = \frac{t_{wo}}{t_{wo} + t_{pb}} \cdot e^{-\mu h},$$

where,  $t_{wo}$  is the wood thickness,  $t_{pb}$  is the lead thickness,  $h$  is the grid height and  $\mu$  is the attenuation coefficient of the wood. In Fig. 22, the effective transmittance of 33.17 keV x-rays is shown as a function of wood thickness under the condition of grid ratio of 15. It was found that the effective transmittance was almost constant in the region above 0.2 mm of wood thickness; especially, it becomes smaller in the region above 0.5 mm. The lead of grid are clearly visible,



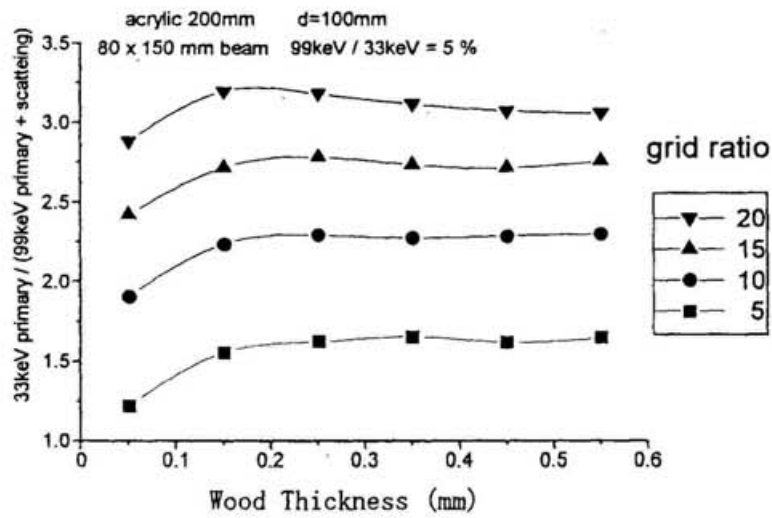


Fig. 21 The ratio of 33.17 keV direct x-rays per 99.51 keV primary and scattered x-rays as a function of wood thickness of x-ray grids

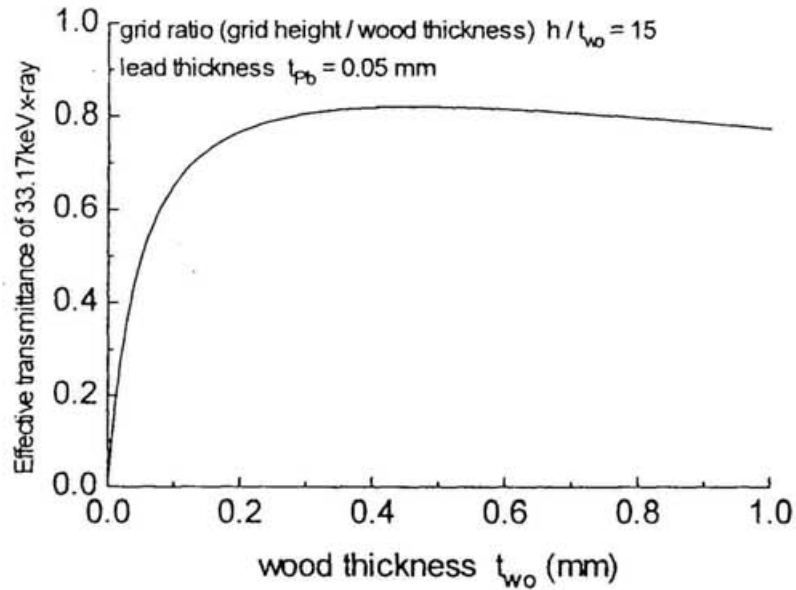


Fig. 22 Effective transmittance of 33.17 keV x-rays as a function of wood thickness of grids under the condition of constant grid ratio of 15. The effective transmittance ( $I/I_0$ ) is defined here as

$$\frac{I}{I_0} = \frac{t_{w0}}{t_{w0} + t_{pb}} \cdot e^{-\mu h},$$

where,  $t_{w0}$  is the the wood thickness,  $t_{pb}$  is the lead thickness,  $h$  is the grid height and  $\mu$  is the attenuation coefficient of the wood.

when its spatial frequency is smaller than that of II-TV system. Thus, 0.25 mm of wood thickness which gave no grid images was adopted as the best x-ray grid for SR coronary angiography. Assuming possibility of manufacturing bigger grid ratio, image contrast  $((a-b)/a)$  is shown in Fig. 23 with the red line, which is as a function of grid height from 1.25 to 80 mm while fixing the wood thickness of 0.25 mm. The contrast saturates around grid height of 10 mm. On the other hand, 33.17 keV primary photons are attenuated as the grid thickness become bigger progressively as shown with the purple line in Fig. 23. Thus, the required maximum grid height should be 10 mm.

I have made simple model images in the case of ideal clinical application with wide exposure area, with the best realizable x-ray grid whose specifications are shown in Fig. 3, and investigated the contrast improvement of images by x-ray grids. The exposure area was assumed to be 150 mm  $\times$  150 mm covering the whole heart sight, and the distance between acrylic and detector to be 100 mm in order to avoid so much penumbra width due to finite source size as in Fig. 24; the distance was minimal to insertion of the x-ray grid with angle adjustment. The ratio of the third higher harmonic against the iodine K-edge energy was assumed to be 1%. The simulated images and profiles are shown in Fig. 25. The contrast of artery model was improved twice by the x-ray grid insertion. The x-ray grid is very effective in this case.

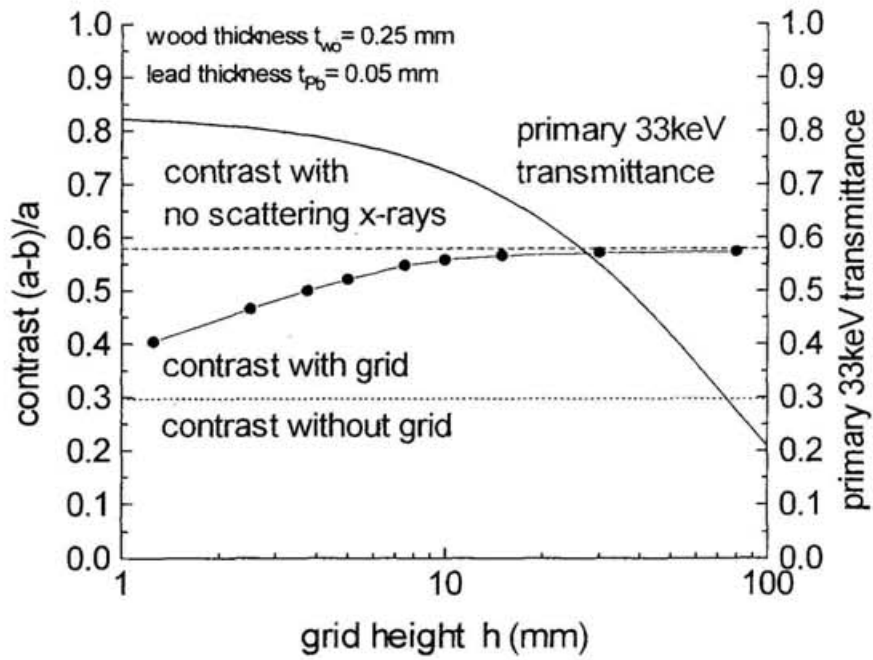


Fig. 23 Image contrast  $(a-b)/a$  and transmittance of primary 33.17 keV x-rays as a function of grid height from 1.25 to 80 mm with fixed value of wood thickness of 0.25 mm

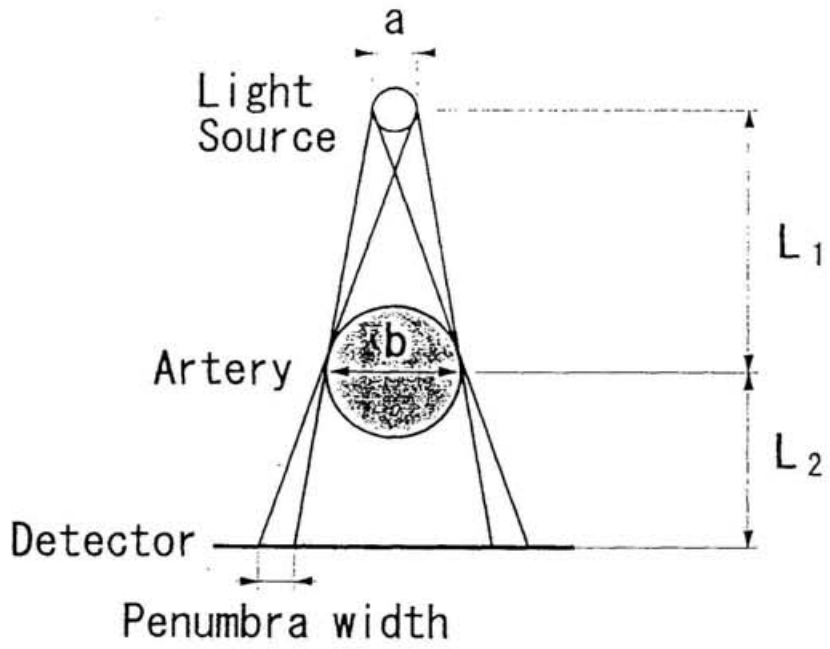
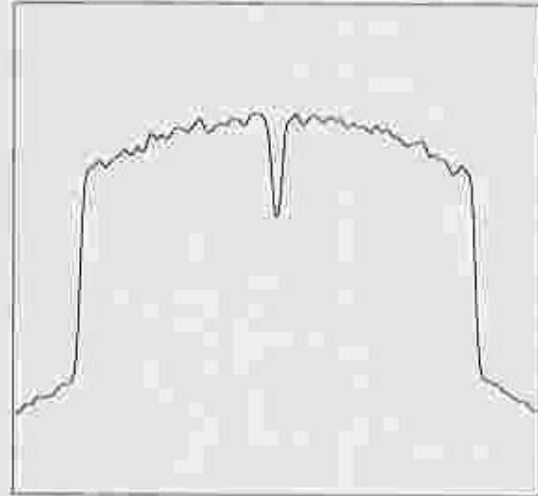
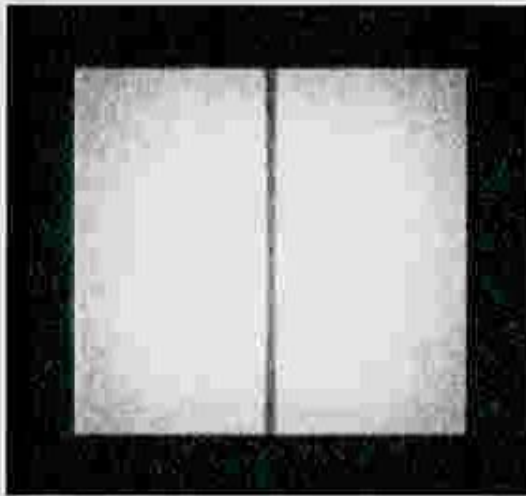
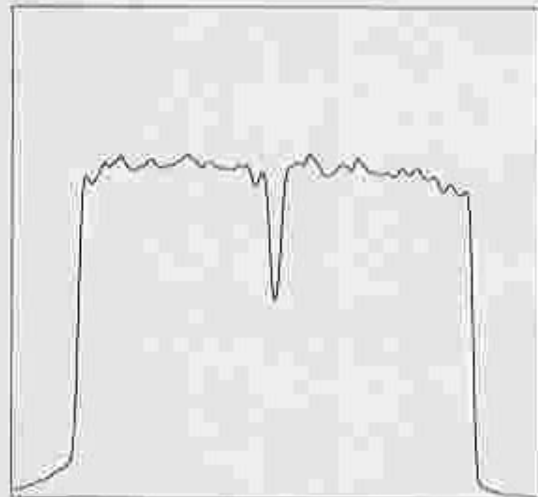
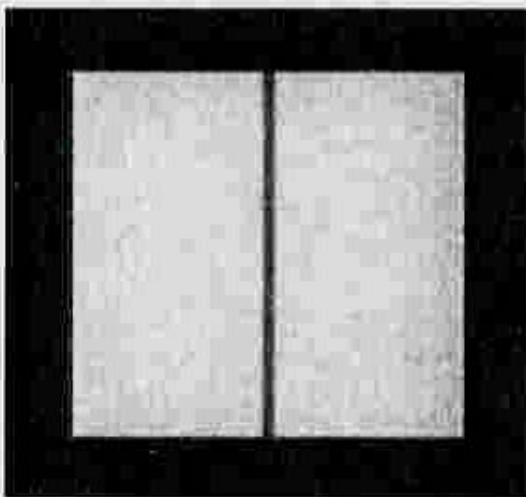


Fig. 24 Penumbra width due to finite light source size  
 Penumbra width =  $a \cdot (L_2 / L_1)$



without grid



with grid

Fig. 25 Simulated images and their profiles in the case of ideal clinical application with wide exposure area of  $150\text{ mm} \times 150\text{ mm}$  covering the whole heart sight, and the distance between acrylic and detector to be 100 mm in order to avoid so much penumbra width due to finite source size. The specifications of the x-ray grid are shown in Fig.3.

### 3. Development of the rotating shutter

#### 3-1 Principle and design

An x-ray shutter which generates pulsed beams is necessary in order first to make blurless artery images and second to suppress the patient's dose as much as possible. Thus, a rotating x-ray shutter was developed in this study. The x-ray shutter consisted of a drum with a hole in the direction of its radius as in Fig. 26 and it rotated at 15 rps. ( Zeman H. D. et al. 1983, LeGrand A. D. et al. 1989 ) X-rays pass through the hole during 2~6 msec, on a frequency of 30 Hz. The x-ray shutter also generated trigger pulses in order to synchronize the read-out starting of the TV system with the x-ray passing. Three different types of sensors for generating trigger pulses were employed; they were a photoelectric sensor, a proximity sensor and a digital encoder. Either one would have survived in an extreme case if radiation damage or other mechanical trouble occurred. In order to make two-dimensional images for coronary angiography, an asymmetric diffraction monochromator ( Kohra K. 1962 ) was employed to magnify vertical x-ray beam size. So, the developed rotating x-ray shutter was arranged in front of the monochromator in order to make a hole of the x-ray shutter as small as possible.

The shape of the hole in the transaxial plane of the drum is shown in Fig. 26. The design of the shape was determined as follows: At the beginning of the irradiation period  $t_e$ , phase (a) in Fig. 26, the plane of the hole wall of the drum is parallel to the synchrotron radiation beam axis. Phase (c) is the end of the irradiation period. Then, at the end of the transition period  $t_t$ , phase (d), synchrotron radiation is completely interrupted by the shutter drum. The shape shown in Fig. 26 is so determined that the x-ray path length in the attenuation material of the drum should be as long as possible in the transition period between phase (c) and (d) in Fig. 26. The reason for the above is that the energy of x-rays which I used was higher than the x-ray energy used in experiment of physical study, and penetration of the x-rays is high and they should be attenuated. The concrete design of the drum is as follows: As the rotating angle in the transition period  $t_t$ , between phase (c) and (d) as in Fig. 26 is twice that of

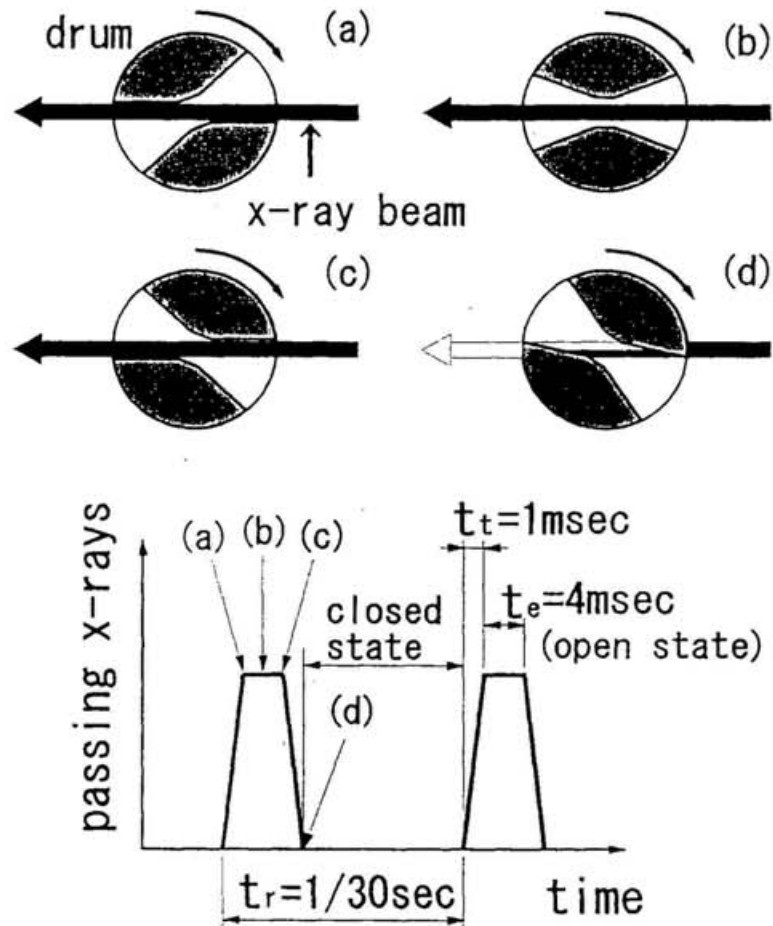


Fig. 26 Time sequential cross section of drum rotating and passing x-ray's quantity as a function of the periodic time

Status (a) is beginning of the irradiation period. Status (b) is center of the irradiation period. Status (c) is end of the irradiation period. Status (d) is end of the transition period and beginning of the drum complete closing period.

- $t_r$  : repetitive period of drum half rotation\*
- $t_e$  : irradiation period of x-rays
- $t_t$  : transition period between x-ray passing and stopping

the beam covering angle  $\theta_b$  in Fig. 27 and the rotating angle in the repetitive period  $t_r$  is  $\pi$ ,  $\theta_b$  is represented by  $t_t$  and the repetitive period  $t_r$  as follows:

$$2\theta_b = \frac{t_t}{t_r} \pi . \quad (7)$$

The radius of the drum,  $R$  is represented by  $\theta_b$  and the synchrotron radiation beam vertical width  $h_b$ , as follows:

$$R = \frac{h_b}{2 \sin \theta_b} . \quad (8)$$

The opening angle of the drum,  $\theta_o$  in Fig. 25 is represented by  $\theta_b$ , the irradiation period  $t_e$  and  $t_r$  as follows:

$$2\theta_o = \frac{t_e}{t_r} \pi + 2\theta_b . \quad (9)$$

The opening height of the drum is as follows:

$$h_o = 2 R \cdot \sin \theta_o . \quad (10)$$

After rotating of  $\theta_o - \theta_b$  clockwise from the state as in Fig. 27 as well as in Fig. 26 (b), the edge of the drum is parallel to the beam axis as in Fig. 26 (c). Thus, the cutting angle of the drum,  $\theta_c$  is as follows:

$$\theta_c = \theta_o - \theta_b . \quad (11)$$

The requirements for the rotating x-ray shutter for medical doctors are as follows: (a) the time structure of the x-ray beam is a pulsed one whose beam spill is either 2, 4 or 6 msec with the frequency of 30 Hz so that the irradiation are synchronized with the timing of the imaging system, (b) in a closing state, the intensity of x-rays of 33.17 keV and 99.51 keV should be attenuated to be less than  $10^{-8}$  of the original photons, (c) transition period  $t_t$  between the irradiation period and close state should be less than 1 msec, because x-rays during this period shouldn't contribute to the images, (d) trigger pulse (TTL signal) should be generate as starting of the irradiation period.

From requirement (a), the repetitive period of synchrotron radiation passing through the x-ray shutter  $t_r$  should be 1/30 sec and the irradiation period  $t_e$  is

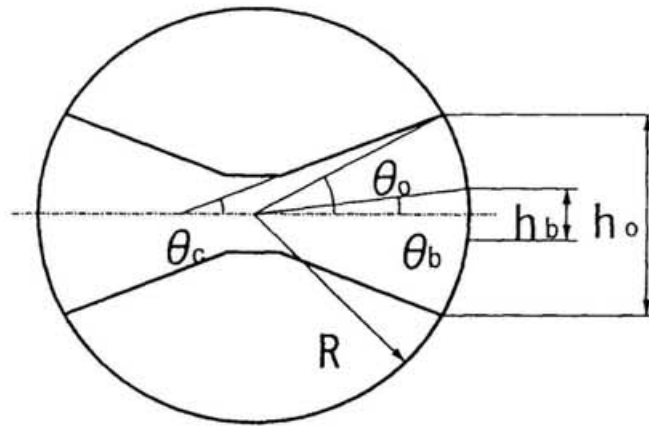


Fig. 27 Design parameters of the x-ray shutter drum

$\theta_b$  is the beam covering angle and it is represented by  $t_t$  and the repetitive period  $t_r$  as  $2\theta_b = (t_t / t_r)\pi$ . The radius of the drum,  $R$  is represented by  $\theta_b$  and the synchrotron radiation beam height,  $h_b$ , as  $R = h_b / (2 \sin \theta_b)$ . The opening angle of the drum,  $\theta_o$  is represented by  $\theta_b$ ,  $t_e$  and  $t_r$  as  $2\theta_o = (t_e / t_r)\pi + 2\theta_b$ . The opening height of the drum is as  $h_b = 2R \cdot \sin \theta_b$ .  $\theta_c$  is given as  $\theta_c = \theta_o - \theta_b$ .

selected to be 2 msec here. On the other hand, from requirement (c), the transition period,  $t_t$ , was assumed to be 1 msec.

With the above parameters and the vertical beam width ( $h_b = 7 \text{ mm}$ ) of synchrotron radiation of NE1 beamline at AR of KEK, the design parameters of the drum were obtained from equations (7) to (11) as follows:

$$2 \theta_b = \frac{3\pi}{100} \text{ rad} = 5.4^\circ ,$$

$$R = 75 \text{ mm},$$

$$2 \theta_o = 0.282 \text{ rad} = 16.2^\circ ,$$

$$h_o = 21.2 \text{ mm},$$

$$\theta_c = 5.4^\circ .$$

As the horizontal beam width was about 80 mm, opening width of the drum was designed to be 90 mm. The drum was designed as above. The other two types of drums for 4 and 6 msec pulse width were also designed the same as above, and provided. I employed stainless steel SUS304 as the material for the drum. Passing through this drum, the x-rays of 33.17 keV attenuate to less than  $10^{-100}$ , and 99.51 keV, the third higher harmonic, deteriorate to less than  $2.2 \times 10^{-18}$  in the case of the closed state, the latter of which rose from the (311) reflection from silicon crystal monochromator as the third higher harmonic x-rays. (Konishi K. et al. 1985) The arrangement of the system including motors and sensors is shown in Fig. 28. The rotation of the drum is driven by the speed variable motor. In order to synchronize the readout start timing of the CCD camera of the II-TV system with the start timing of the x-rays passing through the x-ray shutter, the trigger pulses must be generated by the x-ray shutter controller. Three sensors are used for generating trigger pulses. They are a photoelectric sensor, a proximity sensor and a digital encoder. The photoelectric sensor works for sensing laser beams which pass through a radial hole in the disk. The proximity sensor works for sensing a recess cut on the edge of the disk. These disks are attached to both sides of the drum as in Fig. 28. These disks are set for sensors to work just before the opening position of the x-ray shutter. A pulse motor in Fig. 26 is used for rotating the shutter drum to the closed state when the x-ray shutter

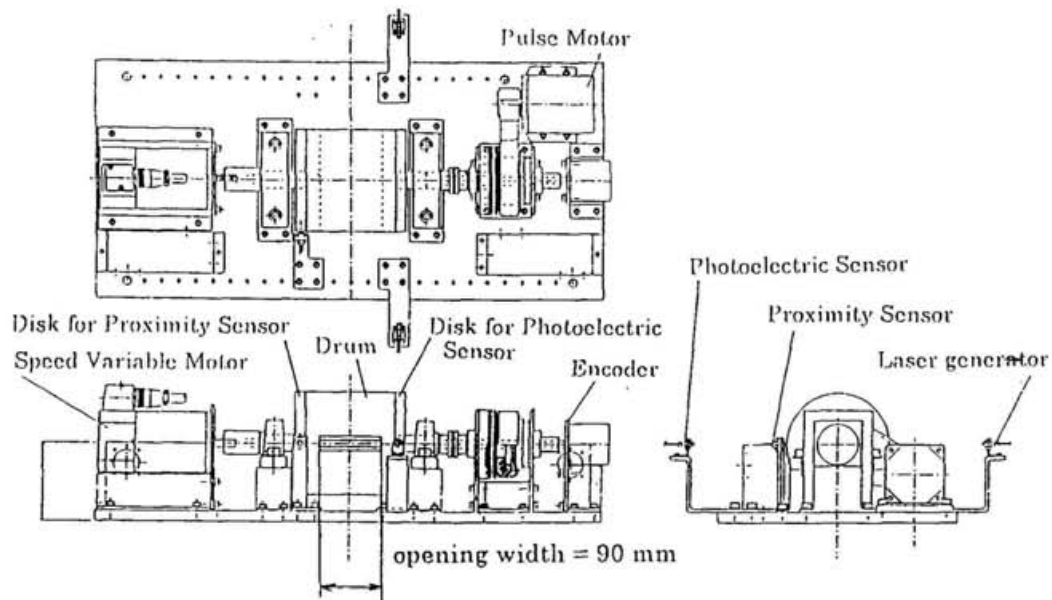


Fig. 28 The rotating x-ray shutter system

The drum is rotated continuously by the speed variable motor. In order to synchronize the timing between the x-rays passing through the x-ray shutter and that of the CCD camera of the II-TV system reading the image signals, the trigger pulses are generated by the three sensors; the photoelectric sensor, the proximity sensor and the digital encoder. A pulse motor is used for deciding shutter drum rotating angle when the x-ray shutter is stopped. After the drum is completely stopped, the drum is controlled to rotate to the closed state.

is stopped. After the drum is completely stopped, the drum is controlled to rotate to the closed state. Even if the x-ray shutter system is stopped by mechanical accidents, the shutter drum shouldn't be kept at the open state, and should be closed promptly in order to avoid useless irradiation to the patients. Input, output, indication and adjustment of the rotating x-ray shutter are shown in Table 3, and specifications of 'open' sensors in use is shown in Table 4.

### 3-2 Safety analysis against thermal load

Safety analysis of the drum to accidental thermal load had to be carried out in order to confirm the safety of the designed drum. It was necessary to confirm that the drum wouldn't melt by the power of synchrotron radiation even in the case of failure in its rotating mechanism. The thermal investigation was carried out using the program code ANSYS for finite element analysis. Considering clinical application at NE1 beamline of the AR in KEK, the total power of the synchrotron radiation was assumed to be 2.96 kW when the ring parameters were 5.0 GeV as the electron beam energy, 70 mA as the electron beam current and 0.93 T as the wiggler magnetic field. As the thermal power of 2.01 kW was absorbed when passing through three beryllium filters with 0.3 mm thickness and an aluminum filter with 1 mm thickness of NE1 beamline, remaining power of 0.95 kW was absorbed at the x-ray shutter drum. The spatial maximum temperature of the drum in the steady state was estimated to be 1,297°C when preceding x-ray shutters may fail and thus synchrotron radiation continuously irradiates onto the stopped x-ray shutter drum, according to the result of the numerical analysis. In this calculation, thermal emission and natural conventional heat transfer are considered. As the melting point of SUS304 is about 1410°C, I found that the x-ray shutter drum would never melt even if it received synchrotron radiation at a certain point over a long period due to rotation failure.

Table 3 Input, Output, Indication and Adjustment of the rotating x-ray shutter

Input	Interlock sequencer ready signal
Output	Trigger pulse $\times$ 3 routes Signal of required drum rotation number Signal when abnormal drum rotation occurs Emergency stop signal
Indication	Required drum rotation number Drum rotation number (rpm and images/sec) 'Open state' sensor Drum stopping angle (only when drum stopping)
Adjustment	Drum rotation number (accuracy 1 rpm) Delay of trigger pulse (accuracy 0.2 msec) Drum stopping angle (accuracy 1 degree)

Table 4 Specifications of used open state sensors

Digital encoder	Rotation angle resolution less than 0.5 degree Response frequency 10 kHz Type E6F-AB3C made by OMRON
Photoelectric sensor	Response time less than 0.25 msec Type FS-L50 & FS-L70 made by KEYENCE
Proximity sensor	Response time less than 1 msec Type EH-110 & ES-X38 made by KEYENCE

### 3-3 Experiment for verification of synchronization

An experiment of the x-ray shutter was carried out at the NE5A beamline of the AR in KEK in order to verify the synchronization between passing of x-rays and sending of the trigger pulses. Synchrotron radiation was monochromatized to 33.17 keV x-rays by (111) silicon double crystal. The x-rays that passed through the x-ray shutter were detected by a PIN diode (HAMAMATSU PHOTONICS, S3584-06) as shown in Fig. 29. When the PIN diode received x-rays, electric current flowed in it, when providing 100 volts to the diode. Voltage signals generated from the current by a circuit. The signals from the PIN diode were compared with those of trigger pulse from the rotating shutter on an oscilloscope to analyze their temporal relation. With adjustment of trigger pulse delay, I found that x-ray pulse and the trigger pulse could be adjusted to synchronize completely as in Fig. 30. In the experiment at NE5A beamline,  $t_s$  was 4.6 msec, as shown in Fig. 30, because of the difference of beam heights  $h_b$  (3 mm at NE5A, while the expecting period was 4.0 msec for 7 mm at NE1). Synchronization of trigger pulse with x-ray pulse was verified from this result.

### 3-4 Application for clinical examination

The rotating x-ray shutter was installed in NE1 beamline for clinical application. (Hyodo K. et al. to be published, Ohtsuka S. et al. to be published) The arrangement of equipment is shown in Fig. 31. Synchrotron radiation was monochromatized by the silicon crystal, after passing through the rotating x-ray shutter. Photon energy of 35 keV was selected for the clinical examinations because of relatively lower photon numbers at the third higher harmonic. A parallel plate ionization chamber which consisted of three of 25  $\mu$  m of Mylar and 100  $\mu$  m of acetate film was inserted in the beamline to monitor the irradiation just upstream of the patient. The ionization chamber was developed by Dr. J. Tada of Spring-8 (Oku Y. et al. submitted). The radiation dose was monitored by the ionization chamber. The monochromatic x-rays that passed the ionization chamber and the patient were detected by the imaging system.

The purpose of the monitoring is to measure the skin dose of the patient to

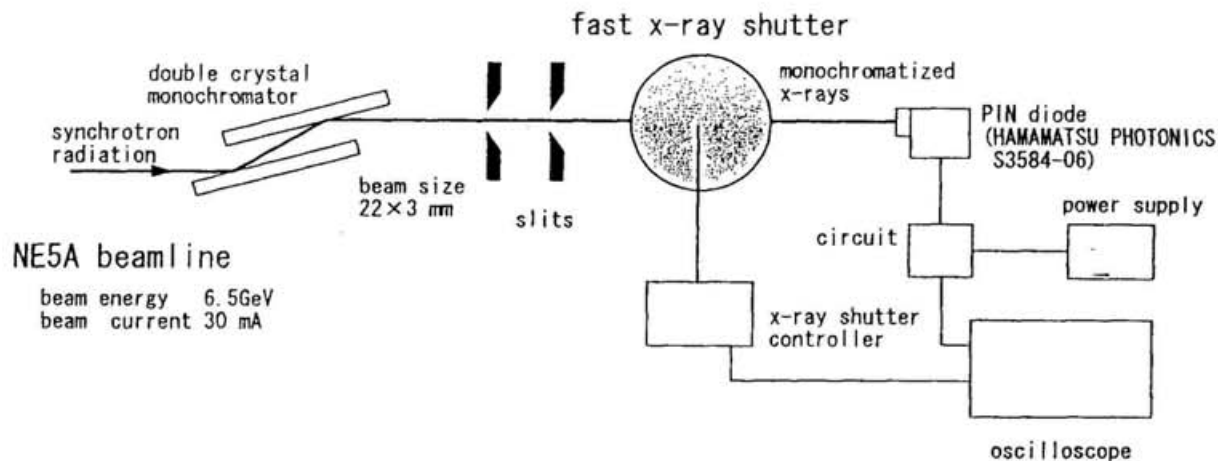


Fig. 29 The arrangement of x-ray shutter experiment  
 Synchrotron radiation was monochromatized to 33.17 keV x-rays by Si (111) double crystal monochromator. The x-rays passed through the x-ray shutter and reached a PIN diode. When the PIN diode received x-rays, electric current flowed in it, when providing 100 volts to the diode. The current was changed to voltage signals by a circuit. The signals were taken into an oscilloscope as well as the trigger pulse from x-ray shutter controller, and they were compared.

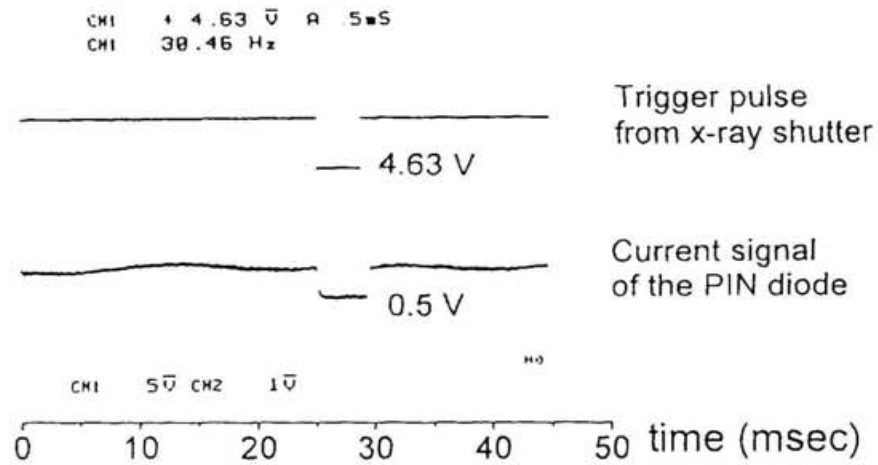


Fig. 30 Synchronizing of the trigger pulse from x-ray shutter controller with current signal of the PIN diode by x-rays passing through the shutter. With adjustment of trigger pulse delay, it is found that x-ray passing and the trigger pulse were completely synchronized.

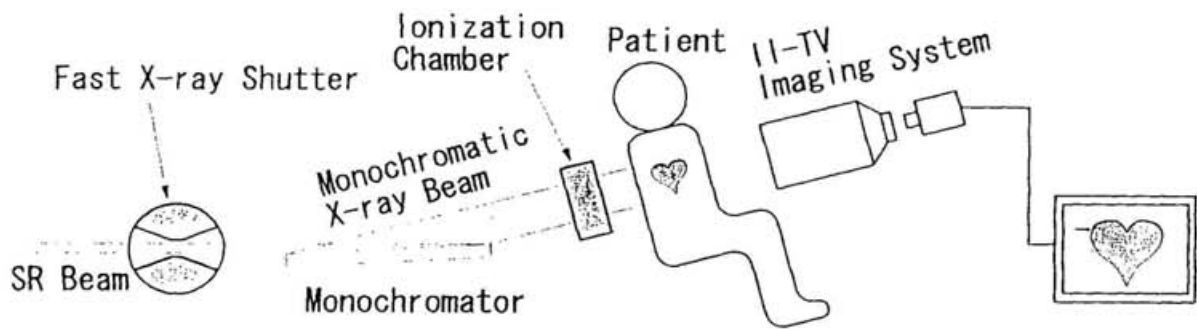


Fig. 31 Arrangement of equipment for clinical application of SR coronary angiography ( Hyodo K. et al. to be published )  
 Synchrotron radiation was monochromatized by the silicon crystal monochromator after passing through the rotating x-ray shutter. The monochromatic x-rays went up to an ionization chamber. The radiation dose was monitored by the ionization chamber. The monochromatic x-rays passed the ionization chamber and the patient, and reached the imaging system.

prevent over exposure. When the dose exceeds the prescribed value, the 'dose interlock system' interrupts the ring current immediately.

The exposure of monochromatic photons is defined as equation (12):

$$X = \Psi_{\gamma} \cdot \left(\frac{\mu_{en}}{\rho}\right)_{air} \cdot \frac{e}{W_{air}} \quad (12)$$

- $X$  : exposure ( C /kg )  
 $\Psi_{\gamma}$  : energy fluence of photons( J / m<sup>2</sup> )  
 $\left(\frac{\mu_{en}}{\rho}\right)_{air}$  : mass energy absorption coefficient of air ( m<sup>2</sup> / kg )  
 $e$  : elementary electric charge  
 $W_{air}$  : W value of air ( J )

Where energy fluence  $\Psi_{\gamma}$  of monoenergetic photons is represented as equation (13):

$$\Psi_{\gamma} = h \nu \cdot \phi \cdot t \quad (13)$$

- $h \nu$  : photon energy ( J )  
 $\phi$  : photon fluence rate ( photons  $\cdot$  sec<sup>-1</sup>  $\cdot$  m<sup>-2</sup> )  
 $t$  : irradiation period ( sec )

The value of the exposure per frame of image and per normalized storage ring current (1 mA) can be calculated by the above equations in C/kg  $\cdot$  image<sup>-1</sup>  $\cdot$  mA<sup>-1</sup>.

As the exposure was monitored for each patient by ionization chamber in the clinical application, the value of exposure per one image and 1 mA of electron storage ring current can be given by dividing monitored exposure by the number of corresponding images and the ring current during the measurement. The image number per each patient could be counted by reading out from a video image later.

As the calculated photon fluence rate of the x-rays whose energy was 35 keV per 1 mA of ring storage current in front of the ionization chamber was  $2.4 \times 10^{14}$  photons  $\cdot$  m<sup>-2</sup>  $\cdot$  sec<sup>-1</sup>, the calculated value of exposure with 4 msec of irradiation

period per one image was  $1.4 \times 10^{-6} \text{ C/kg} \cdot \text{image}^{-1} \cdot \text{mA}^{-1}$ , while the monitored values of the exposure ranged from  $1.0 \times 10^{-6}$  to  $1.3 \times 10^{-6} \text{ C/kg} \cdot \text{image}^{-1} \cdot \text{mA}^{-1}$ . Parameters in the clinical application are shown in Table 5 ( Hyodo K. et al. to be published, Ohtsuka S. et al. to be published ). As the average value of monitored exposure was about 20% less than the estimated value from photon fluence, it was found that the rotating x-ray shutter worked properly and could have restrained the patient dose at the design concept value.

The images for diagnosis were taken without motion blur by heart beat and flicker due to a time lag between x-ray pulses and image reading of TV system in the clinical applications (Hyodo K. et al. to be published, Ohtsuka S. et al. to be published).

Table 5 Parameters in the clinical application ( Hyodo K. et al. to be published )

Beam energy of storage ring AR	5.0 GeV,
NE1 wiggler gap	40 mm
Monochromatic x-ray beam energy	35 keV
X-ray beam size magnification by asymmetric monochromator diffraction	17.4
Al, Be filter thickness and Air pass length	1 mm, 0.9 mm, 5000 mm
Average reflection ratio of monochromator	45%
Energy band width of monochromatic x-rays	0.3%
Device type	multipole wiggler (43 pole)
Device magnetic field	0.79 T
Critical energy of SR	13 keV
Original beam size of SR before the shutter	$80^w \times 7^h$ mm

#### 4. Proposal of an optimized system for intravenous angiography using synchrotron radiation source

##### 4-1 Fixing the basic specifications

The S/N ratio of images by quantum noise is given by;

$$S/N = \frac{I}{\sqrt{I}}, \quad (14)$$

where  $I$  is the photon flux injected into one pixel. The quantum noises per signal should be sufficiently smaller than the contrast of the artery images. Simulation images with various S/N ratios were made by the developed image-simulation program, and investigated. The necessary maximum S/N ratio was chosen based on this investigation. The value of the ratio of the artery shadow depth (a-b in Fig. 15) with which 1% concentration of iodine in weight, against the standard deviation of quantum noise, was decided. If the value of the ratio was 1, the artery shadow could not be completely distinguished in the image; thus, the minimum value was chosen to be 2. The S/N ratio was determined based on the ratio of the artery shadow depth against the standard deviation of the quantum noise to be 60 from Fig. 32. Simulation images and their profiles with various value of the S/N ratio are shown in Figs. 33 and 34. From the S/N ratio, necessary photon flux ( $I$ ) of 3600 into a pixel was obtained by Eq.(14). The necessary total photon flux of 33.17 keV, the iodine K-edge energy, in front of the detector was obtained from the above  $I$  and the ideal exposure area of 150 mm  $\times$  150 mm for coronary angiography; it was  $2.0 \times 10^9$  photons/image considering a pixel size of 0.2 mm.

On the other hand, the contrast deterioration of the images due to 99.51 keV photons, the third higher harmonic, was investigated. The analyzed artery contrast, ((a-b)/a in Fig. 15) against the ratio of 99.51 keV per 33.17 keV photons in front of the phantom is shown in Fig. 35. The incident x-ray beam size was 150 mm  $\times$  150 mm. The acrylic thickness was 160 mm, the distance between the acrylic and the detector was 100 mm, the artery diameter was 5 mm, and the concentration of iodine in weight was 5%. It was found that the contrast improvement became remarkable if 99.51 keV portion is less than 1 %.

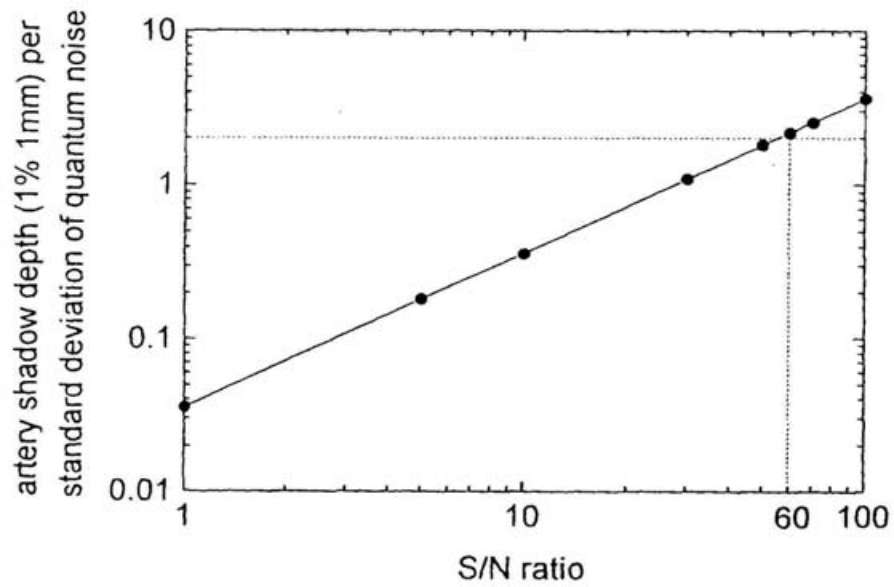
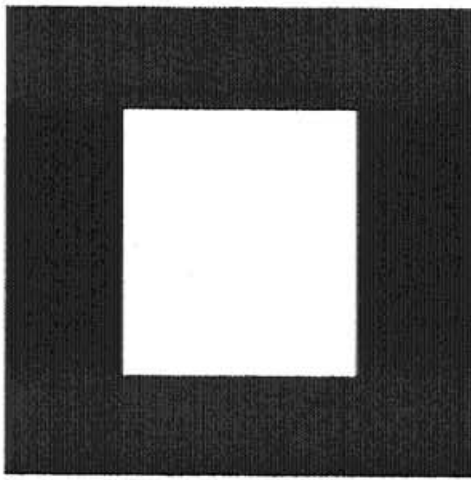
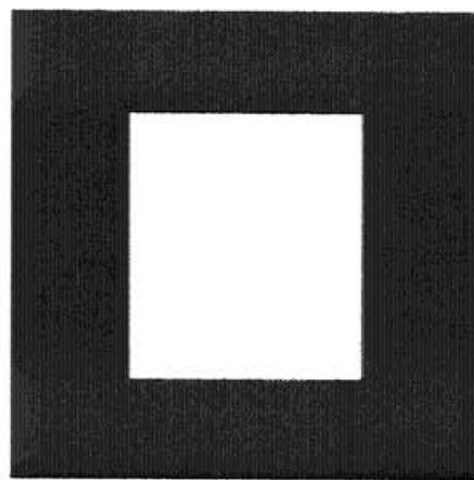


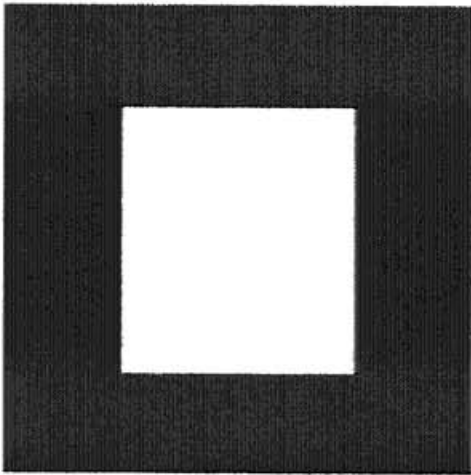
Fig. 32 Artery shadow depth (1% concentration iodine in weight and 1 mm diameter ) against the standard deviation of the quantum noise calculated from the photon flux injected into one pixel, as a function of the S/N ratio of the quantum noise.



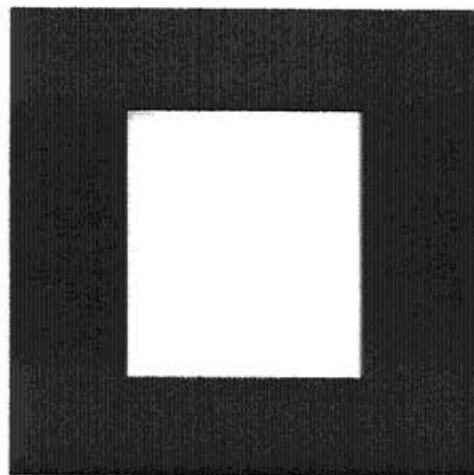
$S/N = 100$



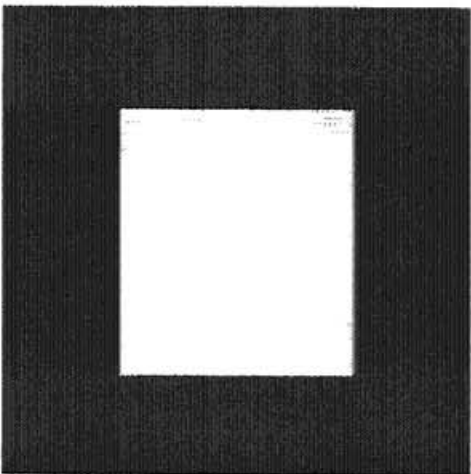
$S/N = 70$



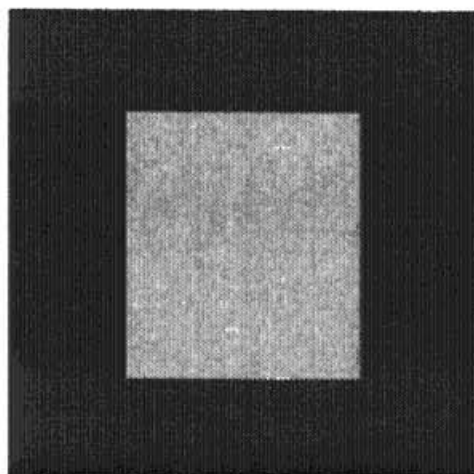
$S/N = 60$



$S/N = 50$



$S/N = 30$



$S/N = 10$

Fig. 32 Simulation images with various values of the S/N ratio

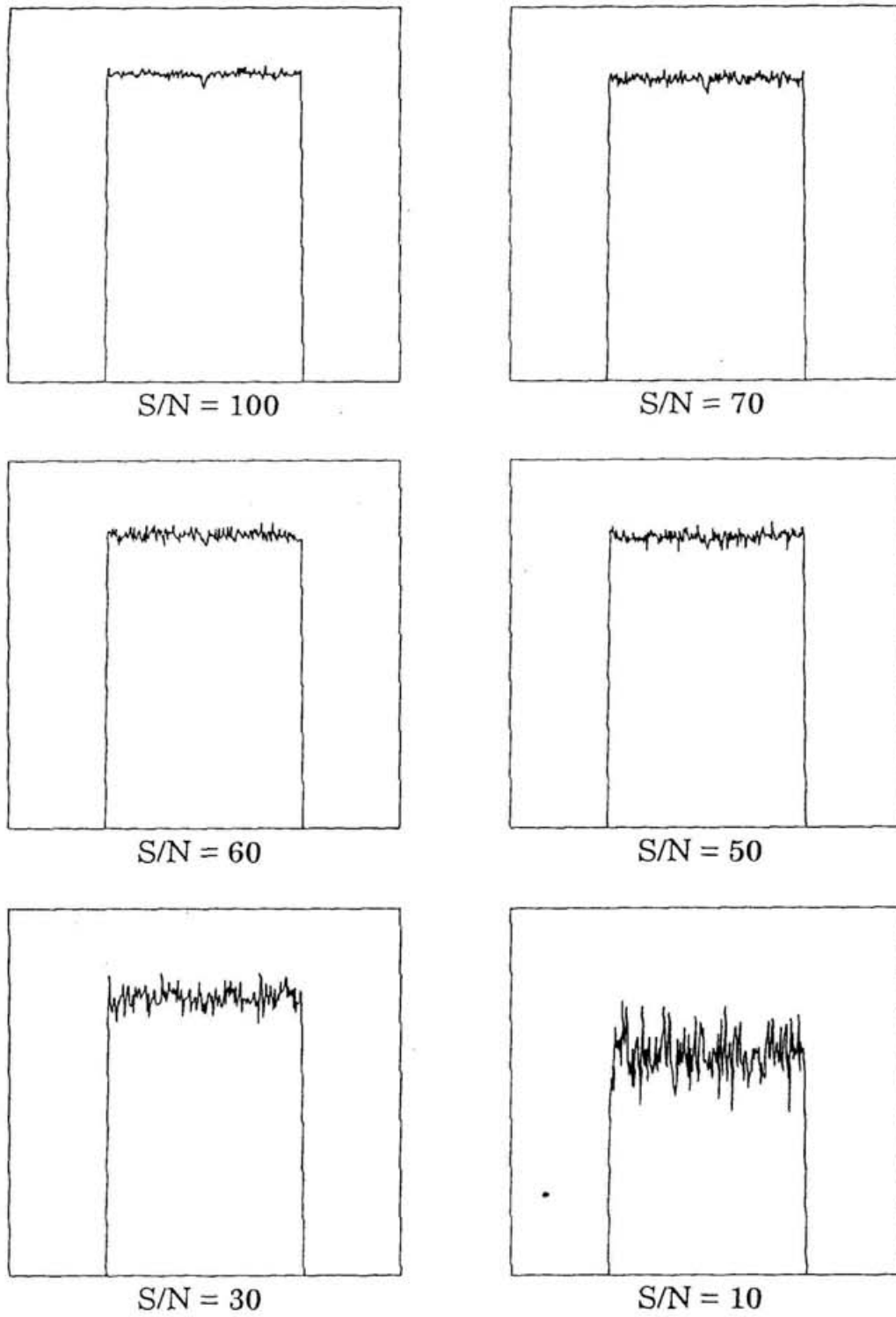


Fig. 34 Simulation image profiles with various values of the S/N ratio

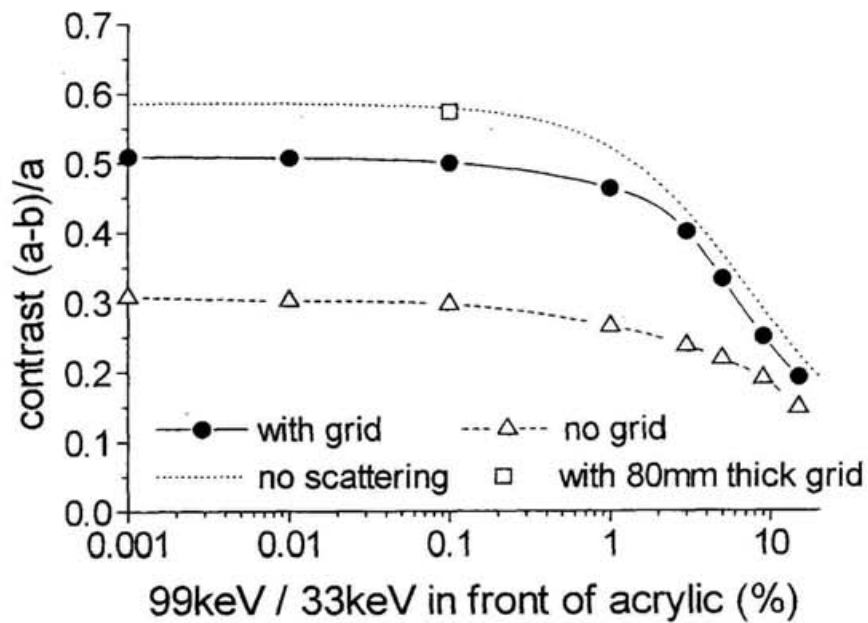


Fig. 35 Artery contrast  $((a-b)/a)$ , as a function of the ratio of the third higher harmonics photon flux against 33.17 keV photons in front of the phantom in the case of the 150 mm  $\times$  150 mm beam required by medical doctors. The acrylic thickness is 160 mm, the distance between acrylic and the detector is 100 mm, the artery diameter is 5 mm, and the concentration of iodine in weight is 5%.

Furthermore, the contamination ratio of the third higher harmonic should be 0.1%, because the contrast when using an x-ray grid was saturated at that point.

At a radiation source, necessary total photon flux of 33.17 keV is  $9.7 \times 10^{11}$  photons/image of the total photons per 4 msec and allowed contamination of the 99.51 keV photons against the 33.17 keV photons is 0.18%, considering photon attenuation process due to passing through three elements such as a beryllium filter with a total 1 mm thickness, an aluminum filter with a 1 mm thickness and across 4 m of air, and the diffraction process at the monochromator. Allowed maximum critical energy of 9.0 keV was obtained from the above allowed contamination of 99.51 keV of 0.18%. While, a stored electron beam current of 500 mA and the number of pole of a superconducting wiggler of 5 were determined as reasonable values with current technologies. From the values of the critical energy, the beam current and the number of the wiggler poles, the electron beam energy to obtain the necessary photon flux of 33.17 keV was determined to be 1.5 GeV. Magnetic field of the wiggler was determined to be 6.0 T by the critical energy and the beam energy. The specifications of the radiation source for SR coronary angiography can be obtained from the necessary photon flux and irradiation period per one image, and the maximum contamination of the third higher harmonic. They are shown in Table 6.

#### 4-2 Design of the storage ring

A conceptual electron storage ring dedicated to coronary angiography to meet the above basic specifications as in Table 6, was designed using the program SAD of KEK (Oide K. et al. since 1986). The Chasman-Green type was adopted as a lattice, because dispersion suppression on the insertion device was easily avoidable of so much emittance growth by exciting the insertion device. The lattice of the designed ring is shown in Fig. 36. Superconducting bending magnets and a wiggler as an insertion device with a field of 4 T and 6 T were adopted. A wiggler with 6 T magnetic field is possible to manufacture (Huke K. et al. 1980, Sugiyama S. et al 1992). The twiss parameters are shown in Fig. 37. The vertical beta functions at the wiggler were set to be small in order to make the wiggler gap as small as possible. The horizontal beta functions at the injector

Table 6 Basic parameters of the radiation source for SR coronary angiography

beam energy	1.5 GeV
magnetic field of insertion device	6.0 T
pole number of insertion device	5 pole
beam current	500 mA

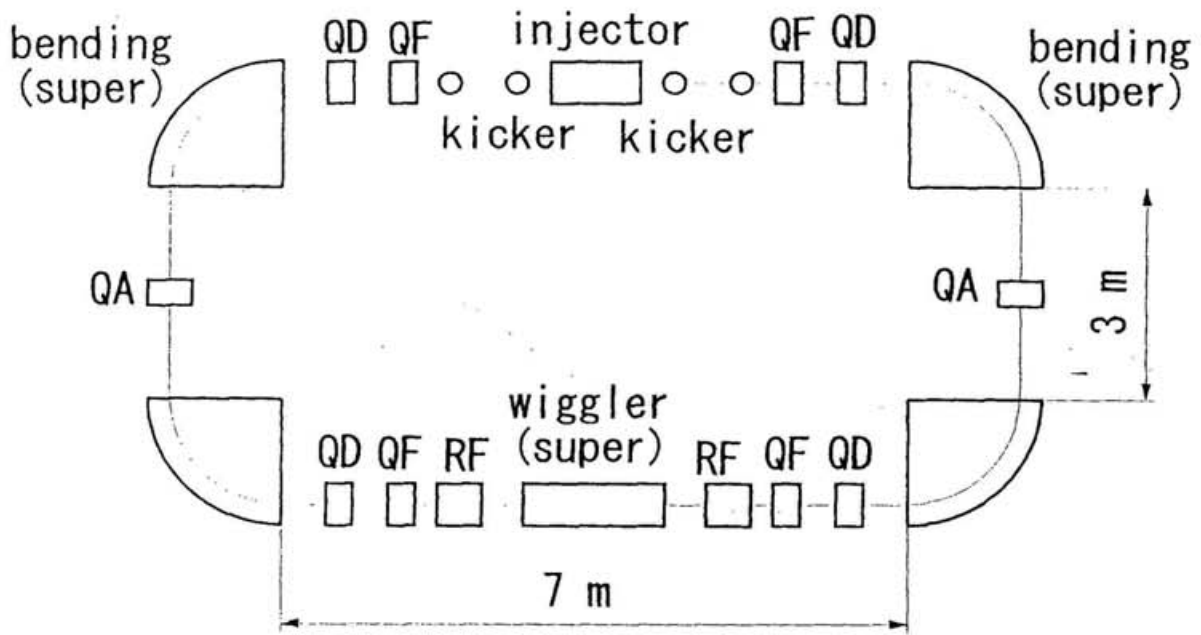


Fig. 36 Lattice of the designed electron storage ring dedicated to SR coronary angiography

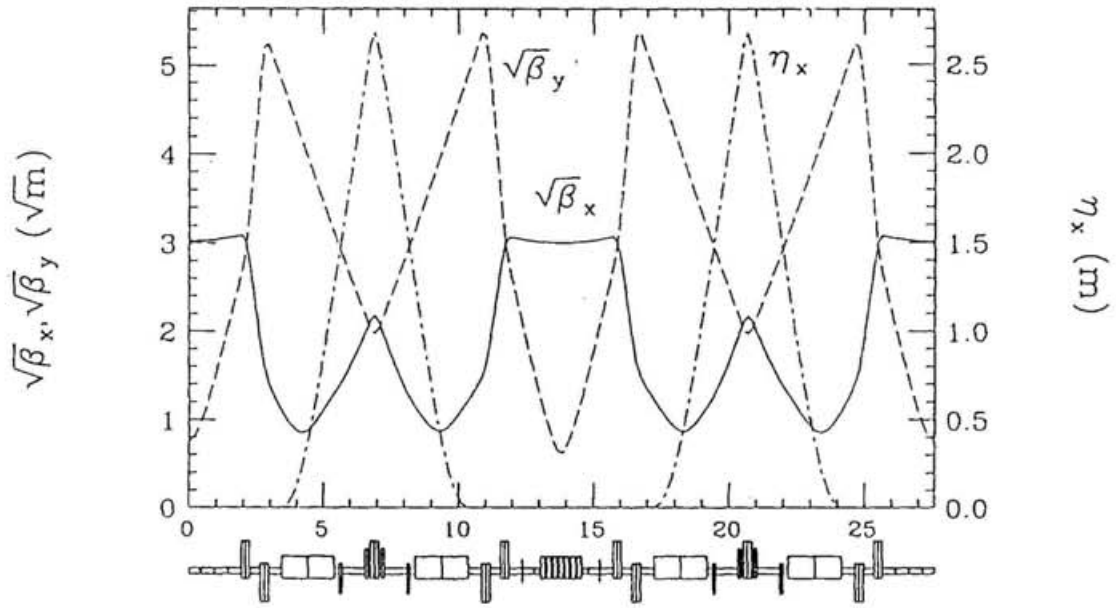


Fig. 37 Twiss parameters of the designed ring

were set to be relatively large in order to make the acceptance at the injection point large. Sextupole magnets were set between the QA magnets and the bending magnets. The dynamic aperture at the injection point is shown in Fig. 38. Based on an assumption that the horizontal and vertical beam size there are 4.22 mm and 0.11 mm, the dynamic aperture is sufficiently wide. The parameters of the ring are given in Table 7. The emittance was set to be relatively large in order to make the storage beam current as large as possible. The synchrotron radiation spectrum of the above-designed medical ring is shown in Fig. 39 with one of AR NE1 under the condition of the first clinical application. They are the total photon number per second when using a lapped single monochromator (integrated intensity of diffracted photons = 0.3% at 33.17 keV). The 33.17 keV photon number of the medical ring was more than that for the AR NE1 clinical application, while 99.51 keV, the harmful third higher harmonic, is opposite.

#### 4-3 Optical Element

A lapped crystal monochromator (Shiwaku H. et al. 1991, Shiwaku et al. 1992, Shiwaku H. 1992) was used for two-dimensional SR coronary angiography in order to obtain a high integrated intensity diffracted from it. Thus, the third higher harmonic was also diffracted and injected into the detector. Since it deteriorates the image contrast, a ratio of its intensity against 33.17 keV should be as small as possible. Thus, a storage ring whose clinical energy of synchrotron radiation is relatively small is suitable for coronary angiography. On the other hand, a multi-layer monochromator is effective for suppressing the third higher harmonic. However, its current technology does not give sufficient image quality for two-dimensional imaging; it is still under development. If the gadolinium is used as a contrast agent, since its K-edge energy is 50.24 keV, the size of a crystal monochromator will be extremely large due to its very small diffraction angle. In this study, a lapped Si (311) crystal which is available was selected as a monochromator.

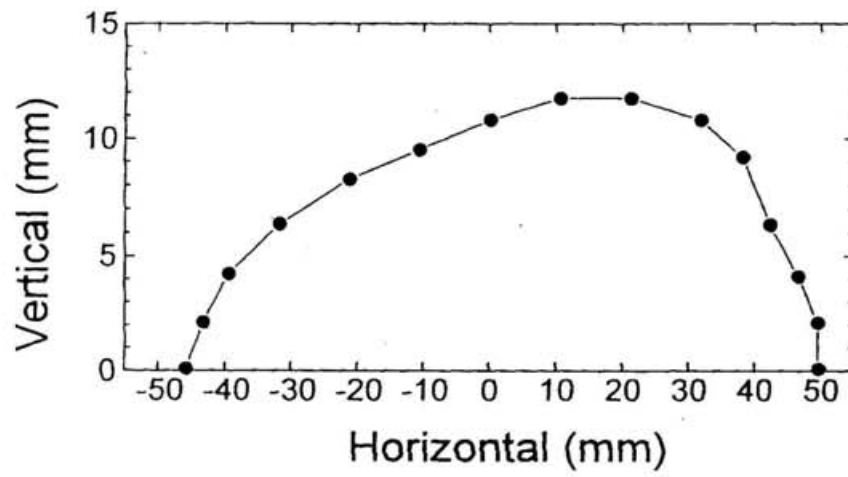


Fig. 38 Dynamic aperture at the injection point

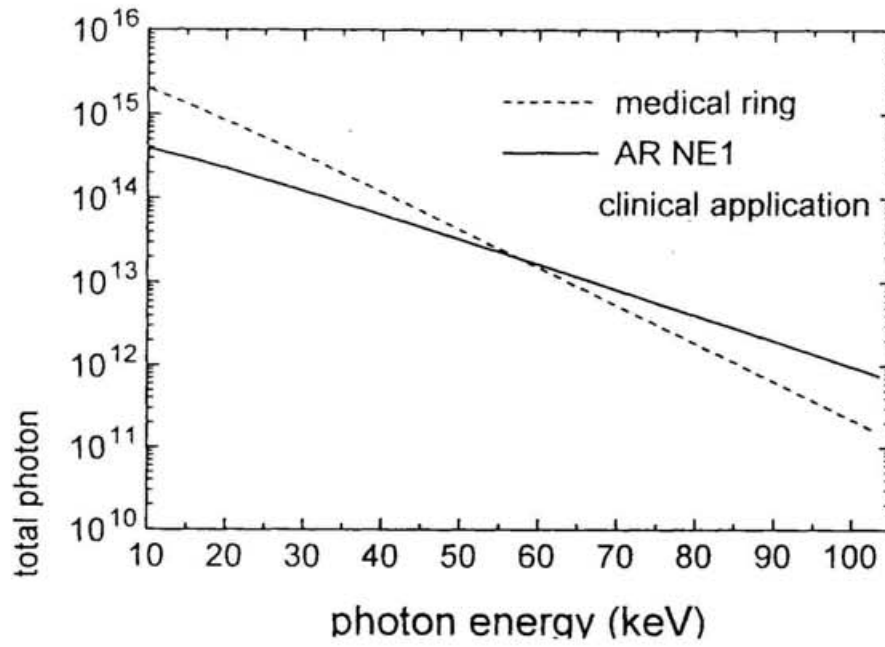


Fig. 39 Synchrotron-radiation spectrum of the above-designed medical ring and of AR NE1 under the condition of the first clinical application of two-dimensional SR coronary angiography

Table 7 Parameters of the storage ring

beam energy	1.5 GeV
beam current	500 mA
magnetic field of insertion device	6.0 T
pole number of insertion device	5 pole
magnetic field of bending magnet	4.0 T
bending radius	1.25 m
bending angle	90°
quadrupole magnet length	30 cm
sextupole magnet length	10 cm
natural emittance	1,970 nm · rad
xy coupling	0.1
beam size $\sigma_x$ at wiggler & injector	4.2 mm
beam size $\sigma_y$ at wiggler & injector	0.1 mm
betatron tune $\nu_x, \nu_y$	2.150, 1.197
radiation energy loss per turn	428 keV
RF frequency	500 MHz
RF voltage per cavity	700 kV
quadrupole magnet field	
QF	13.1, 12.6 T/m
QD	14.6, 14.5 T/m
QA	12.6 T/m
sextupole magnet field	
SF	75.2 T/m <sup>2</sup>
SD	154.8 T/m <sup>2</sup>

#### 4-4 Contrast agent

Iodine is usually used as a contrast agent in x-ray examinations of arteries at hospitals, and was used in the clinical application of coronary angiography using synchrotron radiation (Hyodo K. et al. to be published, Ohtsuka S. et al. to be published). Thus, iodine was adopted as a contrast agent in this image simulation. Recently, the contrast agent of gadolinium has been developed for an NMR examination (Creasy J. L et al. 1990). However, the concentration is very low compared to that of iodine, because of high viscosity of gadolinium. The iodine concentration of the contrast material in clinical coronary angiography using synchrotron radiation was about 5~10% in weight at the coronary arteries (Hyodo K. private communications), and the concentration of gadolinium in the usual NMR examination was less than 1% in weight (Yamasaki K. private communications). Thus, it is difficult to be used in x-ray examinations. If a higher concentration of the gadolinium contrast agent for injection into arteries is developed, it could be effective. Since the K-edge energy of gadolinium is 50.24 keV, a lower exposure to patients is available using monochromatic x-rays of 50.24 keV because of its higher penetration. The differences in the image contrast and exposure between iodine and gadolinium were investigated. The contrast of the artery is obtained by

$$C = 1 - e^{-\mu \rho L}, \quad (14)$$

where  $C$  is the contrast,  $\mu$  is the mass attenuation coefficient ( $\text{cm}^2/\text{g}$ ),  $\rho$  is the density ( $\text{g}/\text{cm}^3$ ), and  $L$  is the contrast material path length (cm).

The image contrast when using iodine and gadolinium as contrast materials is given in Table 8. The absorbed energy of attenuated x-rays in the patient's body and the exposure dose per frame are given in Tables 9 and 10. The absorbed energy is given from attenuated x-ray photon number. The exposure is given by equations (12),(13). In the intravenous digital subtraction angiography (DSA) of carotid artery or renal artery at hospitals, 450 frames of images are taken in one imaging of 15 sec, and three imaging from different directions are done in one examination generally. Total exposure with 1,350 frames (450

Table 8 Contrast of an artery filled by a diluted contrast material

Contrast Material	K-edge Energy (keV)	Mass Att. Coefficient (cm <sup>2</sup> /g)	Density (g/cm <sup>3</sup> )	Att. Coefficient (cm <sup>-1</sup> )	Concentration in Volume (%) *1	Contrast Material Pass Length (cm) *2	Contrast
Iodine	33.17	35.8	4.93	176.5	1.0	$1.0 \times 10^{-3}$	0.162
Gadolinium	50.24	18.1	7.90	143.0	0.66	$6.6 \times 10^{-4}$	0.090

\*1 Concentration of contrast material in weight in coronary arteries is 5 %.

\*2 Diameter of artery is 1 mm.

Table 9 Absorbed energy of attenuated x-rays in the patient's body

Contrast Material	K-edge Energy (keV)	H <sub>2</sub> O Mass Att. Coefficient (cm <sup>2</sup> /g)	Attenuation *1	Incident Photon No. *2	Absorbed photon No.	Absorbed Energy (J)
Iodine	33.17	0.328	$5.26 \times 10^{-3}$	$3.85 \times 10^{11}$	$3.83 \times 10^{11}$	$2.03 \times 10^{-3}$
Gadolinium	50.24	0.226	$2.69 \times 10^{-2}$	$4.56 \times 10^{10}$	$4.44 \times 10^{10}$	$3.57 \times 10^{-4}$

\*1 Body thickness (water equivalent) is 160 mm.

\*2 Incident photon No. per pixel is 3600, in order to obtain an S/N ratio of 60. Total pixel No. is  $5.625 \times 10^5$ , because the exposure area is 150 mm  $\times$  150 mm and the pixel size of the detector is 0.2 mm  $\times$  0.2 mm. Thus, the total incident photon No. to the detector is  $2.025 \times 10^9$ . The response of the detector (II) at 50.24 keV is 1.65 times as that at 33.17 keV. Thus, the total incident photon No. to the detector is  $1.2273 \times 10^9$  when gadolinium is used as the contrast agent.

Table 10 Exposure of the patient per frame

Contrast Material	K-edge Energy (keV)	Energy Fluence (J / m <sup>2</sup> )	Mass Energy Att. Coefficient (m <sup>2</sup> / kg)	Exposure (C /kg)	Exposure (mR)
Iodine	33.17	0.0908	$8.8 \times 10^{-3}$	$2.37 \times 10^{-5}$	91.8
Gadolinium	50.24	0.0163	$4.1 \times 10^{-3}$	$1.98 \times 10^{-6}$	7.67

frames  $\times$  3 directions) is  $3.5 \times 10^{-2}$  C/kg, because the exposure per frame is about  $2.6 \times 10^{-5}$  C/kg. (Hyodo K. private communication) In case of intravenous coronary angiography using SR from the proposed electron storage ring with iodine as a contrast agent, the exposure per frame is  $2.37 \times 10^{-5}$  C/kg from Table 10. Total exposure in an examination with the same frames as DSA (1,350 frames) is  $3.2 \times 10^{-2}$  C/kg. This exposure is less than usual DSA exposure of  $3.5 \times 10^{-2}$  C/kg.

#### 4-5 Penumbra

When the light-source size is finite, and rays are not parallel, a penumbra is generated in the images, as in Fig. 24. The penumbra size is proportional to the ray beam divergence, and is limited by the projection angle of the beam-source size. In the case of imaging by monochromatic x-rays from synchrotron radiation, the penumbra size is generally negligible, because the beam has a very small divergence. However, the divergence of the diffracted beam is larger in the case of coronary angiography using synchrotron radiation, because a lapped silicon monochromator is used to obtain a high integrated intensity of the x-ray beam. The FWHM of 33.17 keV monochromatic x-rays diffracted by Si(311) with an asymmetric angle of 5 degrees lapped by #1200 abrasives is about 15 arcsec (Shiwaku H. 1992). The angle equals 0.073 mrad. When a white synchrotron radiation beam was monochromatized to 33.17 keV by a Si(311) asymmetric monochromator, the spectral width of diffracted x-rays was 75 eV, as in the experiment at the AR NE5A beamline by Hyodo et al (Hyodo K. private communications). The spectral width is equivalent to 0.27 mrad. The convolution divergence angle ( $\theta_m$ ) of the monochromatic beam's FWHM, and the spectral width of the white beam is 0.35 mrad. The total beam divergence ( $\theta_t$ ) is obtained by the sum of this divergence angle ( $\theta_m$ ) generated at the monochromator and the divergence angle ( $\theta_s$ ) of the original x-ray beam. The horizontal and vertical divergence angles of the irradiated x-ray beam are given in Table 11.

In the case of the first clinical application of SR coronary angiography at the AR NE1 beamline, the horizontal and vertical divergence angles are both less

Table 11 Divergence angles of the x-ray beam

	Beam size $2\sigma_x$ (mm)	Beam size $2\sigma_y$ (mm)	Beamline length (m)	Horizontal $\theta_x$ (mrad)	Vertical $\theta_y$ (mrad)	Horizontal $\theta_t$ (mrad)	Vertical $\theta_l$ (mrad)
AR NE1	2.0	0.16	40	0.05	0.004	0.4	0.354
medical ring	8.5	0.22	10	0.85	0.022	1.2	0.372

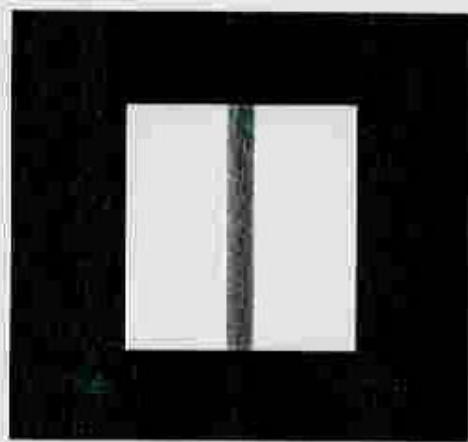
than 0.4 mrad. In the case of a medical ring dedicated to coronary angiography, the horizontal divergence angle is more than 1 mrad.

Using the developed image simulation program, artery images with an injection beam divergence were generated. They are shown in Figs. 40 and 41. The distance between the acrylic and the detector is 500 mm, and the injecting angle in the horizontal plane is chosen according to the normal distribution. The twice of the standard deviation ( $2\sigma$ ) of the normal distribution is from 0 to 1.2 mrad. The differential values of the image profile of Figs. 40 and 41 around the artery are shown in Figs. 42 and 43.

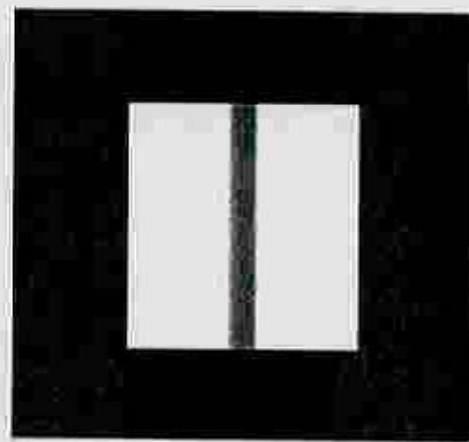
When the standard deviation of the divergence of the incident beam was 0.4 mrad, the penumbra of the artery image was conspicuous. However, when the standard deviation of the injection beam divergence was 1.2 mrad, the edge of the artery image was obviously gradated. Thus, in the case of the clinical application at the AR NE1, although the penumbra was negligible, it deteriorated the image visibility in the case of an examination using the dedicated ring, if the distance from the patient and the detector was set at 500 mm. The images and differential values of the image profile with a distance between the patient and the detector of 100 mm in the case of the standard deviation of the photon-injecting angles of 1.2 mrad (in the case of the medical ring) are shown in Fig. 44. Negligible small penumbra were obtained from the images. Therefore, in the case of using such a dedicated ring, the distance between the patient and the detector should be 100 mm.

#### 4-6 Detector

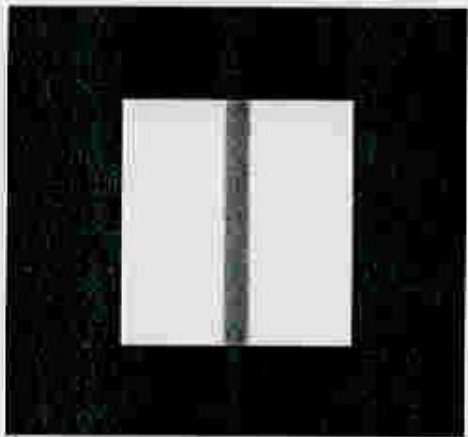
In this study, an image intensifier TV system was adopted as an x-ray detector for coronary angiography. An image intensifier is suitable for dynamic x-ray imaging, and is used in hospitals as an x-ray examination detector. However, the response of the third higher harmonic (99.51 keV) of the image intensifier is greater than that of 33.17 keV x-rays, as in Fig. 20. Thus, the harmful third higher harmonic is relatively enhanced in the images. When using the imaging plate (IP), its response at 99.51 keV against 33.17 keV is smaller than 1, ( Ito M. et al. 1991 ) and its spatial resolution is higher than that



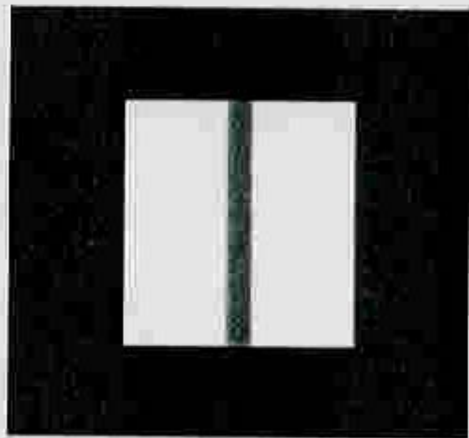
$2\sigma = 0$  mrad



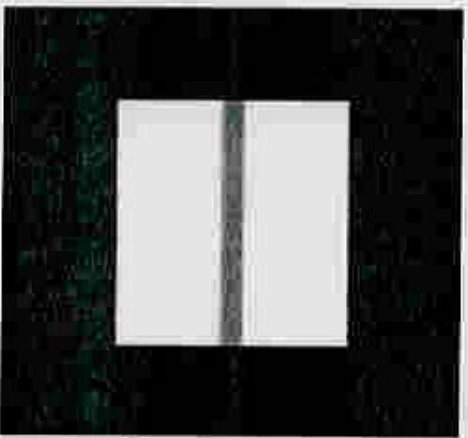
$2\sigma = 0.4$  mrad



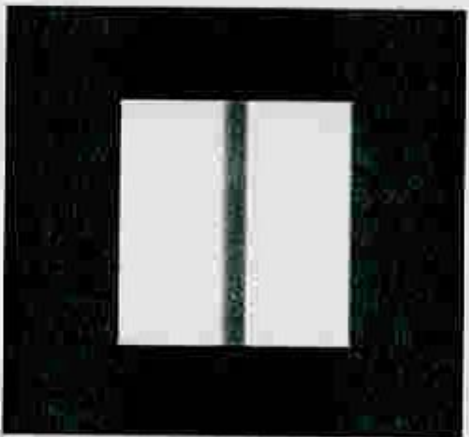
$2\sigma = 0.6$  mrad



$2\sigma = 0.8$  mrad

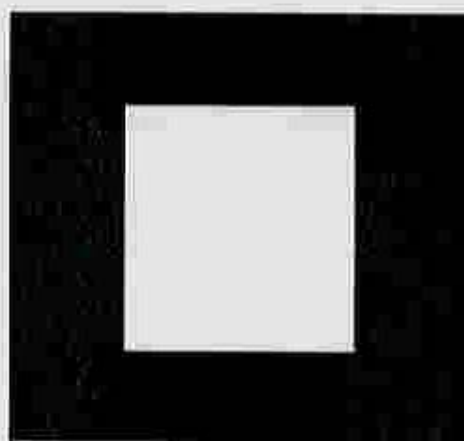


$2\sigma = 1.0$  mrad

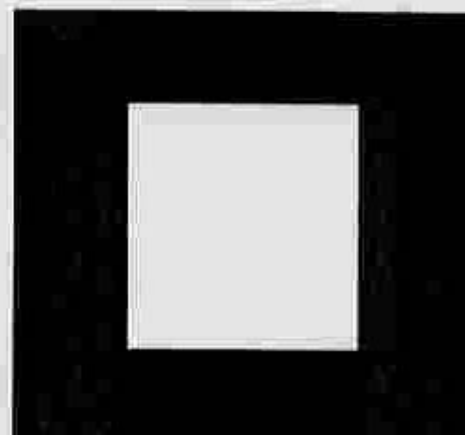


$2\sigma = 1.2$  mrad

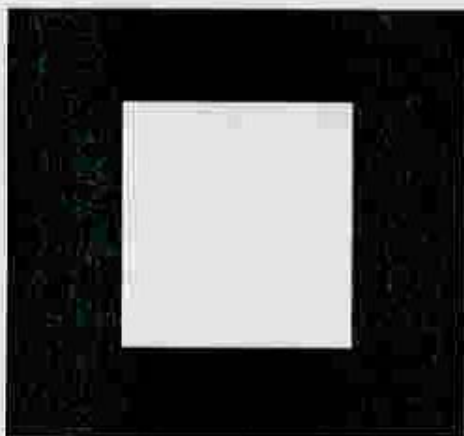
Fig. 40 Simulated images of arteries by 33.17 keV x-ray beams which have various divergences. The distance between the acrylic and the detector is 500 mm, and the injecting angle in the horizontal plane is chosen according to the normal distribution. Twice of the standard deviation ( $2\sigma$ ) of the normal distribution is from 0 to 1.2 mrad. The artery diameter is 5 mm.



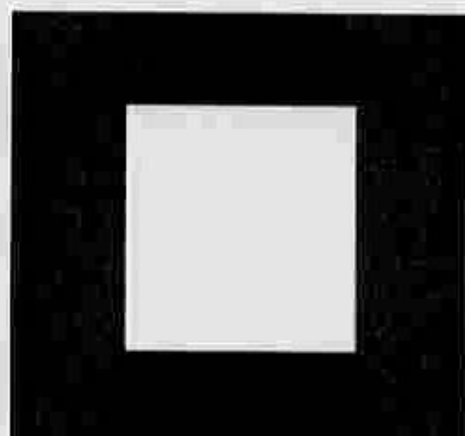
$2\sigma = 0$  mrad



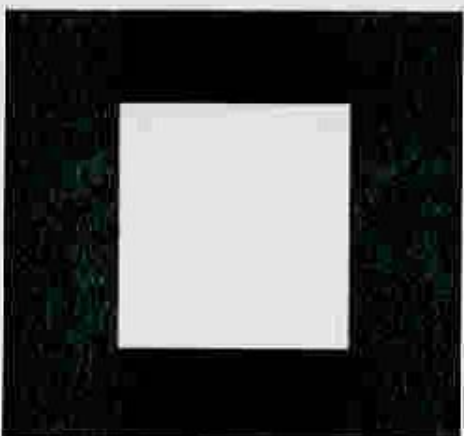
$2\sigma = 0.4$  mrad



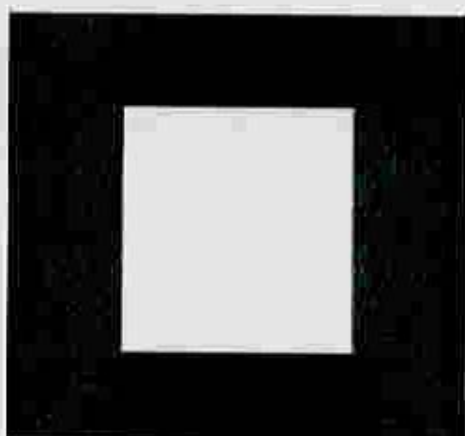
$2\sigma = 0.6$  mrad



$2\sigma = 0.8$  mrad



$2\sigma = 1.0$  mrad



$2\sigma = 1.2$  mrad

Fig. 41 Simulated images of arteries by 33.17 keV x-ray beams which have various divergences. The distance between the acrylic and the detector is 500 mm, and the injecting angle in the horizontal plane is chosen according to the normal distribution. Twice of the standard deviation ( $2\sigma$ ) of the normal distribution is from 0 to 1.2 mrad. The artery diameter is 1 mm.

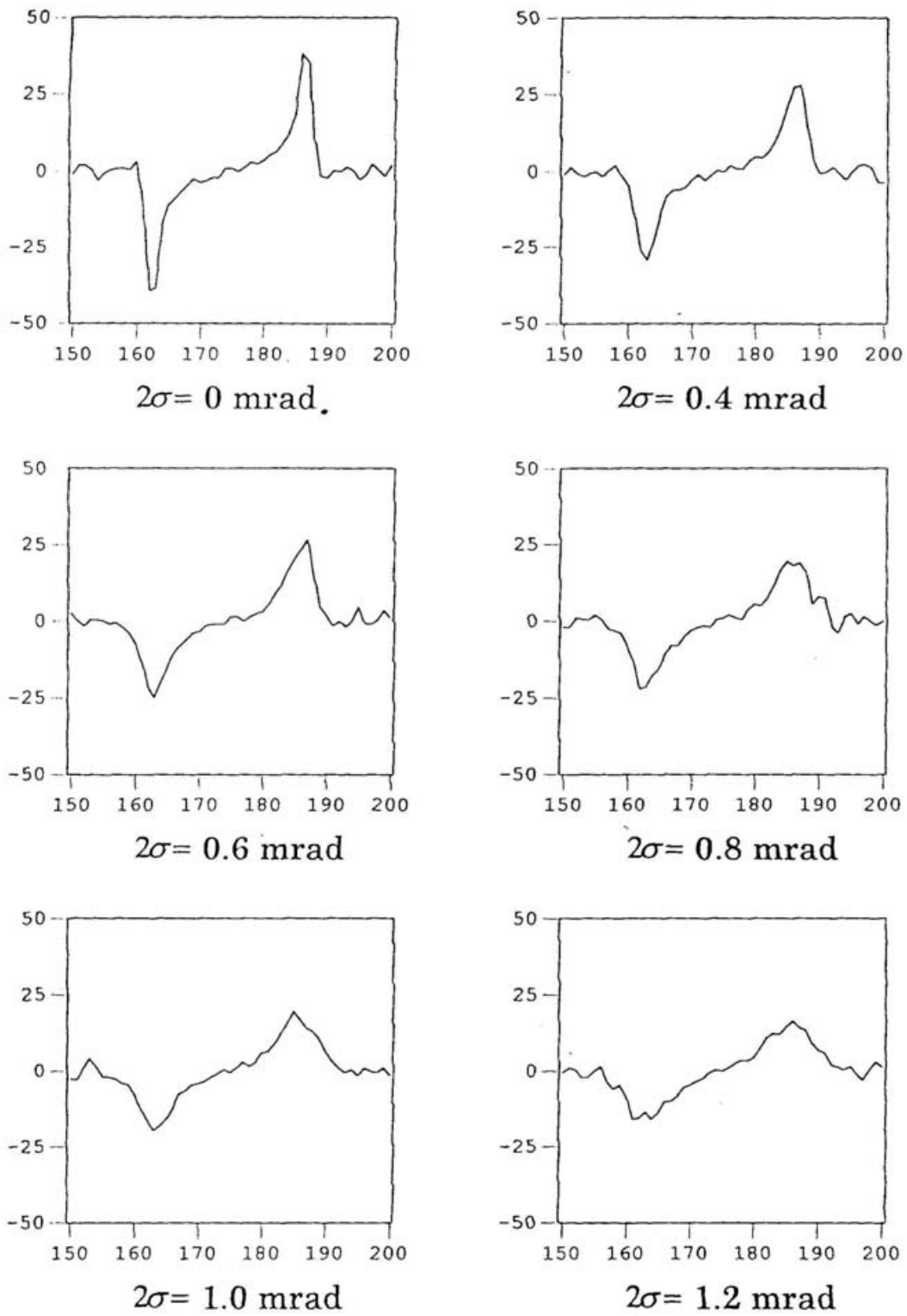


Fig. 42 Profiles of the differential value of images of Fig. 40 around the arteries. The artery diameter is 5 mm.

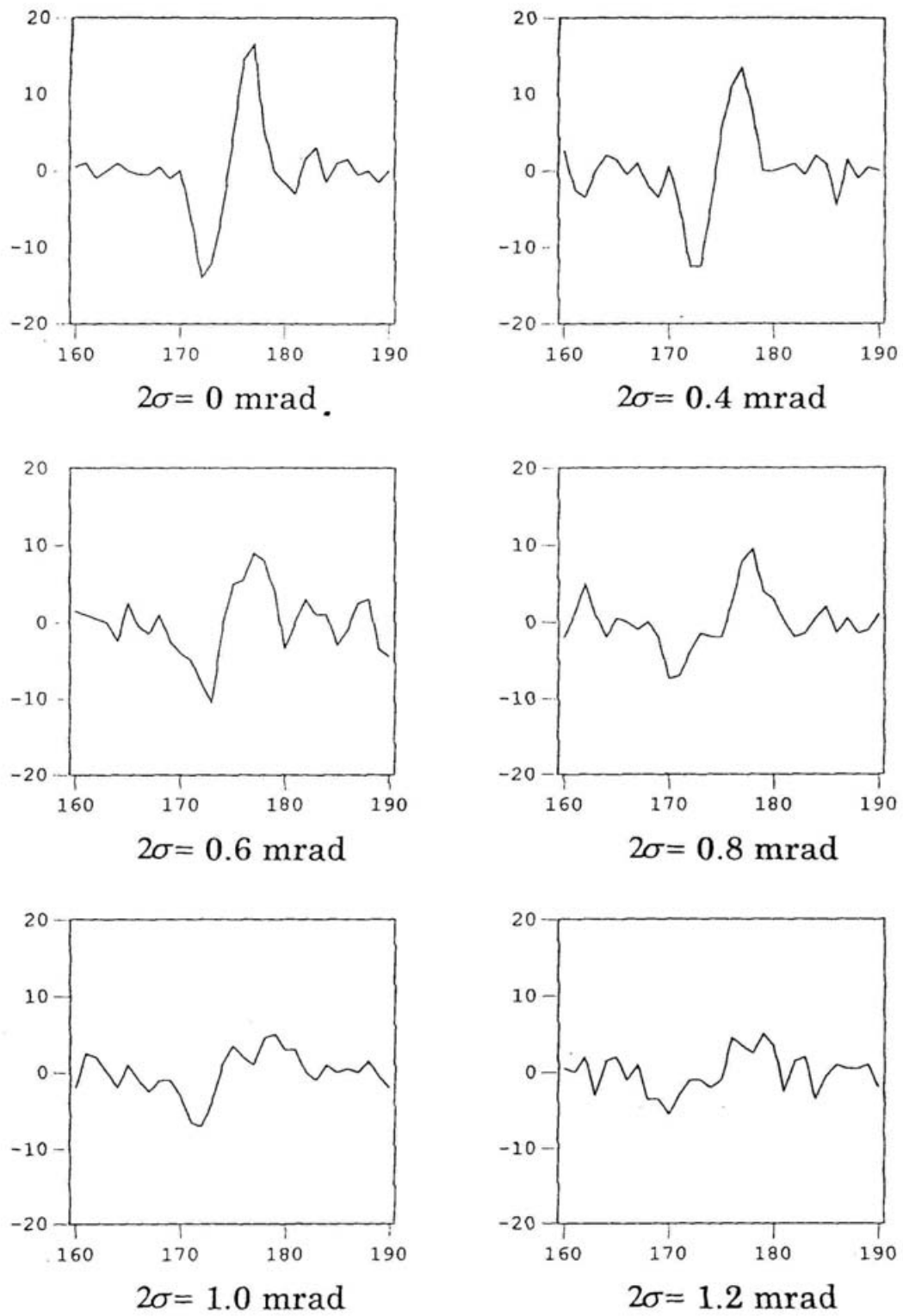


Fig. 43 Profiles of the differential value of images of Fig. 41 around the arteries. The artery diameter is 1 mm.

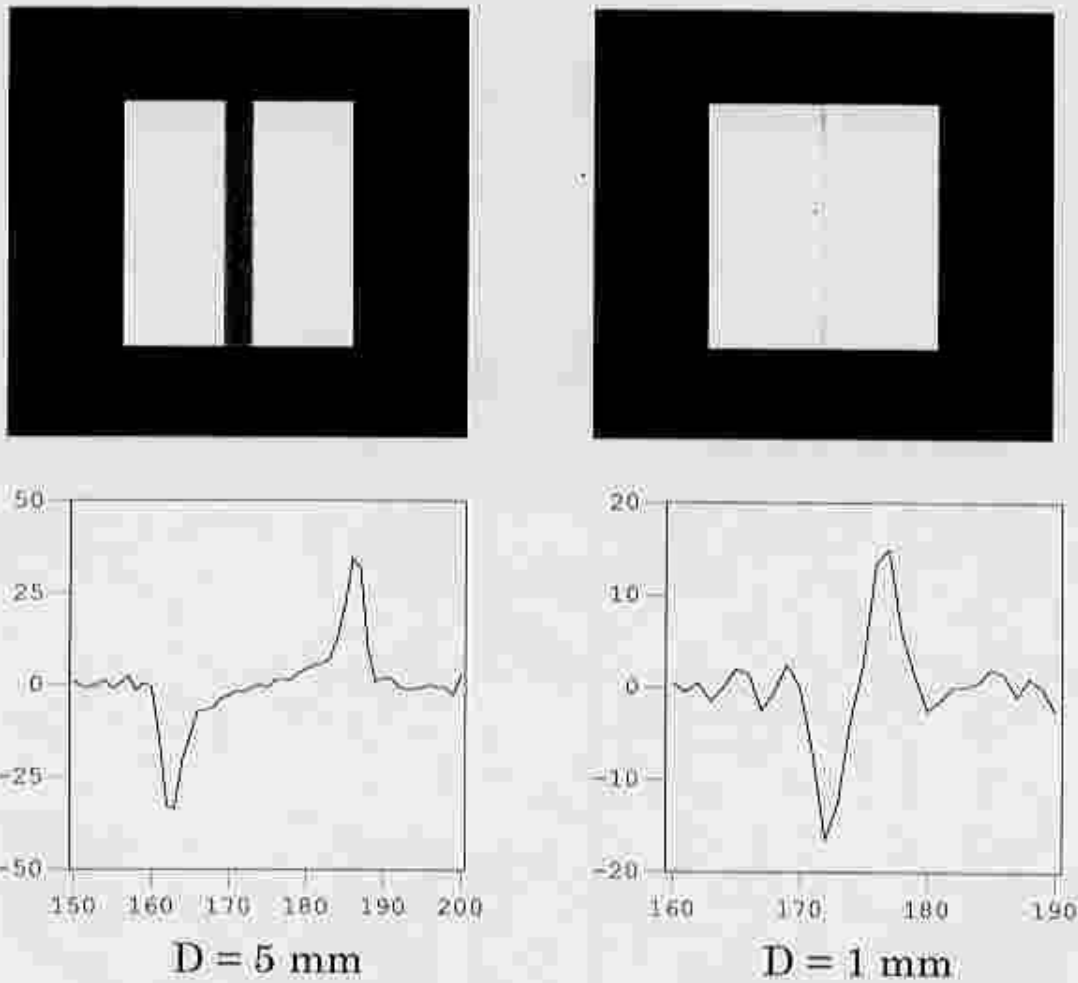


Fig. 44 Simulated images and profiles of their differential value of arteries by 33.17 keV x-ray beams which have various divergences. The distance between the acrylic and the detector is 100 mm, and the injecting angle in the horizontal plane is chosen according to the normal distribution. Twice of the standard deviation ( $2\sigma$ ) of the normal distribution is 1.2 mrad. The artery diameters ( $D$ ) are 5 mm and 1 mm.

of II. Furthermore, since its dynamic range of  $10^4$  is greater than that of II of  $10^3$ , and its image data are recorded as digital data, it will be a useful detector for the current angiography program, if one can change IP's with fast speed capable of dynamic images.

## 5. Conclusions

### 5-1 Summary

Summary regarding image simulation is as follows:

- (1) The two-dimensional image simulation program using the Monte Carlo method was developed in order to investigate the influence of harmful scattered x-rays and the third higher harmonic on image contrast.
- (2) The simulation program was verified by comparison with results of the experiment and simulation by program code EGS4.
- (3) Characteristics of scattered x-rays with various body thickness and exposure area were investigated.
- (4) Images in the case without the x-ray grid and with the x-ray grid in ideal clinical conditions were obtained using the simulation program, and the effect of the x-ray grid to improve image contrast was ascertained.

Summary regarding rotating x-ray shutter is as follows: A rotating shutter to produce pulsed x-ray beams was developed for SR coronary angiography, and applied to the clinical application. It was confirmed that dynamic coronary imaging by the pulsed x-ray was possible, and that the irradiation period per one image was reasonable.

Summary regarding coronary angiography system using a dedicated SR source is as follows:

- (1) The quantum noise value against the photon flux of iodine K-edge energy from radiation source could be an estimated period, and necessary photon flux was obtained by comparing the standard deviation of quantum noises with artery image contrast.
- (2) Characteristics of image contrast and its improvement by x-ray grids against the contamination of the third higher harmonic were investigated by the simulation program, and the allowable contamination limit was determined.
- (3) The required specifications of radiation source for SR coronary angiography were obtained from the necessary photon flux, irradiation period per one image

and allowed contamination of the third higher harmonic. They are proposed as a practical radiation source for screening diagnosis of coronary artery by SR angiography.

(4) Conceptual design of the SR source system for coronary angiography with considerations of other system factors such as the beamline element was carried out, and it was proposed as a dedicated system.

## 5-2 Outcome

Outcome of this study is as follows:

(1) Quantitative characterization of scattered x-rays which were harmful for the two-dimensional coronary imaging method was carried out by investigation of image contrast deterioration by scattered x-rays and the third higher harmonic on image simulation of images made by monochromatic SR x-rays.

(2) A rotating x-ray shutter which generated pulsed x-ray beam and was necessary for two-dimensional SR coronary angiography was developed, and applied to the first clinical examination. The radiation dose whose total per one examination is pointed out as a demerit of the two-dimensional imaging method was suppressed to be minimum physically by the shutter, and the possibility of practical use was shown.

(3) Taking into account the above results and information on the beamline optics, the detectors etc. in the clinical application, the practical synchrotron radiation source system dedicated to medical use was designed using investigations of image characterization.

## Acknowledgments

The author would like to greatly thank Professor Masami Ando of KEK for his assigning a significant theme to this study, his supervision and accurate advice throughout this study. He also would like to thank Dr. Kazuyuki Hyodo of KEK for his lead in performing the experiments in detail, his kindly showing the valuable information of his basic studies and the clinical applications and for his kind advice regarding this study.

He also would like to thank Professor Hitoshi Kanamori, Dr. Nobuyuki Nakamori of Kyoto Institute of Technology, Professor Hideo Hirayama and Dr. Yoshihito Namito of KEK for their kind advice on the simulation methods and their information about x-ray attenuation data, and Dr. Kaoru Iwano of KEK and Mr. Tatsuya Minami of GUAS for their kind advice on using computer systems..

Further, the author would like to acknowledge Dr. Xiao Wei Zhang of KEK and Mr. Hidetaka Koga of ATC for their support in the x-ray shutter experiment, and Dr. Junichiro Tada of JASRI for his kind advice in estimation of the radiation dose with the x-ray shutter and information about the ionization chamber used in the clinical applications.

The author also would like to acknowledge Professor Susumu Kamada, Dr. Kazufumi Ohmi, Dr. Masahiro Kato and Dr. Yukinori Kobayashi of KEK for their advice on the design method of the synchrotron radiation source and instruction of using the storage ring design code.

Furthermore, the author also would like to acknowledge Dr. William Thomlinson, Dr. Jerome Hastings and Dr. Zhong Zhong of NSLS in BNL for their kind help and effective advice in the experiments and their kind machine time allocation at X-17 beamline of NSLS. He also would like to thank Dr. Hideaki Shiwaku of Spring-8 for his information about integrated intensity diffracted by lapped crystal monochromator, and Dr. Yoshiyuki Amemiya of Tokyo Univ. and Mr. Kazuki Ito of GUAS for their advice about x-ray detector response as a function of the photon energy

Last but not least, he would like to thank Dr. Akira Iwata and Kiyoshi Aizawa of Kawasaki Heavy Industries, Ltd. for their encouragement and support throughout this study.

## References

- Akisada A., M. Ando, K. Hyodo, S. Hasegawa, K. Konishi, K. Nishimura, A. Maruhashi, F. Toyofuku, A. Suwa and K. Kohra; Nucl. Instrum. and Methods A246, p713 (1986)
- Berger M. J. and J. H. Hubbell; A computer program and database made by Center for Radiation Research, National Bureau of Standards, Gaithersburg, MD 20899 (9 May 1987)
- Creasy J. L, R. R. Price, T. Presbrey, et al.; Radiology, 175, p280 (1990)
- Dementyev E. N., E. Ya. Dovga, G. N. Kulipanov, A. S. Medvedko, N. A. Mezentsev, V. F. Pindyurin, M. A. Sheromov, A. N. Skrinsky, A. S. Sokolov, V. A. Ushakov and E. I. Zagorodnikov; Nucl. Instrum. and Methods A 246, p726 (1986)
- Dementyev E. N., I. P. Dolbnya, E. I. Zagorodnikov, K. A. Kolesnikov, G. N. Kulipanov, G. Kurylo, A. S. Medvedko, N. A. Mezentsev, V. F. Pindyurin, V. Cheskidov and M. A. Sheromov; Rev. Sci. Instrum. 60, p2264 (1989)
- Dix W.-R., K. Engelke, C.-C. Gluer, W. Graeff, C. P. Hoppner, K.-H. Stellmaschek, T. Wroblewski, W. Bleifeld, K. H. Hohne and W. Kupper; Nucl. Instrum. and Methods A 246, p702 (1986)
- Dix W.-R., W. Graeff, J. Heuer, H. Jabs, W. Kupper and K.-H. Stellmaschek; Rev. Sci. Instrum. 60, p2260 (1989)
- Fukagawa H., C. Noda, Y. Suzuki S. Hasegawa, M. Ando, K. Hyodo, K. Nishimura, M. Akisada, E. Takenaka, R. Hosaka and F. Toyofuku; Rev. Sci. Instrum. 60 (7), p2268 (July 1989)
- Hubbell J. H., Wm. J. Veigele, E. A. Briggs, R. T. Brown, D. T. Cromer, and R. J. Howerton, J. Phys. Chem. Ref. Data 4, 471 (1975)
- Hughes E. B., H. D. Zeman, L. E. Campbell, R. Hofstadter, U. Meyer-Berkhout, J. N. Otis, J. Rolfe, J. P. Stone and S. Wilson; Nucl. Instrum. and Methods 208, p665 (1983)
- Hughes E. B., E. Rubenstein, H. D. Zeman, G. S. Brown, M. Buchbinder, D. C. Harrison, R. Hofstadter, R. S. Kernoff, J. N. Otis and A. C. Thompson; Nucl. Instrum. and Methods A 246, p719 (1986)
- Huke K. and T. Yamakawa; Nucl. Instrum. and Methods 177, p253 (1980)

- Hyodo K., K. Nishimura, and M. Ando, in Handbook on Synchrotron Radiation, edited by S. Ebashi, M. Koch, and E. Rubenstein ( Elsevier, Amsterdam, 1991), 4, p 55
- Hyodo K., H. Shiwaku, S. Yamamoto, H. Kitamura and M. Ando; Rev. Sci. Instrum. 63 (1) p601 ( 1992 )
- Hyodo K., et al.: to be published
- Hyodo K.; private communications
- Ito M. and Y. Amemiya; Nucl. Instrum. and Methods A 310, 369 (1991)
- Kohra K.; J. Phys. Soc. 17,589 (1962)
- Konishi K., F. Toyofuku, K. Nishimura, M. Ando, K. Hyodo, A. Maruhashi, M. Akisada, S. Hasegawa, A. Suwa and E. Takenaka; Jpn. J. Med. & Inf. Sci. 2, p113 (1985)
- LeGrand A. D., W. Schildkamp and B. Blank; Nucl. Instrum. and Methods A275, p442 (1989)
- Nakamori N. and H. Kanamori; Japanese Journal of Radiological Technology, 36 No. 1, p1-9 (1980)
- Namito Y., S. Ban and H. Hirayama; Nucl. Instrum. and Methods A332, p277-283 (1993)
- Nelson W. R., H. Hirayama and David W.O. Rogers; SLAC-Report-265 (December 1985)
- Nishimura K., K. Hyodo, R. Hosaka, M. Ando, M. Akisada, S. Hasegawa and E. Takenaka; Rev. Sci. Instrum. 60 (7) p2260 (1989)
- Oide K. et al.; A computer program complex for accelerator design developed in KEK (since 1986), Home page address; <http://www-acc-theory.kek.jp/SAD/sad.html>
- Ohtsuka S., Y. Sugishita, T. Takeda, Y. Itai, K. Hyodo and M. Ando; Jpn. Circ. J, 61, p 432 ( 1997 )
- Ohtsuka S. et al.; to be published
- Oku Y., K. Aizawa, S. Nakagawa, A. Iwata, K. Hyodo, S. Kamada and M. Ando; Kawasaki Technical Review No. 118, p89, 1993 ( in Japanese )
- Oku Y., K. Aizawa, S. , M. Ando, K. Hyodo, and S. Kamada, IEEE Proceedings of the 1993 Particle Accelerator Conference, 1994, Vol. 2, p. 1468
- Oku Y., K. Aizawa, K. Hyodo and M. Ando; Rev. Sci. Instrum. 66, No.2, Part 2,

- p1451, (Feb. 1995)
- Oku Y., K. Hyodo, M. Ando and J. Tada; submitted Journal of Synchrotron Radiation
- Rubenstein E., E. B. Hughes, L. E. Campbell, R. Hofstadter, R. L. Kirk, T. J. Krolicki, J. P. Stone, S. Wilson, H. D. Zeman, W. R. Brody, A. Macovski and A. C. Thompson; Conf. on Digital Radiography, SPIE 314, p42 (1981)
- Rubenstein E., R. Hofstadter, H. D. Zeman, A. C. Thompson, J. N. Otis, G. S. Brown, J. C. Giacomini, H. J. Gordon, R. S. Kernoff, D. C. Harrison and W. Thomlinson; Proc. Natl. Sci. USA, 83 p9724 (1986)
- Rubenstein E., A. C. Thompson, G. Brown, R. Hofstadter, W. Thomlinson and H. D. Zeman; Nucl. Instrum. and Methods A 291, p80 ( 1990 )
- Shiwaku H., K. Hyodo and M. Ando; Japanese Journal of Applied Physics, 30, 12A, L2065 (1991)
- Shiwaku H., K. Hyodo and M. Ando; Rev. Sci. Instrum. 63 (1), p1201 ( 1992 )
- Shiwaku H.; Ph. D thesis, from The Graduate University for Advanced Studies (1992)
- Sugiyama S., H. Ohgaki, M. Mikado, T. Noguchi, K. Yamada, M. Chiwaki, R. Suzuki, M. Koike, T. Yamazaki and T. Tomimasu; Rev. Sci. Instrum. 63 (1), p313 ( January 1992 )
- Suortti P. and W. Thomlinson; Nucl. Instrum. and Methods A 269, p639 ( 1988 )
- Thomlinson W., D. Chapman, N. Gmur and N. Lazarz; Nucl. Instrum. and Methods A 266, p226 ( 1988 )
- Thomlinson W., N. Gmur, D. Chapman, R. Garrett, N. Lazarz, H. Moulin, A. C. Thompson, H. D. Zeman, G. S. Brown, J. Morrison, P. Reiser, V. Padmanabahn, L. Ong, S. Green, J. Giacomini, H Gordon and E. Rubenstein; Rev. Sci. Instrum. 63 (1) p625 (1992 )
- Thompson A. C., E. Rubenstein, H. D. Zeman, R. Hofstadter, J. N. Otis, J. C. Giacomini, H. J. Gordon, G. S. Brown, W. Thomlinson, R. S. Kernoff; Rev. Sci. Instrum. 60 (7) p1674 ( July 1989 )
- Wiedemann H.; IEEE Transactions on Nucl. Sci., Vol. NS-32, No. 5, (October 1985 )
- Wiedemann H.; Italian Physical Society Conference Proceedings Vol. 10, p299 ( 1988 )

Yamasaki K. private communications

Zeman H. D., E. B. Hughes, J. N. Otis, J. Rolfe and A. C. Thompson: Proceedings  
of the IEEE Nuclear Science Symposium, San Francisco October 19-24, (1983)

## Appendix

1. Simulation program list
2. Differential cross section of coherent scattering and incoherent scattering for 33.17 keV and 99.51 keV x-rays
3. Atomic form factor  $F(x,z)$  and incoherent scattering function  $S(x,z)$  for 33.17 keV and 99.51 keV x-rays

C-----  
 C       Declarations and Parameters  
 C-----

```

CHARACTER*8  OUTFILEA, OUTFILEG
CHARACTER*1  NUM1(0:9), CHA(0:10), CALTYPE
CHARACTER*2  NUM2(0:99)
CHARACTER*1  DORS, EPHOR
REAL  PI, ME
REAL  XEND, XH2OU, XH2OD, YH2OU, YH2OD, ZH2OU, ZH2OD
REAL  DISTWE
REAL  RFREE, EPHOR33, EPHOR99, LOSEPH
REAL  UNIRAN, TH1
REAL  X0, Y0, XR, YR, Z1, X2, Y2, Z2
REAL  XBAI
REAL  TAU, SIGCOH, SIGINC
REAL  THM(0:1000), PITHOMS(0:99, 0:1000), PIKLNIS(0:99, 0:1000)
REAL  PITHOMSH2O(0:99, 0:1000), PIKLNISH2O(0:99, 0:1000)
REAL  PITHOMSI(0:99, 0:1000), PIKLNISI(0:99, 0:1000)
REAL  PITHOMSWO(0:99, 0:1000), PIKLNISWO(0:99, 0:1000)
REAL  PITHOMSPB(0:99, 0:1000), PIKLNISPB(0:99, 0:1000)
REAL  EPH, LEPH, YEND, ZEND
REAL  FTAU, FSIGCOH, FSIGINC
REAL  LRUN, ETAU, ETAUD
REAL  ENE
REAL  WIB, HIB, YIB, ZIB, WIB2U, WIB2D, HIB2U, HIB2D
REAL  ROUACL, ROUI
REAL  EIX, E1Y, E1Z, E0X, E0Y, E0Z, KX, KY, KZ
REAL  MEWI, MEWH2O, MEWIH2O, MEW, MEWFLOUR
REAL  MEWWO, MEWPB
REAL  LWOI, LWO, LWOM, LWO, LPBI, LPBF, LPBM, LPB
REAL  LPBEQ, LEQ
INTEGER  NTH, NTRVL, I, J, K
INTEGER  NPHOT
INTEGER  RAN
INTEGER  RANSU(1:10)
INTEGER  LI
INTEGER  CCOH, CINC
INTEGER  DIGIT1, DIGIT2
INTEGER  CD3I, CD3B, CD9I, CD9B, CS3I, CS3B, CS9I, CS9B
INTEGER  CI3I, CI3B, CI9I, CI9B, CF3I, CF3B, CF9I, CF9B
INTEGER  CGD3I, CGD3B, CGD9I, CGD9B, CGS3I, CGS3B, CGS9I, CGS9B
INTEGER  CGI3I, CGI3B, CGI9I, CGI9B, CGF3I, CGF3B, CGF9I, CGF9B
INTEGER  CGG3I, CGG3B, CGG9I, CGG9B
LOGICAL  FELOS, FWOUT, FDOUT, FGOUT, FINCOH, FIBIN, FIARTIN
LOGICAL  F2J, F2JG, FISCAT, FINWO
LOGICAL  FNOPOL
PARAMETER (PI=3.141592, ME=.511*1E+06)
PARAMETER (NTH=1000, NTRVL=1000)
PARAMETER (XH2OD=0.)
PARAMETER (YH2OU=125., YH2OD=-125., ZH2OU=125., ZH2OD=-125.)
PARAMETER (YGRIDU=150., YGRIDD=-150., ZGRIDU=150., ZGRIDD=-150.)
PARAMETER (YDET=70., ZDET=70.)
PARAMETER (EPHOR33=33.17, EPHOR99=99.51, LOSEPH=10.)
PARAMETER (EPH12=33.17, EPH23=35.98, EPH34=60.)
PARAMETER (ROUACL=1.19, ROUI=4.93)
PARAMETER (ROUWO=0.49, ROUPB=11.34)
PARAMETER (OMEGAKI=0.882, OMEGAKPB=0.968)
PARAMETER (RIKA2=53.8, RIKA1=100., RIKB1=29., RIKB2=6.1)
PARAMETER (RPBKA2=59.3, RPBKA1=100.)
PARAMETER (RPBKB3=11.6, RPBKB1=22.2, RPBKB2=10.2)
PARAMETER (EIKA2=28.3172, EIKA1=28.6120, EIKB1=32.3, EIKB2=33.0)
PARAMETER (EPBKA2=72.804, EPBKA1=74.969)
PARAMETER (EPBKB3=84.450, EPBKB1=84.936, EPBKB2=87.3)

```

C-----

```

INTEGER  XMAX, YMAX
INTEGER  XSCR, YSCR
REAL  XSCRMAX, YSCRMAX, DENSEMAX
PARAMETER(XSCRMAX=350., YSCRMAX=350.)
PARAMETER(XMAX=350, YMAX=350)
PARAMETER(IMAX=1000000)
REAL  DENSE(XMAX, YMAX), DENSENG(XMAX, YMAX)
INTEGER  JBUFF(XMAX, YMAX, I)
PARAMETER (RDAMMY=10.)
COMMON /GRID/H, DWO, DPB, DBL, XEND, XGRID, XGEND
COMMON /ANGLE/THM, PITHOMSWO, PIKLNISWO, PITHOMSPB, PIKLNISPB

```

C----- Acrylic Attenuation functions -----  
C 1 2 3 4 5 6 7  
FTAU(X)=3.4777-2.7010\*X-.58037\*X\*X+.44988\*X\*X\*X-.099249\*X\*X\*X\*X  
% -.17341\*X\*X\*X\*X\*X+.12990\*X\*X\*X\*X\*X\*X-.013523\*X\*X\*X\*X\*X\*X\*X  
% -.014851\*X\*X\*X\*X\*X\*X\*X\*X+.0053234\*X\*X\*X\*X\*X\*X\*X\*X\*X  
% -.00050347\*X\*X\*X\*X\*X\*X\*X\*X\*X\*X  
FSIGCOH(X)=.54943-1.4373\*X+.031150\*X\*X+.34363\*X\*X\*X-.18688\*X\*X\*X\*X  
% -.083771\*X\*X\*X\*X\*X\*X+.047459\*X\*X\*X\*X\*X\*X\*X-.0074510\*X\*X\*X\*X\*X\*X\*X\*X  
% +.00053850\*X\*X\*X\*X\*X\*X\*X\*X\*X+.0037229\*X\*X\*X\*X\*X\*X\*X\*X\*X\*X  
% -.0013514\*X\*X\*X\*X\*X\*X\*X\*X\*X\*X  
FSIGINC(X)=-1.5751+1.2045\*X-.29957\*X\*X-.30516\*X\*X\*X+.14425\*X\*X\*X\*X  
% +.058519\*X\*X\*X\*X\*X-X-.068271\*X\*X\*X\*X\*X\*X+.020999\*X\*X\*X\*X\*X\*X\*X  
% +.0051268\*X\*X\*X\*X\*X\*X\*X\*X-X-.0063029\*X\*X\*X\*X\*X\*X\*X\*X\*X  
% +.0013852\*X\*X\*X\*X\*X\*X\*X\*X\*X\*X

C----- H2O Attenuation functions -----  
C 1 2 3 4 5 6 7  
FTAUH2O(X)=3.6333-2.6540\*X-.47817\*X\*X+.36500\*X\*X\*X-.26016\*X\*X\*X\*X  
% +.11022\*X\*X\*X\*X\*X\*X-.025047\*X\*X\*X\*X\*X\*X\*X+.0027131\*X\*X\*X\*X\*X\*X\*X\*X  
FSIGCOHH2O(X)=.72275-1.6687\*X+.54516\*X\*X-.12796\*X\*X\*X  
% -.20230\*X\*X\*X\*X\*X+.13069\*X\*X\*X\*X\*X-X-.040743\*X\*X\*X\*X\*X\*X  
% +.0066214\*X\*X\*X\*X\*X\*X\*X  
FSIGINCH2O(X)=-1.9590+2.4270\*X-1.5951\*X\*X+.044281\*X\*X\*X  
% +.46840\*X\*X\*X\*X-X-.22796\*X\*X\*X\*X\*X\*X+.032741\*X\*X\*X\*X\*X\*X\*X  
% +.00037069\*X\*X\*X\*X\*X\*X\*X\*X

C----- Iodine Attenuation functions ( TAU ) -----  
C--- over K (150.0keV-33.17keV) ---  
C 1 2 3 4 5 6 7  
FTAUIOK(X)=1.4024+4.8165\*X-4.7830\*X\*X+1.2971\*X\*X\*X-.12780\*X\*X\*X\*X  
C  
C--- below K (5.188keV-33.17keV) ---  
FTAUIBK(X)=4.6808-2.2897\*X-.18847\*X\*X

C----- Iodine Attenuation functions ( COH and INC ) -----  
C 1 2 3 4 5 6 7  
FSIGCOHI(X)=1.1550-.90930\*X+.82994\*X\*X-.75976\*X\*X\*X  
% +.081096\*X\*X\*X\*X\*X+.068894\*X\*X\*X\*X\*X\*X-.016390\*X\*X\*X\*X\*X\*X\*X  
FSIGINCI(X)=-1.8917+.13499\*X+1.2900\*X\*X-.95821\*X\*X\*X  
% +.18066\*X\*X\*X\*X\*X+.031217\*X\*X\*X\*X\*X\*X-.011247\*X\*X\*X\*X\*X\*X\*X

C----- Wood Attenuation functions -----  
C 1 2 3 4 5 6 7  
FTAUWO(X)=3.5236-2.7484\*X-.37621\*X\*X+.27704\*X\*X\*X  
% -.15634\*X\*X\*X\*X-X-.0094983\*X\*X\*X\*X\*X\*X+.040787\*X\*X\*X\*X\*X\*X\*X  
% -.0044162\*X\*X\*X\*X\*X\*X\*X-X-.0048903\*X\*X\*X\*X\*X\*X\*X\*X  
% +.000785\*X\*X\*X\*X\*X\*X\*X\*X\*X\*X+.00014234\*X\*X\*X\*X\*X\*X\*X\*X\*X\*X  
FSIGCOHWO(X)=.66777-1.7671\*X+.50479\*X\*X+.10594\*X\*X\*X  
% -.23882\*X\*X\*X\*X-X-.010028\*X\*X\*X\*X\*X\*X+.029020\*X\*X\*X\*X\*X\*X\*X  
% +.0012032\*X\*X\*X\*X\*X\*X\*X\*X+.00014212\*X\*X\*X\*X\*X\*X\*X\*X\*X  
% -.000059193\*X\*X\*X\*X\*X\*X\*X\*X\*X-X-.00021609\*X\*X\*X\*X\*X\*X\*X\*X\*X  
FSIGINCWO(X)=-1.6426+1.2723\*X-.28736\*X\*X-.31547\*X\*X\*X  
% +.11111\*X\*X\*X\*X\*X+.044465\*X\*X\*X\*X\*X-X-.014770\*X\*X\*X\*X\*X\*X  
% -.0010146\*X\*X\*X\*X\*X\*X\*X-X-.0010616\*X\*X\*X\*X\*X\*X\*X\*X  
% -.00064318\*X\*X\*X\*X\*X\*X\*X\*X\*X+.00042586\*X\*X\*X\*X\*X\*X\*X\*X\*X

C----- Lead Attenuation functions ( TAU ) -----  
C--- K(130.0keV-88.00keV) ---  
C 1 2 3 4 5 6 7  
FTAUPBK(X)=1.6049-6.3643\*X+10.364\*X\*X-5.3968\*X\*X\*X+.84788\*X\*X\*X\*X  
C  
C--- L1(88.00keV-15.86keV) ---  
FTAUPBL1(X)=5.0895-2.2603\*X-.13382\*X\*X  
C  
C--- L2(15.86keV-15.20keV) ---  
FTAUPBL2(X)=6.5003-4.8770\*X+1.0208\*X\*X  
C  
C--- L3(15.20keV-13.04keV) ---  
FTAUPBL3(X)=-6.7495+18.147\*X-9.0806\*X\*X  
C  
C--- M1(13.04keV-5.000keV) ---  
FTAUPBM1(X)=1.0110+5.6711\*X-4.4680\*X\*X

C----- Lead Attenuation functions ( COH and INC ) -----  
C 1 2 3 4 5 6 7

```

FSIGCOHPB(X)=.84108+.78743*X-1.0856*X*X+.13085*X*X*X
%      +.040441*X*X*X*X-.020131*X*X*X*X*X+.0031863*X*X*X*X*X*X
FSIGINCPB(X)=-2.3360+1.0816*X+.061788*X*X-.073134*X*X*X
%      -.16268*X*X*X*X+.10155*X*X*X*X*X-.017813*X*X*X*X*X*X

```

```

C----- II Response functions -----

```

```

FIRES1(X)=47.0283-9.45675*X+.559102*X*X-.00836424*X*X*X
FIRES2(X)=-15.408+2.237*X
FIRES3(X)=-124.362+7.74474*X-.0667544*X*X
FIRES4(X)=100.

```

```

C-----
C      Read filenames and parameters
C-----

```

```

RIK=RIKA2+RIKA1+RIKB1+RIKB2
RIKA2KA1=RIKA2/RIK
RIKA1KB1=(RIKA2+RIKA1)/RIK
RIKB1KB2=(RIKA2+RIKA1+RIKB1)/RIK
RPBK=RPBKA2+RPBKA1+RPBKB3+RPBKB1+RPBKB2
RPBKA2KA1=RPBKA2/RPBK
RPBKA1KB3=(RPBKA2+RPBKA1)/RPBK
RPBKB3KB1=(RPBKA2+RPBKA1+RPBKB3)/RPBK
RPBKB1KB2=(RPBKA2+RPBKA1+RPBKB3+RPBKB1)/RPBK
OPEN(UNIT=1, FILE='xibvi.inp')
c  WRITE(*, '(A)') ' Calculation type charecter?'
  READ(1, '(A1)') CALTYPE
c  WRITE(*, '(A)') ' Injection X-ray Photon Number?'
  READ(1, '(I9)') NPHOT
c  WRITE(*, '(A)') ' Water thickness (mm)? Dont forget ".!"'
  READ(1, '(F6.2)') XH2OU
c  WRITE(*, '(A)') ' Distanse from water to end (mm)? Dont forget ".'"
  READ(1, '(F6.2)') DISTWE
  XEND=XH2OU+DISTWE
c  WRITE(*, '(A)') ' Injection beam width (mm)? Dont forget ".'"
  READ(1, '(F6.2)') WIB
c  WRITE(*, '(A)') ' Injection beam height (mm)? Dont forget ".'"
  READ(1, '(F6.2)') HIB
c  WRITE(*, '(A)') ' 99keV / 33keV ratio in %? Dont forget ".'"
  READ(1, '(F6.2)') R99P33P
c  WRITE(*, '(A)') ' iodine artery diameter (mm)? Dont forget ".'"
  READ(1, '(F6.3)') RI2
c  WRITE(*, '(A)') ' iodine weight ratio in %? Dont forget ".'"
  READ(1, '(F6.2)') WPER100
c  WRITE(*, '(A)') ' Grid thickness (mm)? Dont forget ".'"
  READ(1, '(F11.5)') H
c  WRITE(*, '(A)') ' Wood pixel size of Grid(mm)? Dont forget ".'"
  READ(1, '(F8.3)') DWO
c  WRITE(*, '(A)') ' Pb pixel size of Grid(mm)? Dont forget ".'"
  READ(1, '(F8.3)') DPB
  DBL=DWO+DPB
c  WRITE(*, '(A)') ' Distance form Water to Grid (mm)? Dont forget ".'"
  READ(1, '(F8.3)') DISTWG
CLOSE(1)
X0=XH2OU/2.
Y0=0.
WPER=WPER100*.01
VPER=WPER/ROU1/((1.-WPER)+WPER/ROU1)
R99P33=R99P33P/100.
R33P3399=1./(1.+R99P33)
RI=RI2/2.
WIB2U=WIB/2.
WIB2D=-WIB/2.
HIB2U=HIB/2.
HIB2D=-HIB/2.
WIARTU=Y0+RI
WIARTD=Y0-RI
YDETU=YDET/2.
YDET=-YDET/2.
ZDETU=ZDET/2.
ZDET=-ZDET/2.
XGRID=XH2OU+DISTWG
XGEND=XGRID+H
C+++++
  NUM1(0)='0'
  NUM1(1)='1'
  NUM1(2)='2'

```

```

NUM1(3)=' 3'
NUM1(4)=' 4'
NUM1(5)=' 5'
NUM1(6)=' 6'
NUM1(7)=' 7'
NUM1(8)=' 8'
NUM1(9)=' 9'
CHA(1)=' x'
CHA(2)=CALTYPE
CHA(0)=' a'
CHA(3)=' t'
if(DWO. eq. 0. 15) CHA(3)=' v'
if(DWO. eq. 0. 25) CHA(3)=' w'
if(DWO. eq. 0. 35) CHA(3)=' x'
if(DWO. eq. 0. 45) CHA(3)=' y'
if(distwe. gt. 1000.) then
  cha(4)=' z'
else
  CHA(4)=NUM1(INT(DISTWE/100.))
  if(DISTWE. eq. 20.) CHA(4)=' 9'
endif
if(XH2OU. eq. 60.) cha(5)=' a'
if(xh2ou. eq. 80.) cha(5)=' b'
if(xh2ou. eq. 100.) cha(5)=' c'
if(xh2ou. eq. 120.) cha(5)=' d'
if(xh2ou. eq. 160.) cha(5)=' e'
if(xh2ou. eq. 200.) cha(5)=' f'
if(xh2ou. eq. 240.) cha(5)=' g'
if(xh2ou. eq. 11.) cha(5)=' h'
CHA(8)=NUM1(MOD(INT(R99P33P), 10))
CHA(6)=NUM1(INT(R12))
CHA(7)=NUM1(MOD(INT(WPER100), 10))
OUTFILEA=CHA(1)//CHA(2)//CHA(0)//CHA(4)//CHA(5)//CHA(6)//CHA(7)
% //CHA(8)
OUTFILEG=CHA(1)//CHA(2)//CHA(3)//CHA(4)//CHA(5)//CHA(6)//CHA(7)
% //CHA(8)
C..... Read theta kakuritu bunpu integral .....
OPEN(UNIT=10, FILE='PIAC3317. DAT' )
OPEN(UNIT=20, FILE='PIHO3317. DAT' )
OPEN(UNIT=30, FILE='PII3317. DAT' )
OPEN(UNIT=40, FILE='PIWO3317. DAT' )
OPEN(UNIT=50, FILE='PIPB3317. DAT' )
  READ(10, 110) ENE
  READ(20, 110) ENE
  READ(30, 110) ENE
  READ(40, 110) ENE
  READ(50, 110) ENE
  J=0
  DO 11 I=1, NTH
    READ(10, 100) THM(I), PITHOMS(J, I), PIKLNIS(J, I)
    READ(20, 100) THM(I), PITHOMSH20(J, I), PIKLNISH20(J, I)
    READ(30, 100) THM(I), PITHOMSI(J, I), PIKLNISI(J, I)
    READ(40, 100) THM(I), PITHOMSWO(J, I), PIKLNISWO(J, I)
    READ(50, 105) THM(I), PITHOMSPB(J, I), PIKLNISPB(J, I)
11 CONTINUE
  CLOSE(10)
  CLOSE(20)
  CLOSE(30)
  CLOSE(40)
  CLOSE(50)
  OPEN(UNIT=10, FILE='PIAC9951. DAT' )
  OPEN(UNIT=20, FILE='PIHO9951. DAT' )
  OPEN(UNIT=30, FILE='PII9951. DAT' )
  OPEN(UNIT=40, FILE='PIWO9951. DAT' )
  OPEN(UNIT=50, FILE='PIPB9951. DAT' )
    READ(10, 110) ENE
    READ(20, 110) ENE
    READ(30, 110) ENE
    READ(40, 110) ENE
    READ(50, 110) ENE
    J=1
    DO 12 I=1, NTH
      READ(10, 100) THM(I), PITHOMS(J, I), PIKLNIS(J, I)
      READ(20, 100) THM(I), PITHOMSH20(J, I), PIKLNISH20(J, I)
      READ(30, 100) THM(I), PITHOMSI(J, I), PIKLNISI(J, I)

```

```

      READ(40, 100) THM(I), PITHOMSWO(J, I), PIKLNISWO(J, I)
      READ(50, 105) THM(I), PITHOMSPB(J, I), PIKLNISPB(J, I)
12  CONTINUE
      CLOSE(10)
      CLOSE(20)
      CLOSE(30)
      CLOSE(40)
      CLOSE(50)
C----- Input Number Character -----
      DO 13 I=10, 99
          DIGIT1=MOD(I, 10)
          DIGIT2=INT(I/10)
          NUM2(I)=NUM1(DIGIT2)//NUM1(DIGIT1)
13  CONTINUE
C-----
      DO 15 J=10, 99
          OPEN(UNIT=10, FILE='PIAC' //NUM2(J)//'.DAT')
          OPEN(UNIT=20, FILE='PIHO' //NUM2(J)//'.DAT')
          OPEN(UNIT=30, FILE='PII' //NUM2(J)//'.DAT')
          OPEN(UNIT=40, FILE='PIWO' //NUM2(J)//'.DAT')
          OPEN(UNIT=50, FILE='PIPB' //NUM2(J)//'.DAT')
          READ(10, 110) ENE
          READ(20, 110) ENE
          READ(30, 110) ENE
          READ(40, 110) ENE
          READ(50, 110) ENE
          DO 10 I=1, NTH
              READ(10, 100) THM(I), PITHOMS(J, I), PIKLNIS(J, I)
              READ(20, 100) THM(I), PITHOMSH20(J, I), PIKLNISH20(J, I)
              READ(30, 100) THM(I), PITHOMSI(J, I), PIKLNISI(J, I)
              READ(40, 100) THM(I), PITHOMSWO(J, I), PIKLNISWO(J, I)
              READ(50, 105) THM(I), PITHOMSPB(J, I), PIKLNISPB(J, I)
10  CONTINUE
          CLOSE(10)
          CLOSE(20)
          CLOSE(30)
          CLOSE(40)
          CLOSE(50)
15  CONTINUE
110 FORMAT(F10.5)
100 FORMAT(F10.7, 9X, F10.7, 9X, F10.7)
105 FORMAT(F10.7, 9X, F12.7, 9X, F12.7)
      WRITE(*, '(A)') 'Reading file is over'
C-----
C                                     Main program
C-----
      CD3I=0
      CD3B=0
      CD9I=0
      CD9B=0
      CS3I=0
      CS3B=0
      CS9I=0
      CS9B=0
      CI3I=0
      CI3B=0
      CI9I=0
      CI9B=0
      CF3I=0
      CF3B=0
      CF9I=0
      CF9B=0
      ETAUTD3I=0.
      ETAUTD3B=0.
      ETAUTD9I=0.
      ETAUTD9B=0.
      ETAUTS3I=0.
      ETAUTS3B=0.
      ETAUTS9I=0.
      ETAUTS9B=0.
      ETAUTI3I=0.
      ETAUTI3B=0.
      ETAUTI9I=0.
      ETAUTI9B=0.
      ETAUTF3I=0.

```

ETAUTF3B=0.  
ETAUTF9I=0.  
ETAUTF9B=0.  
ETAUTD3IPSL=0.  
ETAUTD3BPSL=0.  
ETAUTD9IPSL=0.  
ETAUTD9BPSL=0.  
ETAUTS3IPSL=0.  
ETAUTS3BPSL=0.  
ETAUTS9IPSL=0.  
ETAUTS9BPSL=0.  
ETAUTI3IPSL=0.  
ETAUTI3BPSL=0.  
ETAUTI9IPSL=0.  
ETAUTI9BPSL=0.  
ETAUTF3IPSL=0.  
ETAUTF3BPSL=0.  
ETAUTF9IPSL=0.  
ETAUTF9BPSL=0.  
CGD3I=0  
CGD3B=0  
CGD9I=0  
CGD9B=0  
CGS3I=0  
CGS3B=0  
CGS9I=0  
CGS9B=0  
CGI3I=0  
CGI3B=0  
CGI9I=0  
CGI9B=0  
CGF3I=0  
CGF3B=0  
CGF9I=0  
CGF9B=0  
CGG3I=0  
CGG3B=0  
CGG9I=0  
CGG9B=0  
ETAUTGD3I=0.  
ETAUTGD3B=0.  
ETAUTGD9I=0.  
ETAUTGD9B=0.  
ETAUTGS3I=0.  
ETAUTGS3B=0.  
ETAUTGS9I=0.  
ETAUTGS9B=0.  
ETAUTGI3I=0.  
ETAUTGI3B=0.  
ETAUTGI9I=0.  
ETAUTGI9B=0.  
ETAUTGF3I=0.  
ETAUTGF3B=0.  
ETAUTGF9I=0.  
ETAUTGF9B=0.  
ETAUTGG3I=0.  
ETAUTGG3B=0.  
ETAUTGG9I=0.  
ETAUTGG9B=0.  
ETAUTGD3IPSL=0.  
ETAUTGD3BPSL=0.  
ETAUTGD9IPSL=0.  
ETAUTGD9BPSL=0.  
ETAUTGS3IPSL=0.  
ETAUTGS3BPSL=0.  
ETAUTGS9IPSL=0.  
ETAUTGS9BPSL=0.  
ETAUTGI3IPSL=0.  
ETAUTGI3BPSL=0.  
ETAUTGI9IPSL=0.  
ETAUTGI9BPSL=0.  
ETAUTGF3IPSL=0.  
ETAUTGF3BPSL=0.  
ETAUTGF9IPSL=0.  
ETAUTGF9BPSL=0.

```

ETAUTGG3IPSL=0.
ETAUTGG3BPSL=0.
ETAUTGG9IPSL=0.
ETAUTGG9BPSL=0.
PSLOR=FIIRES2(EPHOR33)
C----- Initial random number -----
CALL ORRANSU(RANSU)
C----- Reperat Injection of X-ray -----
DO 20 I=1,NPHOT
C----- Initial position of Injected X-ray -----
RAN=RANSU(9)
CALL NEWRANSU(RAN, UNIRAN)
RANSU(9)=RAN
YIB=WIB*(UNIRAN-. 5)
RAN=RANSU(4)
CALL NEWRANSU(RAN, UNIRAN)
RANSU(4)=RAN
ZIB=HIB*(UNIRAN-. 5)
X1=-1.
Y1=YIB
Z1=ZIB
X2=0.
Y2=YIB
Z2=ZIB
TH1=0.
PHAI1=0.
ETAU=1.
CCOH=0
CINC=0
FELOS=. FALSE.
FIBIN=. FALSE.
F2J=. FALSE.
F2JG=. FALSE.
FNOPOL=. FALSE.
RAN=RANSU(9)
CALL NEWRANSU(RAN, UNIRAN)
RANSU(9)=RAN
IF(UNIRAN. LT. R33P3399) THEN
  EPH=EPHOR33
  EPHOR=' 3'
ELSE
  EPH=EPHOR99
  EPHOR=' 9'
ENDIF
DORS=' D'
EOX=0.
EOY=1.
EOZ=0.
LEPH=LOG10(EPH)
TAU=FTAU(LEPH)
TAU=10. **TAU*ROUACL
ETAUD=EXP(-TAU*(XH20U-XH20D)/10.)
C
C----- Repeat of interactions -----
DO 30 J=1,NTRVL
C-----
930   CONTINUE
C-----
LEPH=LOG10(EPH)
TAU=FTAU(LEPH)
SIGCOH=FSIGCOH(LEPH)
SIGINC=FSIGINC(LEPH)
TAU=10. **TAU*ROUACL
SIGCOH=10. **SIGCOH*ROUACL
SIGINC=10. **SIGINC*ROUACL
MEW=SIGCOH+SIGINC
C----- Decide of free run length -----
7010  CONTINUE
RAN=RANSU(9)
CALL NEWRANSU(RAN, UNIRAN)
RANSU(9)=RAN
IF(UNIRAN. EQ. 0. ) GOTO 7010
RFREE=-10./MEW*ALOG(UNIRAN)
C
C----- Compute next point -----

```

```

OMEGA0D=0.
CALL NEWCOORD (X1, Y1, Z1, X2, Y2, Z2, E0X, E0Y, E0Z, RFREE, TH1, PHA11
%           , OMEGA0D)
IF(OMEGA0D. NE. 0. ) GOTO 20
C----- E-Bector deciding -----
      KX=X2-X1
      KY=Y2-Y1
      KZ=Z2-Z1
      CALL EDECIDE(E0X, E0Y, E0Z, KX, KY, KZ, E1X, E1Y, E1Z, DELTA0D)
      IF(DELTA0D. EQ. 1. ) GOTO 20
      E0X=E1X
      E0Y=E1Y
      E0Z=E1Z
      GOTO 900
c
C----- distinction in the iodine or not -----
      AX=X2-X1
      AY=Y2-Y1
      AZ=Z2-Z1
      AXY=SQRT(AX*AX+AY*AY)
      IF(AXY. EQ. 0. ) GOTO 900
      XR=(AX*AX*X0+AY*AY*X1+AX*AY*(Y0-Y1))/AXY/AXY
      YR=(AY*AY*Y0+AX*AX*Y1+AX*AY*(X0-X1))/AXY/AXY
      CX=XR-X0
      CY=YR-Y0
      CXY=SQRT(CX*CX+CY*CY)
      IF(CXY. GE. R1) GOTO 900
      DXYPAXY=SQRT(R1*R1-CXY*CXY)/AXY
      DX=AX*DXYPAXY
      DY=AY*DXYPAXY
      DZ=AZ*DXYPAXY
      BX=XR-X1
      BY=YR-Y1
      IF((DX*BX+DY*BY). LT. 0. ) GOTO 900
      BXY=SQRT(BX*BX+BY*BY)
      BZ=AZ/AXY*BXY
      EX=BX-DX
      EY=BY-DY
      EZ=BZ-DZ
      EXYZ=SQRT(EX*EX+EY*EY+EZ*EZ)
      IF(EXYZ. GT. RFREE) GOTO 900
      ETAU=ETAU*EXP(-TAU*EXYZ/10. )
C
C----- follow scattering in the iodine -----
      DORS=' I '
      X2=X1+EX
      Y2=Y1+EY
      Z2=Z1+EZ
      IF(EPH. GE. 33. 17) THEN
        F2J=. TRUE.
        X1F=X1
        Y1F=Y1
        Z1F=Z1
        X2F=X2
        Y2F=Y2
        Z2F=Z2
        EPHF=EPH
        ETAUF=ETAU
      ENDIF
      TH1=0.
      PHA11=0.
910 CONTINUE
      LEPH=LOG10(EPH)
      IF(EPH. GE. 33. 17) THEN
        TAU1=FTAUIOK(LEPH)
      ELSE
        TAU1=FTAUIBK(LEPH)
      ENDIF
      SIGCOHI=FSIGCOHI(LEPH)
      SIGINCI=FSIGINCI(LEPH)
      TAUH20=FTAUH20(LEPH)
      SIGCOHH20=FSIGCOHH20(LEPH)
      SIGINCH20=FSIGINCH20(LEPH)
      TAU1=10. **TAUI*ROUI
      SIGCOHI=10. **SIGCOHI*ROUI
      SIGINCI=10. **SIGINCI*ROUI

```

```

TAUH20=10. **TAUH20
SIGCOHH20=10. **SIGCOHH20
SIGINCH20=10. **SIGINCH20
MEWI=SIGCOHI+SIGINCI
MEWH20=SIGCOHH20+SIGINCH20
MEWIH20=MEWI*VPER+MEWH20*(1.-VPER)
TAUIH20=TAUI*VPER+TAUH20*(1.-VPER)
C----- Decide of free run length -----
7020 CONTINUE
      RAN=RANSU(9)
      CALL NEWRANSU(RAN, UNIRAN)
      RANSU(9)=RAN
      IF(UNIRAN.EQ.0.) GOTO 7020
      RFREE=-10./MEWIH20*ALOG(UNIRAN)
C
      ( RFREE UNIT mm )
C----- Compute next point -----
      OMEGA0D=0.
      CALL NEWCOORD (X1, Y1, Z1, X2, Y2, Z2, EOX, EOY, EOZ, RFREE, TH1, PHA11
%
      , OMEGA0D)
      IF(OMEGA0D.NE.0.) GOTO 20
C----- E-Bector deciding -----
      KX=X2-X1
      KY=Y2-Y1
      KZ=Z2-Z1
      CALL EDECIDE(EOX, EOY, EOZ, KX, KY, KZ, E1X, E1Y, E1Z, DELTA0D)
      IF(DELTA0D.EQ.1.) GOTO 20
      EOX=E1X
      EOY=E1Y
      EOZ=E1Z
C-----
      RFRIC=SQRT((X2-X0)*(X2-X0)+(Y2-Y0)*(Y2-Y0))
C----- if P2 is out of artery goto acrylic routine -----
      IF(RFRIC.GE.RI) THEN
        AX=X2-X1
        AY=Y2-Y1
        AZ=Z2-Z1
        AXY=SQRT(AX*AX+AY*AY)
        IF(AXY.EQ.0.) GOTO 20
        XR=(AX*AX*X0+AY*AY*X1+AX*AY*(Y0-Y1))/AXY/AXY
        YR=(AY*AY*Y0+AX*AX*Y1+AX*AY*(X0-X1))/AXY/AXY
        CX=XR-X0
        CY=YR-Y0
        CXY=SQRT(CX*CX+CY*CY)
        IF(CXY.GE.RI) THEN
          GOTO 20
        ENDIF
        DXYPAXY=SQRT(RI*RI-CXY*CXY)/AXY
        DX=AX*DXYPAXY
        DY=AY*DXYPAXY
        XIOUT=XR+DX
        YIOUT=YR+DY
        IF((X2-X1).EQ.0.) THEN
          IF((Y2-Y1).EQ.0.) GOTO 20
          ZIOUT=(YIOUT-Y1)*(Z2-Z1)/(Y2-Y1)+Z1
        ELSE
          ZIOUT=(XIOUT-X1)*(Z2-Z1)/(X2-X1)+Z1
        ENDIF
        X2=XIOUT
        Y2=YIOUT
        Z2=ZIOUT
        TH1=0.
        PHA11=0.
        RFREEIL=SQRT((X2-X1)*(X2-X1)+(Y2-Y1)*(Y2-Y1)+(Z2-Z1)*(Z2-Z1))
        ETAU=ETAU*EXP(-TAUIH20*RFREEIL/10.)
        GOTO 930
      ENDIF
      ETAU=ETAU*EXP(-TAUIH20*RFREE/10.)
      RAN=RANSU(9)
      CALL NEWRANSU(RAN, UNIRAN)
      RANSU(9)=RAN
      FISCAT=.FALSE.
      IF(UNIRAN.LT.VPER) FISCAT=.TRUE.
      IF(FISCAT) THEN
c the part of disiding scattering angle (SIGINCI, MEWI, PITHOMSI, PIKLNISI)
C----- Kind of interaction with atom in iodine -----

```

```

      FINCOH=. FALSE.
      RAN=RANSU(7)
      CALL NEWRANSU(RAN, UNIRAN)
      RANSU(7)=RAN
C      (Tomson scattering or Compton scattering ?)
      IF (UNIRAN.LT.SIGINCI/MEWI) FINCOH=. TRUE.
      RAN=RANSU(9)
      CALL NEWRANSU(RAN, UNIRAN)
      RANSU(9)=RAN
C      ( Scattering angle )
      TH1=0.
      IF(EPH.EQ.33.17) THEN
        LI=0
        GOTO 1065
      ENDIF
C      ( If photon energy is 33.17keV then use PII9951.DAT data )
      IF(EPH.EQ.99.51) THEN
        LI=1
        GOTO 1065
      ENDIF
C      ( If photon energy is 99.51keV then use PII9951.DAT data )
      LI=INT(EPH)
1065  CONTINUE
C..... Thomson scattering .....
      IF (FINCOH) THEN
        CINC=CINC+1
        DO 1072 K2=1, 10
          UNIP1=PIKLNISI(LI, K2*100)/PIKLNISI(LI, NTH)
          IF (UNIRAN.LE.UNIP1) THEN
            K100=(K2-1)*100
            GOTO 1092
          ENDIF
1072  CONTINUE
1092  CONTINUE
        DO 1071 K1=1, 10
          UNIP1=PIKLNISI(LI, K100+K1*10)/PIKLNISI(LI, NTH)
          IF (UNIRAN.LE.UNIP1) THEN
            K10=(K1-1)*10
            GOTO 1091
          ENDIF
1071  CONTINUE
1091  CONTINUE
        DO 1070 K=1, 10
          UNIP1=PIKLNISI(LI, K100+K10+K)/PIKLNISI(LI, NTH)
          IF (UNIRAN.LE.UNIP1) THEN
            TH1=THM(K100+K10+K)
            GOTO 1090
          ENDIF
1070  CONTINUE
1090  CONTINUE
          EPH0=EPH
          EPH=EPH/(1+EPH*1000./ME*(1-COS(TH1)))
          IF (EPH.LE.LOSEPH) THEN
C      ( if energy < min energy , photon is lost )
            FELOS=. TRUE.
            GOTO 20
          ENDIF
          EE0E0E=EPH/EPH0+EPH0/EPH
          CALL PHAI COMPT(TH1, PHAI1, RANSU, EE0E0E, FNOPOL)
        ELSE
C..... Thomson scattering .....
          CCOH=CCOH+1
          DO 1082 K2=1, 10
            UNIP1=PITHOMSI(LI, K2*100)/PITHOMSI(LI, NTH)
            IF (UNIRAN.LE.UNIP1) THEN
              K100=(K2-1)*100
              GOTO 1032
            ENDIF
1082  CONTINUE
1032  CONTINUE
          DO 1081 K1=1, 10
            UNIP1=PITHOMSI(LI, K100+K1*10)/PITHOMSI(LI, NTH)
            IF (UNIRAN.LE.UNIP1) THEN
              K10=(K1-1)*10
              GOTO 1031
            ENDIF

```

```

1081   ENDIF
1031   CONTINUE
      CONTINUE
      DO 1080 K=1, 10
        UNIP1=PITHOMSI(LI, K100+K10+K)/PITHOMSI(LI, NTH)
        IF (UNIRAN. LE. UNIP1) THEN
          TH1=THM(K100+K10+K)
          GOTO 1033
        ENDIF
1080   CONTINUE
1033   CONTINUE
      CALL PHAITHOMS(TH1, PHA11, RANSU, FNOPOL)
ENDIF
ELSE
c the part of disiding scattering angle (SIGINCH20, MEWH20, PITHOMSH20, PIKLNISH20)
C----- Kind of interaction with atom in H2O -----
      FINCOH=. FALSE.
      RAN=RANSU(7)
      CALL NEWRANSU(RAN, UNIRAN)
      RANSU(7)=RAN
C      (Tomson scattering or Compton scattering ?)
      IF (UNIRAN. LT. SIGINCH20/MEWH20) FINCOH=. TRUE.
      RAN=RANSU(9)
      CALL NEWRANSU(RAN, UNIRAN)
      RANSU(9)=RAN
C      ( Scattering angle )
      TH1=0.
      IF(EPH. EQ. 33. 17) THEN
        LI=0
        GOTO 2065
      ENDIF
C      ( If photon energy is 33. 17keV then use PI9951. DAT data )
      IF(EPH. EQ. 99. 51) THEN
        LI=1
        GOTO 2065
      ENDIF
C      ( If photon energy is 99. 51keV then use PI9951. DAT data )
      LI=INT(EPH)
2065   CONTINUE
C..... Compton scattering .....
      IF (FINCOH) THEN
        CINC=CINC+1
        DO 2072 K2=1, 10
          UNIP1=PIKLNISH20(LI, K2*100)/PIKLNISH20(LI, NTH)
          IF (UNIRAN. LE. UNIP1) THEN
            K100=(K2-1)*100
            GOTO 2092
          ENDIF
2072   CONTINUE
2092   CONTINUE
        DO 2071 K1=1, 10
          UNIP1=PIKLNISH20(LI, K100+K1*10)/PIKLNISH20(LI, NTH)
          IF (UNIRAN. LE. UNIP1) THEN
            K10=(K1-1)*10
            GOTO 2091
          ENDIF
2071   CONTINUE
2091   CONTINUE
        DO 2070 K=1, 10
          UNIP1=PIKLNISH20(LI, K100+K10+K)/PIKLNISH20(LI, NTH)
          IF (UNIRAN. LE. UNIP1) THEN
            TH1=THM(K100+K10+K)
            GOTO 2090
          ENDIF
2070   CONTINUE
2090   CONTINUE
          EPH0=EPH
          EPH=EPH/(1+EPH*1000. /ME*(1-COS(TH1)))
          IF (EPH. LE. LOSEPH) THEN
C      ( if energy < min energy , photon is lost )
            FELOS=. TRUE.
            GOTO 20
          ENDIF
          EE0E0E=EPH/EPH0+EPH0/EPH
          CALL PHAICOMPT(TH1, PHA11, RANSU, EE0E0E, FNOPOL)

```

```

ELSE
C..... Thomson scattering .....
    CCOH=CCOH+1
    DO 2082 K2=1, 10
        UNIP1=PITHOMSH20(LI, K2*100)/PITHOMSH20(LI, NTH)
        IF (UNIRAN. LE. UNIP1) THEN
            K100=(K2-1)*100
            GOTO 2032
        ENDIF
2082 CONTINUE
2032 CONTINUE
    DO 2081 K1=1, 10
        UNIP1=PITHOMSH20(LI, K100+K1*10)/PITHOMSH20(LI, NTH)
        IF (UNIRAN. LE. UNIP1) THEN
            K10=(K1-1)*10
            GOTO 2031
        ENDIF
2081 CONTINUE
2031 CONTINUE
    DO 2080 K=1, 10
        UNIP1=PITHOMSH20(LI, K100+K10+K)/PITHOMSH20(LI, NTH)
        IF (UNIRAN. LE. UNIP1) THEN
            TH1=THM(K100+K10+K)
            GOTO 2033
        ENDIF
2080 CONTINUE
2033 CONTINUE
        CALL PHAITHOMS(TH1, PHA11, RANSU, FNOPOL)
    ENDIF
    ENDIF
    GOTO 910
C----- flouresent genereting in Iodine -----
920 CONTINUE
    DORS=' F'
    F2J=. FALSE.
    X1=X1F
    Y1=Y1F
    Z1=Z1F
    X2=X2F
    Y2=Y2F
    Z2=Z2F
    EPH=EPHF
    ETAU=ETAUF
    TH1=0.
    PHA11=0.
    LEPH=LOG10(EPH)
    IF(EPH. GE. 33. 17) THEN
        TAU1=FTAU1OK(LEPH)
    ELSE
        TAU1=FTAU1BK(LEPH)
    ENDIF
    TAU1=10. **TAU1*ROUI
7030 CONTINUE
    RAN=RANSU(9)
    CALL NEWRANSU(RAN, UNIRAN)
    RANSU(9)=RAN
    IF(UNIRAN. EQ. 0. ) GOTO 7030
    RFREE=-10. /TAU1/VPER*ALOG(UNIRAN)
    ( RFREE UNIT mm )
C
C----- Compute next point -----
    OMEGA0D=0.
    CALL NEWCOORD (X1, Y1, Z1, X2, Y2, Z2, E0X, E0Y, E0Z, RFREE, TH1, PHA11
    % , OMEGA0D)
    IF(OMEGA0D. NE. 0. ) GOTO 20
C-----
    RFRIC=SQRT((X2-X0)*(X2-X0)+(Y2-Y0)*(Y2-Y0))
    IF(RFRIC. GE. R1) GOTO 20
    RAN=RANSU(9)
    CALL NEWRANSU(RAN, UNIRAN)
    RANSU(9)=RAN
    IF(UNIRAN. GE. OMEGAKI) GOTO 20
    RAN=RANSU(9)
    CALL NEWRANSU(RAN, UNIRAN)
    RANSU(9)=RAN
    TH1=UNIRAN*PI

```

```

RAN=RANSU(7)
CALL NEWRANSU(RAN, UNIRAN)
RANSU(7)=RAN
  PHA11=(UNIRAN-. 5)*2*PI
LEPH=LOG10(EPH)
SIGCOH1=FSIGCOH1(LEPH)
SIGINCI=FSIGINCI(LEPH)
TAUH20=FTAUH20(LEPH)
SIGCOHH20=FSIGCOHH20(LEPH)
SIGINCH20=FSIGINCH20(LEPH)
SIGCOH1=10. **SIGCOH1*ROUI
SIGINCI=10. **SIGINCI*ROUI
TAUH20=10. **TAUH20
SIGCOHH20=10. **SIGCOHH20
SIGINCH20=10. **SIGINCH20
MEW1=SIGCOH1+SIGINCI
MEWH20=TAUH20+SIGCOHH20+SIGINCH20
MEWFLOUR=MEW1*VPER+MEWH20*(1. -VPER)
ETAU=ETAU*EXP(-MEWFLOUR*RFREE)
C----- deciding flourecent photon energy -----
RAN=RANSU(9)
CALL NEWRANSU(RAN, UNIRAN)
RANSU(9)=RAN
  IF(UNIRAN.LT. RIKAKA1) THEN
    EPH=EIKA2
  ELSE
    IF(UNIRAN.LT. RIKAIKB1) THEN
      EPH=EIKAI
    ELSE
      IF(UNIRAN.LT. RIKB1KB2) THEN
        EPH=EIKB1
      ELSE
        EPH=EIKB2
      ENDIF
    ENDIF
  ENDIF
C----- No-polarization set -----
  FNOPOL=. TRUE.
C-----
  GOTO 910
C----- unless photon pass through iodine artery, come here -----
  900 CONTINUE
C----- In the water or not ? -----
  FWOUT=. FALSE.
  IF (X2. GE. XH2OU) FWOUT=. TRUE.
  IF (X2. LE. XH2OD) FWOUT=. TRUE.
  IF (Y2. GE. YH2OU) FWOUT=. TRUE.
  IF (Y2. LE. YH2OD) FWOUT=. TRUE.
  IF (Z2. GE. ZH2OU) FWOUT=. TRUE.
  IF (Z2. LE. ZH2OD) FWOUT=. TRUE.
  IF (FWOUT) GOTO 40
  IF(DORS. EQ. 'D') DORS='S'
C----- Through rate by photo-electron -----
  ETAU=ETAU*EXP(-TAU*RFREE/10.)
C----- Kind of interaction with atom -----
  FINCOH=. FALSE.
  LEPH=LOG10(EPH)
  TAU=FTAU(LEPH)
  SIGCOH=FSIGCOH(LEPH)
  SIGINC=FSIGINC(LEPH)
  TAU=10. **TAU*ROUACL
  SIGCOH=10. **SIGCOH*ROUACL
  SIGINC=10. **SIGINC*ROUACL
  MEW=SIGCOH+SIGINC
  RAN=RANSU(7)
  CALL NEWRANSU(RAN, UNIRAN)
  RANSU(7)=RAN
C (Tomson scattering or Compton scattering ?)
  IF (UNIRAN.LT. SIGINC/MEW) FINCOH=. TRUE.
  RAN=RANSU(9)
  CALL NEWRANSU(RAN, UNIRAN)
  RANSU(9)=RAN
C ( Scattering angle )
  TH1=0.
  IF(EPH. EQ. 33.17) THEN

```

```

      LI=0
      GOTO 65
    ENDIF
C    ( If photon energy is 99.51keV then use PIAC9951.DAT data )
    IF(EPH.EQ.99.51) THEN
      LI=1
      GOTO 65
    ENDIF
C    ( If photon energy is 99.51keV then use PIAC9951.DAT data )
    LI=INT(EPH)
65   CONTINUE
C..... Compton scattering .....
    IF (FINCOH) THEN
      CINC=CINC+1
      DO 72 K2=1,10
        UNIP1=PIKLNIS(LI,K2*100)/PIKLNIS(LI,NTH)
        IF (UNIRAN.LE.UNIP1) THEN
          K100=(K2-1)*100
          GOTO 92
        ENDIF
72   CONTINUE
92   CONTINUE
      DO 71 K1=1,10
        UNIP1=PIKLNIS(LI,K100+K1*10)/PIKLNIS(LI,NTH)
        IF (UNIRAN.LE.UNIP1) THEN
          K10=(K1-1)*10
          GOTO 91
        ENDIF
71   CONTINUE
91   CONTINUE
      DO 70 K=1,10
        UNIP1=PIKLNIS(LI,K100+K10+K)/PIKLNIS(LI,NTH)
        IF (UNIRAN.LE.UNIP1) THEN
          TH1=THM(K100+K10+K)
          GOTO 90
        ENDIF
70   CONTINUE
90   CONTINUE
      EPH0=EPH
      EPH=EPH/(1+EPH*1000./ME*(1-COS(TH1)))
      IF (EPH.LE.LOSEPH) THEN
C    ( if energy < min energy , photon is lost )
        FELOS=.TRUE.
        GOTO 20
      ENDIF
      EEQEOE=EPH/EPH0+EPH0/EPH
      CALL PHAICOMPT(TH1,PHAI1,RANSU,EEQEOE,FNOPOL)
    ELSE
C..... Thomson scattering .....
      CCOH=CCOH+1
      DO 82 K2=1,10
        UNIP1=PITHOMS(LI,K2*100)/PITHOMS(LI,NTH)
        IF (UNIRAN.LE.UNIP1) THEN
          K100=(K2-1)*100
          GOTO 32
        ENDIF
82   CONTINUE
32   CONTINUE
      DO 81 K1=1,10
        UNIP1=PITHOMS(LI,K100+K1*10)/PITHOMS(LI,NTH)
        IF (UNIRAN.LE.UNIP1) THEN
          K10=(K1-1)*10
          GOTO 31
        ENDIF
81   CONTINUE
31   CONTINUE
      DO 80 K=1,10
        UNIP1=PITHOMS(LI,K100+K10+K)/PITHOMS(LI,NTH)
        IF (UNIRAN.LE.UNIP1) THEN
          TH1=THM(K100+K10+K)
          GOTO 33
        ENDIF
80   CONTINUE
33   CONTINUE
      CALL PHAITHOMS(TH1,PHAI1,RANSU,FNOPOL)

```

```

ENDIF
30 CONTINUE
C----- Count photons which come out yet -----
GOTO 20
40 CONTINUE
C----- Foward scattering or Back scattering ? -----
IF (X2. LE. X1) THEN
C ( Out of water and foward scattering then go next flow )
GOTO 20
ENDIF
C----- Position on the ditector -----
XBAI=(XGRID-X1)/(X2-X1)
YGRID=Y1+XBAI*(Y2-Y1)
ZGRID=Z1+XBAI*(Z2-Z1)
C----- In the ditector or not ? -----
FGOUT=. FALSE.
IF(YGRID. GE. YGRIDU) FGOUT=. TRUE.
IF(YGRID. LE. YGRIDD) FGOUT=. TRUE.
IF(ZGRID. GE. ZGRIDU) FGOUT=. TRUE.
IF(ZGRID. LE. ZGRIDD) FGOUT=. TRUE.
IF (FGOUT) THEN
GOTO 20
ENDIF
C----- Calculate the last running distanse in the water -----
XBAIW=(XH2OU-X1)/(X2-X1)
XWEND=XH2OU
YWEND=Y1+XBAIW*(Y2-Y1)
ZWEND=Z1+XBAIW*(Z2-Z1)
LRUN=SQRT((XWEND-X1)*(XWEND-X1)+(YWEND-Y1)*(YWEND-Y1)
% +(ZWEND-Z1)*(ZWEND-Z1))
C----- Calculate through rate by last phot-electron -----
etaubak=etau
ETAU=ETAU*EXP(-TAU*LRUN/10.)
c IF(ETAU.LT..0000001) GOTO 20
C----- Position on the ditector -----
XBAI=(XEND-X1)/(X2-X1)
YEND=Y1+XBAI*(Y2-Y1)
ZEND=Z1+XBAI*(Z2-Z1)
C----- In the ditector face or not ? -----
FDOUT=. FALSE.
IF(YEND. GE. YDETU) FDOUT=. TRUE.
IF(YEND. LE. YDETD) FDOUT=. TRUE.
IF(ZEND. GE. ZDETU) FDOUT=. TRUE.
IF(ZEND. LE. ZDETD) FDOUT=. TRUE.
IF (FDOUT) THEN
GOTO 7000
ENDIF
c!!!!!!!!!!!!!!!!!! II response plus !!!!!!!!!!!!!!!!!!!!!!!!!!!!!!!!!!!!!!!!!!!!!!!
c
IF(EPH.LT.EPH12) THEN
PSL=FI IRES1(EPH)
ELSE
IF(EPH.LT.EPH23) THEN
PSL=FI IRES2(EPH)
ELSE
IF(EPH.LT.EPH34) THEN
PSL=FI IRES3(EPH)
ELSE
PSL=FI IRES4(EPH)
ENDIF
ENDIF
ENDIF
c
c!!!!!!!!!!!!!!!!!!!!!!!!!!!!!!!!!!!!!!!!!!!!!!!!!!!!!!!!!!!!!!!!!!!!!!!!!!!!!!!!!!!!
c!!!!!!!!!!!!!!!!!!!!!!!!!!!!!!!!!!!!!!!!!!!!!!!!!!!!!!!!!!!!!!!!!!!!!!!!!!!!!!!!!!!!
cXXXXXXXXXXXXXXXXXXXXXXXXXXXXXXXXXXXXXXXXXXXXXXXXXXXXXXXXXXXXXXXXXXXXXXXXXXXX
XSCR=INT((YEND+YDET/2.)/YDET*XSCRMAX)+1
YSCR=INT((ZEND+ZDET/2.)/ZDET*YSCRMAX)+1
IF(XSCR.LT.1) goto 8000
IF(YSCR.LT.1) goto 8000
IF(XSCR.GT.INT(XSCRMAX)) goto 8000
IF(YSCR.GT.INT(YSCRMAX)) goto 8000
DENSENG(XSCR, YSCR)=DENSENG(XSCR, YSCR)+ETAU*PSL/PSLOR
cXXXXXXXXXXXXXXXXXXXXXXXXXXXXXXXXXXXXXXXXXXXXXXXXXXXXXXXXXXXXXXXXXXXXXXXXXXXX
Ccccccccccccccc Photon count in front of the Grid ccccccccccccccccccc
IF(EPHOR.EQ.'3') THEN

```

```

IF(DORS. EQ. 'S') THEN
  FIBIN=. FALSE.
  IF((YGRID. LE. WIB2U). AND. (YGRID. GE. WIB2D). AND.
%   (ZGRID. LE. HIB2U). AND. (ZGRID. GE. HIB2D)) FIBIN=. TRUE.
  IF (FIBIN) THEN
    FIARTIN=. FALSE.
    IF((YGRID. LE. WIARTU). AND. (YGRID. GE. WIARTD)) FIARTIN=. TRUE.
    IF(FIARTIN) THEN
      CS3I=CS3I+1
      ETAUTS3I=ETAUTS3I+ETAU
      ETAUTS3IPSL=ETAUTS3IPSL+ETAU*PSL/PSLOR
    ELSE
      CS3B=CS3B+1
      ETAUTS3B=ETAUTS3B+ETAU
      ETAUTS3BPSL=ETAUTS3BPSL+ETAU*PSL/PSLOR
    ENDIF
  ENDIF
ENDIF
ENDIF
IF(DORS. EQ. 'D') THEN
  FIBIN=. FALSE.
  IF((YGRID. LE. WIB2U). AND. (YGRID. GE. WIB2D). AND.
%   (ZGRID. LE. HIB2U). AND. (ZGRID. GE. HIB2D)) FIBIN=. TRUE.
  IF (FIBIN) THEN
    FIARTIN=. FALSE.
    IF((YGRID. LE. WIARTU). AND. (YGRID. GE. WIARTD)) FIARTIN=. TRUE.
    IF(FIARTIN) THEN
      CD3I=CD3I+1
      ETAUTD3I=ETAUTD3I+ETAU
      ETAUTD3IPSL=ETAUTD3IPSL+ETAU*PSL/PSLOR
    ELSE
      CD3B=CD3B+1
      ETAUTD3B=ETAUTD3B+ETAU
      ETAUTD3BPSL=ETAUTD3BPSL+ETAU*PSL/PSLOR
    ENDIF
  ENDIF
ENDIF
ENDIF
IF(DORS. EQ. 'I') THEN
  FIBIN=. FALSE.
  IF((YGRID. LE. WIB2U). AND. (YGRID. GE. WIB2D). AND.
%   (ZGRID. LE. HIB2U). AND. (ZGRID. GE. HIB2D)) FIBIN=. TRUE.
  IF (FIBIN) THEN
    FIARTIN=. FALSE.
    IF((YGRID. LE. WIARTU). AND. (YGRID. GE. WIARTD)) FIARTIN=. TRUE.
    IF(FIARTIN) THEN
      C13I=C13I+1
      ETAUTI3I=ETAUTI3I+ETAU
      ETAUTI3IPSL=ETAUTI3IPSL+ETAU*PSL/PSLOR
    ELSE
      C13B=C13B+1
      ETAUTI3B=ETAUTI3B+ETAU
      ETAUTI3BPSL=ETAUTI3BPSL+ETAU*PSL/PSLOR
    ENDIF
  ENDIF
ENDIF
ENDIF
IF(DORS. EQ. 'F') THEN
  FIBIN=. FALSE.
  IF((YGRID. LE. WIB2U). AND. (YGRID. GE. WIB2D). AND.
%   (ZGRID. LE. HIB2U). AND. (ZGRID. GE. HIB2D)) FIBIN=. TRUE.
  IF (FIBIN) THEN
    FIARTIN=. FALSE.
    IF((YGRID. LE. WIARTU). AND. (YGRID. GE. WIARTD)) FIARTIN=. TRUE.
    IF(FIARTIN) THEN
      CF3I=CF3I+1
      ETAUTF3I=ETAUTF3I+ETAU
      ETAUTF3IPSL=ETAUTF3IPSL+ETAU*PSL/PSLOR
    ELSE
      CF3B=CS3B+1
      ETAUTF3B=ETAUTF3B+ETAU
      ETAUTF3BPSL=ETAUTF3BPSL+ETAU*PSL/PSLOR
    ENDIF
  ENDIF
ENDIF
ENDIF
ELSE
  IF(DORS. EQ. 'S') THEN
    FIBIN=. FALSE.

```

```

% IF((YGRID. LE. WIB2U). AND. (YGRID. GE. WIB2D). AND.
(ZGRID. LE. HIB2U). AND. (ZGRID. GE. HIB2D)) FIBIN=. TRUE.
IF (FIBIN) THEN
FIARTIN=. FALSE.
IF((YGRID. LE. WIARTU). AND. (YGRID. GE. WIARTD)) FIARTIN=. TRUE.
IF(FIARTIN) THEN
CS9I=CS9I+1
ETAUTS9I=ETAUTS9I+ETAU
ETAUTS9IPSL=ETAUTS9IPSL+ETAU*PSL/PSLOR
ELSE
CS9B=CS9B+1
ETAUTS9B=ETAUTS9B+ETAU
ETAUTS9BPSL=ETAUTS9BPSL+ETAU*PSL/PSLOR
ENDIF
ENDIF
ENDIF
IF(DORS. EQ. ' D ' ) THEN
FIBIN=. FALSE.
% IF((YGRID. LE. WIB2U). AND. (YGRID. GE. WIB2D). AND.
(ZGRID. LE. HIB2U). AND. (ZGRID. GE. HIB2D)) FIBIN=. TRUE.
IF (FIBIN) THEN
FIARTIN=. FALSE.
IF((YGRID. LE. WIARTU). AND. (YGRID. GE. WIARTD)) FIARTIN=. TRUE.
IF(FIARTIN) THEN
CD9I=CD9I+1
ETAUTD9I=ETAUTD9I+ETAU
ETAUTD9IPSL=ETAUTD9IPSL+ETAU*PSL/PSLOR
ELSE
CD9B=CD9B+1
ETAUTD9B=ETAUTD9B+ETAU
ETAUTD9BPSL=ETAUTD9BPSL+ETAU*PSL/PSLOR
ENDIF
ENDIF
ENDIF
IF(DORS. EQ. ' I ' ) THEN
FIBIN=. FALSE.
% IF((YGRID. LE. WIB2U). AND. (YGRID. GE. WIB2D). AND.
(ZGRID. LE. HIB2U). AND. (ZGRID. GE. HIB2D)) FIBIN=. TRUE.
IF (FIBIN) THEN
FIARTIN=. FALSE.
IF((YGRID. LE. WIARTU). AND. (YGRID. GE. WIARTD)) FIARTIN=. TRUE.
IF(FIARTIN) THEN
CI9I=CI9I+1
ETAUTI9I=ETAUTI9I+ETAU
ETAUTI9IPSL=ETAUTI9IPSL+ETAU*PSL/PSLOR
ELSE
CI9B=CI9B+1
ETAUTI9B=ETAUTI9B+ETAU
ETAUTI9BPSL=ETAUTI9BPSL+ETAU*PSL/PSLOR
ENDIF
ENDIF
ENDIF
IF(DORS. EQ. ' F ' ) THEN
FIBIN=. FALSE.
% IF((YGRID. LE. WIB2U). AND. (YGRID. GE. WIB2D). AND.
(ZGRID. LE. HIB2U). AND. (ZGRID. GE. HIB2D)) FIBIN=. TRUE.
IF (FIBIN) THEN
FIARTIN=. FALSE.
IF((YGRID. LE. WIARTU). AND. (YGRID. GE. WIARTD)) FIARTIN=. TRUE.
IF(FIARTIN) THEN
CF9I=CF9I+1
ETAUTF9I=ETAUTF9I+ETAU
ETAUTF9IPSL=ETAUTF9IPSL+ETAU*PSL/PSLOR
ELSE
CF9B=CF9B+1
ETAUTF9B=ETAUTF9B+ETAU
ETAUTF9BPSL=ETAUTF9BPSL+ETAU*PSL/PSLOR
ENDIF
ENDIF
ENDIF
ENDIF
8000 continue
$$$$$$$$$$$$$$$$$$$$ Grid Passing Routine $$$$$$$$$$$$$$$$$$$$$$
7000 CONTINUE
GOTO 1020

```

C----- flourescent genereting in Pb -----

1010 CONTINUE

IF(DPB.EQ.0.) GOTO 20

DORS= G

F2JG=.FALSE.

X1=X1FG

Y1=Y1FG

Z1=Z1FG

X2=X2FG

Y2=Y2FG

Z2=Z2FG

EPH=EPHFG

ETAU=ETAUFG

TH1=0.

PHAI1=0.

CALL AHEADPASS(X1, Y1, Z1, X2, Y2, Z2, NBL,

% LWOI, LWOI, LWOF, LWOM, LWO, LPBI, LPBF, LPBM, LPB)

IF(LPB.EQ.0.) GOTO 20

LEPH=LOG10(EPH)

TAUPB=FTAUPBK(LEPH)

TAUPB=10.\*\*TAUPB\*ROUPB

TAUWO=FTAUWO(LEPH)

TAUWO=10.\*\*TAUWO\*ROUWO

LPBEQ=LPB\*TAUPB/TAUWO

LEQ=LWO+LPBEQ

C----- Decide of free run length -----

RAN=RANSU(9)

CALL NEWRANSU(RAN, UNIRAN)

RANSU(9)=RAN

RFREE=-10./TAUWO\*ALOG(UNIRAN)

C ( RFREE UNIT mm )

C-----

IF(RFREE.GE.LEQ) GOTO 20

CALL XPOSITION(RFREE, TAUWO, TAUPB, NBL, X1, Y1, Z1, X2, Y2, Z2,

% LWOI, LWOI, LWOF, LWOM, LWO, LPBI, LPBF, LPBM, LPB)

C-----

NBL1=INT(Y1/DBL)

POBL1=Y1-DBL\*REAL(NBL1)

FINWO=.FALSE.

IF(POBL1.LT.DWO) FINWO=.TRUE.

IF(FINWO) GOTO 20

RAN=RANSU(9)

CALL NEWRANSU(RAN, UNIRAN)

RANSU(9)=RAN

IF(UNIRAN.GE.OMEGAKPB) GOTO 20

LEPH=LOG10(EPH)

SIGCOHPB=FSIGCOHPB(LEPH)

SIGINCPB=FSIGINCPB(LEPH)

SIGCOHWO=FSIGCOHWO(LEPH)

SIGINCWO=FSIGINCWO(LEPH)

SIGCOHPB=10.\*\*SIGCOHPB\*ROUPB

SIGINCPB=10.\*\*SIGINCPB\*ROUPB

SIGCOHWO=10.\*\*SIGCOHWO\*ROUWO

SIGINCWO=10.\*\*SIGINCWO\*ROUWO

MEWPB=SIGCOHPB+SIGINCPB

MEWWO=SIGCOHWO+SIGINCWO

MEWFLOURG=MEWPB\*LPB+MEWWO\*LWO

ETAU=ETAU\*EXP(-MEWFLOURG\*RFREE)

RAN=RANSU(9)

CALL NEWRANSU(RAN, UNIRAN)

RANSU(9)=RAN

TH1=UNIRAN\*PI

RAN=RANSU(7)

CALL NEWRANSU(RAN, UNIRAN)

RANSU(7)=RAN

PHAI1=(UNIRAN-.5)\*2\*PI

C----- Compute next point -----

OMEGAOD=0.

CALL NEWCOORD (X1, Y1, Z1, X2, Y2, Z2, EOX, EOY, EOZ, RFREE, TH1, PHAI1

% , OMEGAOD)

IF(OMEGAOD.NE.0.) GOTO 20

C----- deciding flourescent photon energy -----

RAN=RANSU(9)

CALL NEWRANSU(RAN, UNIRAN)

RANSU(9)=RAN

```

IF(UNIRAN.LT.RPBKA2KA1) THEN
  EPH=EPBKA2
ELSE
  IF(UNIRAN.LT.RPBKA1KB3) THEN
    EPH=EPBKA1
  ELSE
    IF(UNIRAN.LT.RPBKB3KB1) THEN
      EPH=EPBKB3
    ELSE
      IF(UNIRAN.LT.RPBKB1KB2) THEN
        EPH=EPBKB1
      ELSE
        EPH=EPBKB2
      ENDIF
    ENDIF
  ENDIF
ENDIF
ENDIF
C----- No-polarization set -----
      FNOPOL=.TRUE.
C-----
c+++++
1020  CONTINUE
      IF(EPH.GE.88.) THEN
        F2JG=.TRUE.
        X1FG=X1
        Y1FG=Y1
        Z1FG=Z1
        X2FG=X2
        Y2FG=Y2
        Z2FG=Z2
        EPHFG=EPH
        ETAUFG=ETAU
      ENDIF
c..... correct from XWEND to XGRID .....
        X2=XGRID
        Y2=YGRID
        Z2=ZGRID
c.....
1000  CONTINUE
      IF(X1.EQ.X2) THEN
        GOTO 20
      ENDIF
      IF(X1.LT.X2) THEN
        CALL AHEADPASS(X1, Y1, Z1, X2, Y2, Z2, NBL,
%           LW01, LW0F, LW0M, LW0, LPB1, LPBF, LPBM, LPB)
      ELSE
        CALL BACKPASS(X1, Y1, Z1, X2, Y2, Z2, NBL,
%           LW01, LW0F, LW0M, LW0, LPB1, LPBF, LPBM, LPB)
      ENDIF
C-----
      LEPH=LOG10(EPH)
      TAUWO=FTAUWO(LEPH)
      SIGCOHWO=FSIGCOHWO(LEPH)
      SIGINCWO=FSIGINCWO(LEPH)
      TAUWO=10.**TAUWO*ROUWO
      SIGCOHWO=10.**SIGCOHWO*ROUWO
      SIGINCWO=10.**SIGINCWO*ROUWO
      MEWWO=SIGCOHWO+SIGINCWO
C.....
      IF(EPH.GT.88.00) THEN
        TAUPB=FTAUPBK(LEPH)
      ELSE
        IF(EPH.GT.15.86) THEN
          TAUPB=FTAUPBL1(LEPH)
        ELSE
          IF(EPH.GT.15.20) THEN
            TAUPB=FTAUPBL2(LEPH)
          ELSE
            IF(EPH.GT.13.04) THEN
              TAUPB=FTAUPBL3(LEPH)
            ELSE
              TAUPB=FTAUPBM1(LEPH)
            ENDIF
          ENDIF
        ENDIF
      ENDIF

```

```

C      ENDIF
C      SIGCOHPB=FSIGCOHPB(LEPH)
C      SIGINCPB=FSIGINCPB(LEPH)
C-----
C      TAUPB=10. **TAUPB*ROUPB
C      SIGCOHPB=10. **SIGCOHPB*ROUPB
C      SIGINCPB=10. **SIGINCPB*ROUPB
C      MEWPB=SIGCOHPB+SIGINCPB
C-----
C      LPBEQ=LPB*MEWPB/MEWVO
C      LEQ=LWO+LPBEQ
C-----
C      Decide of free run length -----
C      RAN=RANSU(9)
C      CALL NEWRANSU(RAN, UNIRAN)
C      RANSU(9)=RAN
C      RFREE=-10. /MEWVO*ALOG(UNIRAN)
C      ( RFREE UNIT mm )
C-----
C      IF (RFREE. LT. LEQ) THEN
%      CALL XPOSITION(RFREE, MEWVO, MEWPB, NBL, X1, Y1, Z1, X2, Y2, Z2,
%      LW01, LWO, LWOM, LWO, LPB1, LPBF, LPBM, LPB)
C      ETAU=ETAU*EXP(-TAUWO*LWO/10. -TAUPB*LPB/10. )
C      IF (ETAU. LT. 1. E-8) THEN
C      GOTO 20
C      ENDIF
C-----
C      CALL SCANGLE(TH1, PHA11, EPH, FELOS, Y1, FNOPL)
C      IF(FELOS) THEN
C      GOTO 20
C      ENDIF
C-----
C      Compute ahead point -----
C      AX=X2-X1
C      AY=Y2-Y1
C      AZ=Z2-Z1
C      DA=SQRT(AX*AX+AY*AY+AZ*AZ)
C      IF(DA. LE. 0. ) THEN
C      GOTO 20
C      ENDIF
C-----
C      Compute next point -----
C      OMEGA0D=0.
C      CALL NEWCOORD (X1, Y1, Z1, X2, Y2, Z2, EOX, EOY, EOZ, RDAMMY, TH1, PHA11
%      , OMEGA0D)
C      IF(OMEGA0D. NE. 0. ) GOTO 20
C-----
C      E-Bector deciding -----
C      KX=X2-X1
C      KY=Y2-Y1
C      KZ=Z2-Z1
C      CALL EDECIDE(EOX, EOY, EOZ, KX, KY, KZ, E1X, E1Y, E1Z, DELTA0D)
C      IF(DELTA0D. EQ. 1. ) GOTO 20
C      EOX=E1X
C      EOY=E1Y
C      EOZ=E1Z
C-----
C      X3=X1-(X2-X1)
C      Y3=Y1-(Y2-Y1)
C      Z3=Z1-(Z2-Z1)
C      X2=X1
C      Y2=Y1
C      Z2=Z1
C      X1=X3
C      Y1=Y3
C      Z1=Z3
C      GOTO 1000
C      ENDIF
C      IF(X1. GE. X2) THEN
C      GOTO 20
C      ENDIF
C-----
C      Position on the ditector -----
C      XBAl=(XEND-X1)/(X2-X1)
C      YEND=Y1+XBAl*(Y2-Y1)
C      ZEND=Z1+XBAl*(Z2-Z1)
C-----
C      In the ditector face or not ? -----
C      FDOU=. FALSE.
C      IF(YEND. GE. YDETU) FDOU=. TRUE.

```



```

% IF((YEND. LE. WIB2U). AND. (YEND. GE. WIB2D). AND.
  (ZEND. LE. HIB2U). AND. (ZEND. GE. HIB2D)) FIBIN=. TRUE.
  IF (FIBIN) THEN
    FIARTIN=. FALSE.
    IF((YEND. LE. WIARTU). AND. (YEND. GE. WIARTD)) FIARTIN=. TRUE.
    IF(FIARTIN) THEN
      CGI3I=CGI3I+1
      ETAUTGI3I=ETAUTGI3I+ETAU
      ETAUTGI3IPSL=ETAUTGI3IPSL+ETAU*PSL/PSLOR
    ELSE
      CGI3B=CGI3B+1
      ETAUTGI3B=ETAUTGI3B+ETAU
      ETAUTGI3BPSL=ETAUTGI3BPSL+ETAU*PSL/PSLOR
    ENDIF
  ENDIF
ENDIF
IF(DORS. EQ. ' F ' ) THEN
  FIBIN=. FALSE.
% IF((YEND. LE. WIB2U). AND. (YEND. GE. WIB2D). AND.
  (ZEND. LE. HIB2U). AND. (ZEND. GE. HIB2D)) FIBIN=. TRUE.
  IF (FIBIN) THEN
    FIARTIN=. FALSE.
    IF((YEND. LE. WIARTU). AND. (YEND. GE. WIARTD)) FIARTIN=. TRUE.
    IF(FIARTIN) THEN
      CGF3I=CGF3I+1
      ETAUTGF3I=ETAUTGF3I+ETAU
      ETAUTGF3IPSL=ETAUTGF3IPSL+ETAU*PSL/PSLOR
    ELSE
      CGF3B=CGF3B+1
      ETAUTGF3B=ETAUTGF3B+ETAU
      ETAUTGF3BPSL=ETAUTGF3BPSL+ETAU*PSL/PSLOR
    ENDIF
  ENDIF
ENDIF
IF(DORS. EQ. ' G ' ) THEN
  FIBIN=. FALSE.
% IF((YEND. LE. WIB2U). AND. (YEND. GE. WIB2D). AND.
  (ZEND. LE. HIB2U). AND. (ZEND. GE. HIB2D)) FIBIN=. TRUE.
  IF (FIBIN) THEN
    FIARTIN=. FALSE.
    IF((YEND. LE. WIARTU). AND. (YEND. GE. WIARTD)) FIARTIN=. TRUE.
    IF(FIARTIN) THEN
      CGG3I=CGG3I+1
      ETAUTGG3I=ETAUTGG3I+ETAU
      ETAUTGG3IPSL=ETAUTGG3IPSL+ETAU*PSL/PSLOR
    ELSE
      CGG3B=CGG3B+1
      ETAUTGG3B=ETAUTGG3B+ETAU
      ETAUTGG3BPSL=ETAUTGG3BPSL+ETAU*PSL/PSLOR
    ENDIF
  ENDIF
ENDIF
ELSE
IF(DORS. EQ. ' S ' ) THEN
  FIBIN=. FALSE.
% IF((YEND. LE. WIB2U). AND. (YEND. GE. WIB2D). AND.
  (ZEND. LE. HIB2U). AND. (ZEND. GE. HIB2D)) FIBIN=. TRUE.
  IF (FIBIN) THEN
    FIARTIN=. FALSE.
    IF((YEND. LE. WIARTU). AND. (YEND. GE. WIARTD)) FIARTIN=. TRUE.
    IF(FIARTIN) THEN
      CGS9I=CGS9I+1
      ETAUTGS9I=ETAUTGS9I+ETAU
      ETAUTGS9IPSL=ETAUTGS9IPSL+ETAU*PSL/PSLOR
    ELSE
      CGS9B=CGS9B+1
      ETAUTGS9B=ETAUTGS9B+ETAU
      ETAUTGS9BPSL=ETAUTGS9BPSL+ETAU*PSL/PSLOR
    ENDIF
  ENDIF
ENDIF
IF(DORS. EQ. ' D ' ) THEN
  FIBIN=. FALSE.
% IF((YEND. LE. WIB2U). AND. (YEND. GE. WIB2D). AND.
  (ZEND. LE. HIB2U). AND. (ZEND. GE. HIB2D)) FIBIN=. TRUE.

```



```

DENSEMAY=0.
DO 51 YSCR=1, YMAX
DO 56 XSCR=1, XMAX
IF(DENSENG(XSCR, YSCR). GT. DENSEMAY)
DENSEMAY=DENSENG(XSCR, YSCR)
%
56 CONTINUE
51 CONTINUE
-----
C
C Output data
C-----
DO 67 YSCR=1, YMAX
DO 66 XSCR=1, XMAX
DENSENG(XSCR, YSCR)=DENSENG(XSCR, YSCR)/DENSEMAY*255. 99
JBUFF(XSCR, YSCR, 1)=INT(DENSENG(XSCR, YSCR))
66 CONTINUE
67 CONTINUE
OPEN (UNIT=1, FILE=OUTFILEA//'.mat')
DO YSCR=1, YMAX
WRITE(1, 210) (JBUFF(XSCR, YSCR, 1), XSCR=1, XMAX)
ENDDO
CLOSE(1)
210 FORMAT(' ', 1000(I3, '.', '.'), I3)
cYYYYYYYYYYYYYYYYYYYY with grid int data output YYYYYYYYYYYYYYYYYYYYYYYYYYYY
DENSEMAY=0.
DO 50 YSCR=1, YMAX
DO 55 XSCR=1, XMAX
IF(DENSE(XSCR, YSCR). GT. DENSEMAY) DENSEMAY=DENSE(XSCR, YSCR)
55 CONTINUE
50 CONTINUE
-----
C
C Output data
C-----
DO 60 YSCR=1, YMAX
DO 61 XSCR=1, XMAX
DENSE(XSCR, YSCR)=DENSE(XSCR, YSCR)/DENSEMAY*255. 99
JBUFF(XSCR, YSCR, 1)=INT(DENSE(XSCR, YSCR))
61 CONTINUE
60 CONTINUE
OPEN (UNIT=1, FILE=OUTFILEG//'.mat')
DO YSCR=1, YMAX
WRITE(1, 210) (JBUFF(XSCR, YSCR, 1), XSCR=1, XMAX)
ENDDO
CLOSE(1)
cYYYYYYYYYYYYYYYYYYYYYYYYYYYYYYYYYYYYYYYYYYYYYYYYYYYYYYYYYYYYYYYYYYYYYYY
OPEN (UNIT=1, FILE=OUTFILEG//'.num')
WRITE(1, 301) XH2OU
WRITE(1, 302) DISTWE
WRITE(1, 531) DISTWG
WRITE(1, 303) WIB
WRITE(1, 304) HIB
WRITE(1, 305) YDET
WRITE(1, 306) ZDET
WRITE(1, 307) R99P33P
WRITE(1, 308) RI2
WRITE(1, 309) WPER100
WRITE(1, 300)
WRITE(1, 530) H
WRITE(1, 540) DWO
WRITE(1, 545) DPB
WRITE(1, 300)
WRITE(1, 310) NPHOT
WRITE(1, 300)
WRITE(1, 380)
WRITE(1, 350)
WRITE(1, 351)
WRITE(1, 360) CD3I, CD3B, CD9I, CD9B
WRITE(1, 361) CS3I, CS3B, CS9I, CS9B
WRITE(1, 362) CI3I, CI3B, CI9I, CI9B
WRITE(1, 363) CF3I, CF3B, CF9I, CF9B
WRITE(1, 300)
WRITE(1, 381)
WRITE(1, 350)
WRITE(1, 351)
WRITE(1, 364) ETAUTD3I, ETAUTD3B, ETAUTD9I, ETAUTD9B
WRITE(1, 365) ETAUTS3I, ETAUTS3B, ETAUTS9I, ETAUTS9B

```

```

WRITE(1, 366) ETAUT13I, ETAUT13B, ETAUT19I, ETAUT19B
WRITE(1, 367) ETAUTF3I, ETAUTF3B, ETAUTF9I, ETAUTF9B
WRITE(1, 300)
WRITE(1, 391)
WRITE(1, 350)
WRITE(1, 351)
WRITE(1, 364) ETAUTD3IPSL, ETAUTD3BPSL, ETAUTD9IPSL, ETAUTD9BPSL
WRITE(1, 365) ETAUTS3IPSL, ETAUTS3BPSL, ETAUTS9IPSL, ETAUTS9BPSL
WRITE(1, 366) ETAUT13IPSL, ETAUT13BPSL, ETAUT19IPSL, ETAUT19BPSL
WRITE(1, 367) ETAUTF3IPSL, ETAUTF3BPSL, ETAUTF9IPSL, ETAUTF9BPSL
WRITE(1, 300)
WRITE(1, 382)
WRITE(1, 350)
WRITE(1, 351)
WRITE(1, 360) CGD3I, CGD3B, CGD9I, CGD9B
WRITE(1, 361) CGS3I, CGS3B, CGS9I, CGS9B
WRITE(1, 362) CGI3I, CGI3B, CGI9I, CGI9B
WRITE(1, 363) CGF3I, CGF3B, CGF9I, CGF9B
WRITE(1, 369) CCG3I, CCG3B, CCG9I, CCG9B
WRITE(1, 300)
WRITE(1, 383)
WRITE(1, 350)
WRITE(1, 351)
WRITE(1, 364) ETAUTGD3I, ETAUTGD3B, ETAUTGD9I, ETAUTGD9B
WRITE(1, 365) ETAUTGS3I, ETAUTGS3B, ETAUTGS9I, ETAUTGS9B
WRITE(1, 366) ETAUTGI3I, ETAUTGI3B, ETAUTGI9I, ETAUTGI9B
WRITE(1, 367) ETAUTGF3I, ETAUTGF3B, ETAUTGF9I, ETAUTGF9B
WRITE(1, 368) ETAUTGG3I, ETAUTGG3B, ETAUTGG9I, ETAUTGG9B
WRITE(1, 300)
WRITE(1, 393)
WRITE(1, 350)
WRITE(1, 351)
WRITE(1, 364) ETAUTGD3IPSL, ETAUTGD3BPSL, ETAUTGD9IPSL, ETAUTGD9BPSL
WRITE(1, 365) ETAUTGS3IPSL, ETAUTGS3BPSL, ETAUTGS9IPSL, ETAUTGS9BPSL
WRITE(1, 366) ETAUTGI3IPSL, ETAUTGI3BPSL, ETAUTGI9IPSL, ETAUTGI9BPSL
WRITE(1, 367) ETAUTGF3IPSL, ETAUTGF3BPSL, ETAUTGF9IPSL, ETAUTGF9BPSL
WRITE(1, 368) ETAUTGG3IPSL, ETAUTGG3BPSL, ETAUTGG9IPSL, ETAUTGG9BPSL
WRITE(1, 300)
WRITE(1, 389)
WRITE(1, 384)
WRITE(1, 385)
WRITE(1, 386)
WRITE(1, 387)
WRITE(1, 388)
WRITE(1, 389)
-
CLOSE(1)
300 FORMAT(' ')
310 FORMAT(' ', 'Total Photons      =', I10)
301 FORMAT(' ', 'Water Thickness              =', F7.1)
302 FORMAT(' ', 'Distance from Water to Detector =', F7.1)
531 FORMAT(' ', 'Distance from Water to Grid face=', F7.1)
303 FORMAT(' ', 'Injection beam width (mm)      =', F7.2)
304 FORMAT(' ', 'Injection beam height (mm)     =', F7.2)
305 FORMAT(' ', 'Detector width (mm)           =', F7.2)
306 FORMAT(' ', 'Detector height (mm)          =', F7.2)
307 FORMAT(' ', '99keV / 33keV ratio in %      =', F7.2)
308 FORMAT(' ', 'iodine artery diameter (mm)    =', F7.2)
309 FORMAT(' ', 'iodine weight ratio in %      =', F7.2)
530 FORMAT(' ', 'Grid thickness (mm)           =', F7.3)
540 FORMAT(' ', 'Wood pixel size of Grid (mm)   =', F7.3)
545 FORMAT(' ', 'Pb pixel size of Grid (mm)     =', F7.3)
380 FORMAT(' ', '*** Photon count in front of Grid ***')
381 FORMAT(' ', '*** Total photons in front of Grid (Real) ***')
391 FORMAT(' ', '*** Total photons in front of Grid (II res) ***')
382 FORMAT(' ', '*** Photon count after passing Grid ***')
383 FORMAT(' ', '*** Total photons after passing Grid (Real) ***')
393 FORMAT(' ', '*** Total photons after passing Grid (II res) ***')
384 FORMAT(' ', 'D : Direct photons in the beam area')
385 FORMAT(' ', 'S : Scattering photons in the beam area')
386 FORMAT(' ', 'I : Photons passing Iodine in the beam area')
387 FORMAT(' ', 'F : Iodine flouresence photons in the beam area')
388 FORMAT(' ', 'G : Grid flouresence photons in the beam area')
389 FORMAT(' ', '-----')
350 FORMAT(' ', 'DorS', 8X, '33.17 keV ', 16X, '99.51 keV ')
351 FORMAT(5X, ' in Artery   out Artery   in Artery   out Artery')

```

```

360 FORMAT( ' ' D ' , I10.3X, I10.3X, I10.3X, I10)
361 FORMAT( ' ' S ' , I10.3X, I10.3X, I10.3X, I10)
362 FORMAT( ' ' I ' , I10.3X, I10.3X, I10.3X, I10)
363 FORMAT( ' ' F ' , I10.3X, I10.3X, I10.3X, I10)
369 FORMAT( ' ' G ' , I10.3X, I10.3X, I10.3X, I10)
364 FORMAT( ' ' D ' , F11.3, 2X, F11.3, 2X, F11.3, 2X, F11.3)
365 FORMAT( ' ' S ' , F11.3, 2X, F11.3, 2X, F11.3, 2X, F11.3)
366 FORMAT( ' ' I ' , F11.3, 2X, F11.3, 2X, F11.3, 2X, F11.3)
367 FORMAT( ' ' F ' , F11.3, 2X, F11.3, 2X, F11.3, 2X, F11.3)
368 FORMAT( ' ' G ' , F11.3, 2X, F11.3, 2X, F11.3, 2X, F11.3)

```

```

STOP
END

```

```

C
C*****
C          Culculate initial random number
C-----

```

```

SUBROUTINE ORRANSU(RANSU)
  INTEGER RANSU(1:10), AMARI
  REAL UNIRAN, MU
  PARAMETER (MU=2.0**31)
  DO 10 I=1, 10
    UNIRAN=REAL(I)*0.1
    RANSU(I)=INT(UNIRAN*MU)
    AMARI=MOD(RANSU(I), 2)
    IF (AMARI.EQ.0) RANSU(I)=RANSU(I)+1
  10 CONTINUE
  RETURN
END

```

```

CC*****
C          Calculation next random number
C-----

```

```

SUBROUTINE NEWRANSU(RAN, UNIRAN)
  REAL UNIRAN, MU
  INTEGER RAN, LAM, C, T30
  PARAMETER (LAM=843314861, C=453816693, T30=2**30, MU=2.0**31)
  RAN=LAM*RAN+C
  IF (RAN.LT.0) RAN=(RAN+T30)+T30
  UNIRAN=REAL(RAN)/MU
  RETURN
END

```

```

CC*****
C          E-Bector deciding
C-----

```

```

SUBROUTINE EDECIDE(E0X, E0Y, E0Z, KX, KY, KZ, E1X, E1Y, E1Z, DELTA0D)
  REAL E1X, E1Y, E1Z, E0X, E0Y, E0Z, KX, KY, KZ
  DELTA0D=0.
  E0K=E0X*KX+E0Y*KY+E0Z*KZ
  IF(E0K.LT.0.0001) THEN
    E1X=E0X
    E1Y=E0Y
    E1Z=E0Z
  ELSE
    ETA=(KX*KX+KY*KY+KZ*KZ)/(E0X*KX+E0Y*KY+E0Z*KZ)
    ALPHA=ETA*E0X-KX
    BETA=ETA*E0Y-KY
    GAMMA=ETA*E0Z-KZ
    DELTA=SQRT(ALPHA*ALPHA+BETA*BETA+GAMMA*GAMMA)
    IF(DELTA.EQ.0.) THEN
      DELTA0D=1.
      GOTO 200
    ENDIF
    E1X=ALPHA/DELTA
    E1Y=BETA/DELTA
    E1Z=GAMMA/DELTA
  ENDIF
  200 CONTINUE
  RETURN
END

```

```

C*****
C          PHAI1(Compton) decideing
C-----

```

```

SUBROUTINE PHAI1COMPT(TH1, PHAI1, RANSU, EE0E0E, FNOPOL)
  INTEGER RAN, RANSU(1:10)
  LOGICAL FNOPOL
  PARAMETER (PI=3.141592, ME=.511*1E+06)

```

```

      IF(FNOPOL) GOTO 200
100 CONTINUE
      RAN=RANSU(4)
      CALL NEWRANSU(RAN, UNIRAN)
      RANSU(4)=RAN
      PHAI1P4=PI/2. *UNIRAN
      Y=(EE0E0E-2. *SIN(TH1)*SIN(TH1)*COS(PHAI1P4)*COS(PHAI1P4))/EE0E0E
      RAN=RANSU(9)
      CALL NEWRANSU(RAN, UNIRAN)
      RANSU(9)=RAN
      IF(UNIRAN. GT. Y) GOTO 100
200 CONTINUE
      RAN=RANSU(4)
      CALL NEWRANSU(RAN, UNIRAN)
      RANSU(4)=RAN
      IF(UNIRAN. LT. 0. 5) THEN
      IF(UNIRAN. LT. 0. 25) THEN
        PHAI1=PHAI1P4
      ELSE
        PHAI1=PI-PHAI1P4
      ENDIF
      ELSE
      IF(UNIRAN. GT. 0. 75) THEN
        PHAI1=-PHAI1P4
      ELSE
        PHAI1=-(PI-PHAI1P4)
      ENDIF
      ENDIF
      RETURN
      END

```

C\*\*\*\*\*

C PHAI1(Thomson) decideing

C-----

```

      SUBROUTINE PHAI1THOMS(TH1, PHAI1, RANSU, FNOPOL)
      INTEGER RAN, RANSU(1:10)
      LOGICAL FNOPOL
      PARAMETER (PI=3. 141592, ME=. 511*1E+06)
      IF(FNOPOL) GOTO 200
100 CONTINUE
      RAN=RANSU(4)
      CALL NEWRANSU(RAN, UNIRAN)
      RANSU(4)=RAN
      PHAI1P4=PI/2. *UNIRAN
      Y=1. -SIN(TH1)*SIN(TH1)*COS(PHAI1P4)*COS(PHAI1P4)
      RAN=RANSU(9)
      CALL NEWRANSU(RAN, UNIRAN)
      RANSU(9)=RAN
      IF(UNIRAN. GT. Y) GOTO 100
200 CONTINUE
      RAN=RANSU(4)
      CALL NEWRANSU(RAN, UNIRAN)
      RANSU(4)=RAN
      IF(UNIRAN. LT. 0. 5) THEN
      IF(UNIRAN. LT. 0. 25) THEN
        PHAI1=PHAI1P4
      ELSE
        PHAI1=PI-PHAI1P4
      ENDIF
      ELSE
      IF(UNIRAN. GT. 0. 75) THEN
        PHAI1=-PHAI1P4
      ELSE
        PHAI1=-(PI-PHAI1P4)
      ENDIF
      ENDIF
      RETURN
      END

```

C\*\*\*\*\*

C Calcuration next point

C-----

```

      SUBROUTINE NEWCOORD(X1, Y1, Z1, X2, Y2, Z2, EX, EY, EZ, RFREE, TH, PHAI
% , OMEGA0D)
      REAL LAMDA
      PARAMETER(PI=3. 141592)
c common /icommon/i

```

```

C-----
IF (RFREE.LT. 0. 001) GOTO 40
C-----
AX=X2-X1
AY=Y2-Y1
AZ=Z2-Z1
DA=SQRT(AX*AX+AY*AY+AZ*AZ)
IF(DA.EQ. 0.) THEN
  OMEGAOD=1.
  GOTO 40
ENDIF
BX=RFREE*COS(TH)*AX/DA
BY=RFREE*COS(TH)*AY/DA
BZ=RFREE*COS(TH)*AZ/DA
IF((AY.EQ. 0.). OR. (AZ.EQ. 0.)) THEN
  IF(AY.NE. 0.) THEN
    THT=ACOS(AX/DA)
    IF(AY.GT. 0.) THT=-THT
  ENDIF
  IF(AZ.NE. 0.) THEN
    THT=ACOS(AX/DA)
    IF(AZ.GT. 0.) THT=-THT
  ENDIF
  IF(EZ.NE. 0.) THEN
    PHAIE=ACOS(EY/(SQRT(EY*EY+EZ*EZ)))
    IF(EZ.LT. 0.) THEN PHAIE=-PHAIE
    PHAI=PHAI+PHAIE
  ENDIF
  CX=0.
  CY=RFREE*SIN(TH)*COS(PHAI)
  CZ=RFREE*SIN(TH)*SIN(PHAI)
  IF(AY.NE. 0.) THEN
    CX=CX*SIN(THT)
    CY=CX*COS(THT)
  ENDIF
  IF(AZ.NE. 0.) THEN
    CX=CZ*SIN(THT)
    CZ=CZ*COS(THT)
  ENDIF
ELSE
C-----
OMEGAXY=AX*EY-AY*EX
OMEGAXZ=AX*EZ-AZ*EX
OMEGAZY=AZ*EY-AY*EZ
OMEGAYZ=AY*EZ-AZ*EY
IF((OMEGAZY.EQ. 0.). OR. (OMEGAYZ.EQ. 0.)) THEN
  OMEGAOD=1.
  GOTO 40
ENDIF
OMEGAXYZY=OMEGAXY/OMEGAZY
OMEGAXYZZ=OMEGAXZ/OMEGAYZ
LAMDA=RFREE*SIN(TH)*COS(PHAI)
AAA=1+OMEGAXYZY*OMEGAXYZY+OMEGAXYZZ*OMEGAXYZZ
BBB=LAMDA*(AY*OMEGAXYZY/OMEGAZY+AZ*OMEGAXYZZ/OMEGAYZ)
CCC=(AY*AY/OMEGAZY/OMEGAZY+AZ*AZ/OMEGAYZ/OMEGAYZ)
% *LAMDA*LAMDA-RFREE*RFREE*SIN(TH)*SIN(TH)
IF(ABS(CCC).LT. 0. 00001) THEN
  CCC=-1.
  CCC=CCC+1.
ENDIF
% IF((ABS(AAA).GT. 100000000.). OR. (ABS(BBB).GT. 100000000.). OR.
  (ABS(CCC).GT. 100000000.)) THEN
  OMEGAOD=1.
  GOTO 40
ENDIF
XXX=BBB*BBB-AAA*CCC
IF(XXX.LT. 0.) XXX=0.
IF(PHAI.GE. 0.) THEN
  CX=(-BBB+SQRT(XXX))/AAA
ELSE
  CX=(-BBB-SQRT(XXX))/AAA
ENDIF
CY=-OMEGAXYZZ*CX-AZ*LAMDA/OMEGAYZ
CZ=-OMEGAXYZY*CX-AY*LAMDA/OMEGAZY
ENDIF

```



```

ELSE
C NBL > 0
  IF (NBL.GT.0) THEN
    IF (POBL1.LT.DWO) THEN
      LYWOI=DWO-POBL1
      LYPBI=DWO
    ELSE
      LYWOI=0.
      LYPBI=DBL-POBL1
    ENDIF
    IF (POBL2.LT.DWO) THEN
      LYWOF=POBL2
      LYPBF=0.
    ELSE
      LYWOF=DWO
      LYPBF=POBL2-DWO
    ENDIF
    IF (NBL.EQ.1) THEN
      LYWOM=0.
      LYPBM=0.
    ELSE
      LYWOM=DWO
      LYPBM=DPB
    ENDIF
C-----
C NBL < 0
  ELSE
    IF (POBL1.LT.DWO) THEN
      LYWOI=POBL1
      LYPBI=0.
    ELSE
      LYWOI=DWO
      LYPBI=POBL1-DWO
    ENDIF
    IF (POBL2.LT.DWO) THEN
      LYWOF=POBL2
      LYPBF=0.
    ELSE
      LYWOF=DWO
      LYPBF=POBL2-DWO
    ENDIF
  ENDIF
C-----
C ABS(NBL) = 1
  IF (ABS(NBL).EQ.1) THEN
    LYWOM=0.
    LYPBM=0.
C-----
C ABS(NBL) > 1
  ELSE
    LYWOM=DWO
    LYPBM=DPB
  ENDIF
C-----
  ENDIF
C*****
C LYWO, LYPB
C*****
  IF (NBL.EQ.0) THEN
    LYWO=LYWOI+LYWOF
    LYPB=LYPBI+LYPBF
  ELSE
    LYWO=LYWOI+LYWOF+LYWOM*(NBL-1)
    LYPB=LYPBI+LYPBF+LYPBM*(NBL-1)
  ENDIF
C*****
C LWOI, LWOF, LWOM, LWO, LPBI, LPBF, LPBM, LPB,
C*****
  IF ((LYWO.EQ.0.) .AND. (LYPB.EQ.0.)) THEN
    IF (POBL1.LT.DWO) THEN
      LWO=LGRID
      LPB=0.
    ELSE
      LWO=0.
      LPB=LGRID

```

```

ENDIF
  LWOI=LWO
  LPBI=LPB
  LWOI=0.
  LPBI=0.
  LWOM=0.
  LPBM=0.
C-----
ELSE
  RWO=LYWO/(LYWO+LYPB)
  RPB=LYPB/(LYWO+LYPB)
  LWO=LGRID*RWO
  LPB=LGRID*RPB
  IF(LYWO.EQ.0.) THEN
    LWOI=0.
    LWOM=0.
    LWOI=0.
  ELSE
    LWOI=LWO*LYWOI/LYWO
    LWOF=LWO*LYWOF/LYWO
    LWOM=LWO*LYWOM/LYWO
  ENDIF
  IF(LYPB.EQ.0.) THEN
    LPBI=0.
    LPBM=0.
    LPBF=0.
  ELSE
    LPBI=LPB*LYPBI/LYPB
    LPBF=LPB*LYPBF/LYPB
    LPBM=LPB*LYPBM/LYPB
  ENDIF
ENDIF
C*****
  LWOI=ABS(LWOI)
  LWOM=ABS(LWOM)
  LWOI=ABS(LWOI)
  LPBI=ABS(LPBI)
  LPBM=ABS(LPBM)
  LPBF=ABS(LPBF)
  LPB=ABS(LPBI)
C-----
  X0=X1
  Y0=Y1
  Z0=Z1
  X1=X2
  Y1=Y2
  Z1=Z2
  RETURN
END
CC*****
C      Length of x-ray passing through the Grid ( Back )
C-----
SUBROUTINE BACKPASS(X0, Y0, Z0, X1, Y1, Z1, NBL,
%          LWOI, LWOF, LWOM, LWO, LPBI, LPBF, LPBM, LPB)
REAL LWOI, LWOF, LWOM, LWO, LPBI, LPBF, LPBM, LPB
REAL LYWOI, LYWOF, LYWOM, LYWO, LYPBI, LYPBF, LYPBM, LYPB
REAL LGRID, XGRID, XGEND
REAL LSAV
COMMON /GRID/H, DWO, DPB, DBL, XEND, XGRID, XGEND
C----- Position on the entrance of the Grid -----
  XS=XGRID
  XGBAI=(XS-X0)/(X1-X0)
  YS=Y0+XGBAI*(Y1-Y0)
  ZS=Z0+XGBAI*(Z1-Z0)
  X2=X1
  Y2=Y1
  Z2=Z1
  X1=XS
  Y1=YS
  Z1=ZS
C-----
  LGRID=SQRT((X2-X1)*(X2-X1)+(Y2-Y1)*(Y2-Y1)+(Z2-Z1)*(Z2-Z1))
C-----
  IF(Y1.GE.0.) THEN

```

```

      NBL1=INT(Y1/DBL)
    ELSE
      NBL1=INT(Y1/DBL)-1
    ENDIF
    IF(Y2. GE. 0. )THEN
      NBL2=INT(Y2/DBL)
    ELSE
      NBL2=INT(Y2/DBL)-1
    ENDIF
    NBL=NBL2-NBL1
    POBL1=Y1-DBL*REAL(NBL1)
    POBL2=Y2-DBL*REAL(NBL2)
C*****
C  LYWO1, LYPBI, LYWOF, LYPBF, LYWOM, LYPBM
C*****
C  NBL = 0
    IF (NBL. EQ. 0) THEN
      IF (POBL1. LT. DWO) THEN
        IF (POBL2. LT. DWO) THEN
          LYWO1=POBL2-POBL1
          LYPBI=0.
        ELSE
          LYWO1=DWO-POBL1
          LYPBI=POBL2-DWO
        ENDIF
      ELSE
        IF (POBL2. LT. DWO) THEN
          LYWO1=DWO-POBL1
          LYPBI=POBL2-DWO
        ELSE
          LYWO1=0.
          LYPBI=POBL2-POBL1
        ENDIF
      ENDIF
      LYWOF=0.
      LYPBF=0.
      LYWOM=0.
      LYPBM=0.
C+++++
C-----
    ELSE
C  NBL > 0
      IF (NBL. GT. 0) THEN
        IF (POBL1. LT. DWO) THEN
          LYWO1=DWO-POBL1
          LYPBI=DWO
        ELSE
          LYWO1=0.
          LYPBI=DBL-POBL1
        ENDIF
        IF (POBL2. LT. DWO) THEN
          LYWOF=POBL2
          LYPBF=0.
        ELSE
          LYWOF=DWO
          LYPBF=POBL2-DWO
        ENDIF
        IF (NBL. EQ. 1) THEN
          LYWOM=0.
          LYPBM=0.
        ELSE
          LYWOM=DWO
          LYPBM=DPB
        ENDIF
C.....
C  NBL < 0
    ELSE
      IF (POBL1. LT. DWO) THEN
        LYWO1=POBL1
        LYPBI=0.
      ELSE
        LYWO1=DWO
        LYPBI=POBL1-DWO
      ENDIF
      IF (POBL2. LT. DWO) THEN

```

```

        LYWOF=POBL2
        LYPBF=0.
    ELSE
        LYWOF=DWO
        LYPBF=POBL2-DWO
    ENDIF
ENDIF
C-----
C ABS(NBL) = 1
  IF (ABS(NBL).EQ.1) THEN
        LYWOM=0.
        LYPBM=0.
C-----
C ABS(NBL) > 1
  ELSE
        LYWOM=DWO
        LYPBM=DPB
  ENDIF
C-----
  ENDIF
C*****
C LYWO, LYPB
C*****
  IF (NBL.EQ.0) THEN
        LYWO=LYWOI+LYWOF
        LYPB=LYPBI+LYPBF
  ELSE
        LYWO=LYWOI+LYWOF+LYWOM*(NBL-1)
        LYPB=LYPBI+LYPBF+LYPBM*(NBL-1)
  ENDIF
C*****
C LWOI, LWO, LWOF, LWOM, LWO, LPBI, LPBF, LPBM, LPB,
C*****
  IF ((LYWO.EQ.0.).AND.(LYPB.EQ.0.)) THEN
        IF (POBL1.LT.DWO) THEN
                LWO=LGRID
                LPB=0.
        ELSE
                LWO=0.
                LPB=LGRID
        ENDIF
        LWOI=LWO
        LPBI=LPB
        LWOF=0.
        LPBF=0.
        LWOM=0.
        LPBM=0.
C-----
  ELSE
        RWO=LYWO/(LYWO+LYPB)
        RPB=LYPB/(LYWO+LYPB)
        LWO=LGRID*RWO
        LPB=LGRID*RPB
        IF(LYWO.EQ.0.) THEN
                LWOI=0.
                LWOM=0.
                LWOF=0.
        ELSE
                LWOI=LWO*LYWOI/LYWO
                LWOF=LWO*LYWOF/LYWO
                LWOM=LWO*LYWOM/LYWO
        ENDIF
        IF(LYPB.EQ.0.) THEN
                LPBI=0.
                LPBM=0.
                LPBF=0.
        ELSE
                LPBI=LPB*LYPBI/LYPB
                LPBF=LPB*LYPBF/LYPB
                LPBM=LPB*LYPBM/LYPB
        ENDIF
  ENDIF
C*****
  LWOI=ABS(LWOI)
  LWOM=ABS(LWOM)

```

```

LWOF=ABS(LWOF)
LWO=ABS(LWO)
LPBI=ABS(LPBI)
LPBM=ABS(LPBM)
LPBF=ABS(LPBF)
LPB=ABS(LPB)
C-----
IF(LWOF.NE.0.) THEN
  LSAV=LWOI
  LWOI=LWOF
  LWOF=LSAV
ENDIF
IF(LPBF.NE.0.) THEN
  LSAV=LPBI
  LPBI=LPBF
  LPBF=LSAV
ENDIF
X0=X2
Y0=Y2
Z0=Z2
RETURN
END
CC*****
C      Position of x-ray scattering in the Grid
C-----
SUBROUTINE XPOSITION(RFREE, MEWVO, MEWPB, NBL, X0, Y0, Z0, X1, Y1, Z1,
%      LWOI, LWOF, LWOM, LWO, LPBI, LPBF, LPBM, LPB)
REAL RFREE
REAL MEWVO, MEWPB
REAL LWOI, LWOF, LWOM, LWO, LPBI, LPBF, LPBM, LPB
REAL LWOI2, LWOM2, LWOF2, LWO2, LPBI2, LPBM2, LPBF2, LPB2
REAL LPBEQI
REAL LREALY, LREAL, LEQ1, LEQM, LEQF2, LEQF2Y
COMMON /GRID/H, DWO, DPB, DBL, XEND, XGRID, XGEND
C-----
      NBL=0
      LWOI2=0.
      LWOM2=0.
      LWOF2=0.
      LWO2=0.
      LPBI2=0.
      LPBM2=0.
      LPBF2=0.
      LPB2=0.
      LPBEQI=LPBI/MEWVO*MEWPB
C-----
IF (NBL.EQ.0) THEN
  IF ((LWOI.EQ.0.).OR.(LPBI.EQ.0.)) THEN
    IF (LWOI.EQ.0.) THEN
      LPBI2=RFREE/MEWPB*MEWVO
      X2=LPBI2/LPBI*(X1-X0)+X0
      Y2=LPBI2/LPBI*(Y1-Y0)+Y0
      Z2=LPBI2/LPBI*(Z1-Z0)+Z0
    ENDIF
    IF (LPBI.EQ.0.) THEN
      LWOI2=RFREE
      X2=LWOI2/LWOI*(X1-X0)+X0
      Y2=LWOI2/LWOI*(Y1-Y0)+Y0
      Z2=LWOI2/LWOI*(Z1-Z0)+Z0
    ENDIF
  ELSE
    IF (Y1.GT.Y0) THEN
      IF (RFREE.LT.LWOI) THEN
        LWOI2=RFREE
        X2=LWOI2/(LWOI+LPBI)*(X1-X0)+X0
        Y2=LWOI2/(LWOI+LPBI)*(Y1-Y0)+Y0
        Z2=LWOI2/(LWOI+LPBI)*(Z1-Z0)+Z0
      ELSE
        LWOI2=LWOI
        LPBI2=(RFREE-LWOI)/MEWPB*MEWVO
        X2=(LWOI2+LPBI2)/(LWOI+LPBI)*(X1-X0)+X0
        Y2=(LWOI2+LPBI2)/(LWOI+LPBI)*(Y1-Y0)+Y0
        Z2=(LWOI2+LPBI2)/(LWOI+LPBI)*(Z1-Z0)+Z0
      ENDIF
    ELSE
      LPB2=LPB
      LPBF2=LPBF
      LPBM2=LPBM
      LPBEQI=LPBI/MEWVO*MEWPB
    ENDIF
  ENDIF
ELSE
  LPB2=LPB
  LPBF2=LPBF
  LPBM2=LPBM
  LPBEQI=LPBI/MEWVO*MEWPB
ENDIF
END

```

```

IF (RFREE. LT. LPBEQ1) THEN
  LPB12=RFREE/MEWPB*MEWVO
  X2=LPB12/(LWOI+LPBI)*(X1-X0)+X0
  Y2=LPB12/(LWOI+LPBI)*(Y1-Y0)+Y0
  Z2=LPB12/(LWOI+LPBI)*(Z1-Z0)+Z0
ELSE
  LPB12=LPBI
  LWOI2=(RFREE-LPBEQ1)
  X2=(LWOI2+LPB12)/(LWOI+LPBI)*(X1-X0)+X0
  Y2=(LWOI2+LPB12)/(LWOI+LPBI)*(Y1-Y0)+Y0
  Z2=(LWOI2+LPB12)/(LWOI+LPBI)*(Z1-Z0)+Z0
ENDIF
ENDIF
ENDIF
  LWO2=LWOI2
  LPB2=LPB12
ELSE
C-----
  LEQ1=LWOI+LPBI*MEWPB/MEWVO
  LEQM=LWOM+LPBM*MEWPB/MEWVO
  IF (RFREE. LT. LEQ1) THEN
    NBS=0
  ELSE
    IF (LEQM. EQ. 0.) THEN
      NBS=1
    ELSE
      NBS=INT((RFREE-LEQ1)/LEQM)+1
    ENDIF
  ENDIF
  IF (NBS. EQ. 0) THEN
    IF ((LWOI. EQ. 0.) OR (LPBI. EQ. 0.)) THEN
      IF (LWOI. EQ. 0.) THEN
        LPB12=RFREE/MEWPB*MEWVO
        X2=LPB12/LPBI*(X1-X0)+X0
        Y2=LPB12/LPBI*(Y1-Y0)+Y0
        Z2=LPB12/LPBI*(Z1-Z0)+Z0
      ENDIF
      IF (LPBI. EQ. 0.) THEN
        LWOI2=RFREE
        X2=LWOI2/LWOI*(X1-X0)+X0
        Y2=LWOI2/LWOI*(Y1-Y0)+Y0
        Z2=LWOI2/LWOI*(Z1-Z0)+Z0
      ENDIF
    ELSE
      IF (Y1. GT. Y0) THEN
        IF (RFREE. LT. LWOI) THEN
          LWOI2=RFREE
          X2=LWOI2/(LWOI+LPBI)*(X1-X0)+X0
          Y2=LWOI2/(LWOI+LPBI)*(Y1-Y0)+Y0
          Z2=LWOI2/(LWOI+LPBI)*(Z1-Z0)+Z0
        ELSE
          LWOI2=LWOI
          LPB12=(RFREE-LWOI)/MEWPB*MEWVO
          X2=(LWOI2+LPB12)/(LWOI+LPBI)*(X1-X0)+X0
          Y2=(LWOI2+LPB12)/(LWOI+LPBI)*(Y1-Y0)+Y0
          Z2=(LWOI2+LPB12)/(LWOI+LPBI)*(Z1-Z0)+Z0
        ENDIF
      ELSE
        IF (RFREE. LT. LPBEQ1) THEN
          LPB12=RFREE/MEWPB*MEWVO
          X2=LPB12/(LWOI+LPBI)*(X1-X0)+X0
          Y2=LPB12/(LWOI+LPBI)*(Y1-Y0)+Y0
          Z2=LPB12/(LWOI+LPBI)*(Z1-Z0)+Z0
        ELSE
          LPB12=LPBI
          LWOI2=(RFREE-LPBEQ1)
          X2=(LWOI2+LPB12)/(LWOI+LPBI)*(X1-X0)+X0
          Y2=(LWOI2+LPB12)/(LWOI+LPBI)*(Y1-Y0)+Y0
          Z2=(LWOI2+LPB12)/(LWOI+LPBI)*(Z1-Z0)+Z0
        ENDIF
      ENDIF
    ENDIF
  ENDIF
  LWO2=LWOI2
  LPB2=LPB12
ELSE

```

```

C-----
      LEQF2=RFREE-LEQI-LEQM*REAL(NBLS-1)
      LREAL=(Y1-Y0)
      LREAL=SQRT((X1-X0)*(X1-X0)+(Y1-Y0)*(Y1-Y0)
%          +(Z1-Z0)*(Z1-Z0))
      LEQF2Y=LEQF2*LREAL/LREAL
      IF (Y1.GT.Y0) THEN
      IF (LEQF2Y.LE.DWO) THEN
          LWOF2=LEQF2
          LPBF2=0.
      ELSE
          LWOF2=DWO*LREAL/LREAL
          LPBF2=(LEQF2Y-DWO)/MEWPB*MEWWO*LREAL/LREAL
      ENDIF
      ELSE
      IF (LEQF2Y.LE.DPB*MEWPB/MEWWO) THEN
          LWOF2=0.
          LPBF2=LEQF2/MEWPB*MEWWO
      ELSE
          LWOF2=(LEQF2Y-DPB*MEWPB/MEWWO)*LREAL/LREAL
          LPBF2=DPB*LREAL/LREAL
      ENDIF
      ENDIF
      LWO2=LWOI2+LWOM2*REAL(NBLS-1)+LWOF2
      LPB2=LPBI2+LPBM2*REAL(NBLS-1)+LPBF2
      X2=(LWO2+LPB2)/(LWO+LPB)*(X1-X0)+X0
      Y2=(LWO2+LPB2)/(LWO+LPB)*(Y1-Y0)+Y0
      Z2=(LWO2+LPB2)/(LWO+LPB)*(Z1-Z0)+Z0
      ENDIF
      ENDIF
      NBL=NBLS
      LWOI=LWOI2
      LWOM=LWOM2
      LWOF=LWOF2
      LWO=LWO2
      LPBI=LPBI2
      LPBM=LPBM2
      LPBF=LPBF2
      LPB=LPB2
      X0=X1
      Y0=Y1
      Z0=Z1
      X1=X2
      Y1=Y2
      Z1=Z2

```

```

C-----
      RETURN
      END
CC*****
C      Deciding scattering angle
C-----

```

```

SUBROUTINE SCANGLE(TH1, PHA11, EPH, FELOS, Y1, FNOPOL)
REAL MEWWO, SIGINCWO, MEWPB, SIGINCPB
REAL MEW, SIGINC
REAL THM(0:1000)
REAL LR
REAL PITHOMSWO(0:99, 0:1000), PIKLNISWO(0:99, 0:1000)
REAL PITHOMSPB(0:99, 0:1000), PIKLNISPB(0:99, 0:1000)
INTEGER RAN
INTEGER RANSU(1:10)
LOGICAL FELOS, FINCOH, FINWO, FNOPOL
PARAMETER (PI=3.141592, ME=.511*1E+06)
PARAMETER (RE=2.81794092E-15, C=2.99792458E+08)
PARAMETER (NTH=1000)
PARAMETER (LOSEPH=10.)
PARAMETER (ROUWO=0.49, ROUPB=11.34)
COMMON /ANGLE/THM, PITHOMSWO, PIKLNISWO, PITHOMSPB, PIKLNISPB
COMMON /RANDAW/RANSU
COMMON /MEWSIG/MEWWO, SIGCOHWO, SIGINCWO, MEWPB, SIGCOHPB, SIGINCPB
COMMON /GRID/H, DWO, DPB, DBL, XEND, XGRID, XGEND

```

```

C-----
      NBL1=INT(Y1/DBL)
      POBL1=Y1-DBL*REAL(NBL1)
      FINWO=.FALSE.
      IF(POBL1.LT.DWO) FINWO=.TRUE.

```

```

IF(FINWO) THEN
  MEW=MEWWO
  SIGINC=SIGINCWO
ELSE
  MEW=MEWPB
  SIGINC=SIGINCPB
ENDIF
C----- Kind of interaction with atom -----
RAN=RANSU(9)
CALL NEWRANSU(RAN, UNIRAN)
RANSU(9)=RAN
C (Tomson scattering or Compton scattering ?)
FINCOH=.FALSE.
IF (UNIRAN.LT.SIGINC/MEW) FINCOH=.TRUE.
RAN=RANSU(4)
CALL NEWRANSU(RAN, UNIRAN)
RANSU(4)=RAN
C ( Scattering angle )
TH1=0.
IF(EPH.EQ.99.51) THEN
  LR=0.
  GOTO 65
ENDIF
C ( If photon energy is 99.51keV then use PIA9951.DAT data )
  LR=EPH
65 CONTINUE
  LI=INT(LR)
C..... Compton scattering .....
IF (FINCOH) THEN
  DO 72 K2=1, 10
  IF(FINWO) THEN
    UNIP1=PIKLNISWO(LI, K2*100)/PIKLNISWO(LI, NTH)
  ELSE
    UNIP1=PIKLNISPB(LI, K2*100)/PIKLNISPB(LI, NTH)
  ENDIF
  IF (UNIRAN.LE.UNIP1) THEN
    K100=(K2-1)*100
    GOTO 92
  ENDIF
72 CONTINUE
92 CONTINUE
  DO 71 K1=1, 10
  IF(FINWO) THEN
    UNIP1=PIKLNISWO(LI, K100+K1*10)/PIKLNISWO(LI, NTH)
  ELSE
    UNIP1=PIKLNISPB(LI, K100+K1*10)/PIKLNISPB(LI, NTH)
  ENDIF
  IF (UNIRAN.LE.UNIP1) THEN
    K10=(K1-1)*10
    GOTO 91
  ENDIF
71 CONTINUE
91 CONTINUE
  DO 70 K=1, 10
  IF(FINWO) THEN
    UNIP1=PIKLNISWO(LI, K100+K10+K)/PIKLNISWO(LI, NTH)
  ELSE
    UNIP1=PIKLNISPB(LI, K100+K10+K)/PIKLNISPB(LI, NTH)
  ENDIF
  IF (UNIRAN.LE.UNIP1) THEN
    TH1=THM(K100+K10+K)
    GOTO 90
  ENDIF
70 CONTINUE
90 CONTINUE
  EPH0=EPH
  EPH=EPH/(1+EPH*1000./ME*(1-COS(TH1)))
  IF (EPH.LE.LOSEPH) THEN
C ( if energy < min energy , photon is lost )
    FELOS=.TRUE.
    GOTO 30
  ENDIF
  EE0E0E=EPH/EPH0+EPH0/EPH
  CALL PHA1COMPT(TH1, PHA11, RANSU, EE0E0E, FNOPOL)
ELSE

```

```

C----- Thomson scattering -----
      DO 82 K2=1.10
      IF(FINWO) THEN
        UNIPI=PITHOMSWO(LI, K2*100)/PITHOMSWO(LI, NTH)
      ELSE
        UNIPI=PITHOMSPB(LI, K2*100)/PITHOMSPB(LI, NTH)
      ENDIF
      IF (UNIRAN. LE. UNIPI) THEN
        K100=(K2-1)*100
        GOTO 32
      ENDIF
82    CONTINUE
32    CONTINUE
      DO 81 K1=1.10
      IF(FINWO) THEN
        UNIPI=PITHOMSWO(LI, K100+K1*10)/PITHOMSWO(LI, NTH)
      ELSE
        UNIPI=PITHOMSPB(LI, K100+K1*10)/PITHOMSPB(LI, NTH)
      ENDIF
      IF (UNIRAN. LE. UNIPI) THEN
        K10=(K1-1)*10
        GOTO 31
      ENDIF
81    CONTINUE
31    CONTINUE
      DO 80 K=1.10
      IF(FINWO) THEN
        UNIPI=PITHOMSWO(LI, K100+K10+K)/PITHOMSWO(LI, NTH)
      ELSE
        UNIPI=PITHOMSPB(LI, K100+K10+K)/PITHOMSPB(LI, NTH)
      ENDIF
      IF (UNIRAN. LE. UNIPI) THEN
        TH1=THM(K100+K10+K)
        GOTO 33
      ENDIF
80    CONTINUE
33    CONTINUE
        CALL PHAITHOMS(TH1, PHA11, RANSU, FNOPOL)
      ENDIF
30    CONTINUE
C-----
      RETURN
      END
C*****

```

